

UNCLASSIFIED

AD NUMBER

ADB004731

LIMITATION CHANGES

TO:

Approved for public release; distribution is unlimited.

FROM:

Distribution authorized to U.S. Gov't. agencies only; Critical Technology; MAR 1975. Other requests shall be referred to Federal Aviation Administration, Supersonic Transport Office, 800 Independence Avenue, SW, Washington, DC 20590. This document contains export-controlled technical data.

AUTHORITY

faa ltr, 26 apr 1977

THIS PAGE IS UNCLASSIFIED

THIS REPORT HAS BEEN DELIMITED
AND CLEARED FOR PUBLIC RELEASE
UNDER DOD DIRECTIVE 5200.20 AND
NO RESTRICTIONS ARE IMPOSED UPON
ITS USE AND DISCLOSURE.

DISTRIBUTION STATEMENT A

APPROVED FOR PUBLIC RELEASE;
DISTRIBUTION UNLIMITED.

Report No. FAA-SS-73-11-4

Handwritten initials and a circled number '1'.

**SST Technology
Follow-On Program—Phase II
NOISE SUPPRESSOR/NOZZLE DEVELOPMENT
VOLUME IV**

AD B O U 4 7 3 1

**PERFORMANCE TECHNOLOGY
SUMMARY**

R. S. Armstrong

**Boeing Commercial Airplane Company
P.O. Box 3707
Seattle, Washington 98124**

AD No. _____
FILE COPY



D6-42479

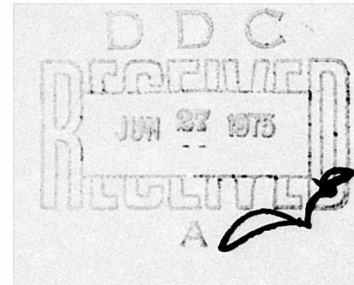
March 1975

FINAL REPORT

Task III

Approved for U.S. Government only. This document is exempted from public availability because of restrictions imposed by the Export Control Act. Transmittal of this document outside the U.S. Government must have prior approval of the Supersonic Transport Office.

**Prepared for
FEDERAL AVIATION ADMINISTRATION
Supersonic Transport Office
800 Independence Avenue, S.W.
Washington, D.C. 20590**



The contents of this report reflect the views of the Boeing Commercial Airplane Company, which is responsible for the facts and the accuracy of the data presented herein. The contents do not necessarily reflect the official views or policy of the Department of Transportation. This report does not constitute a standard, specification, or regulation.

SEARCHED		
INDEXED	SERIALIZED	FILED
APR 19 1964		
FBI - MEMPHIS		
13		

1. Report No. 19 FAA-SS 73-11-4	2. Government Accession No.	3. Recipient's Catalog No. 12 93p.	
4. Title and Subtitle SST TECHNOLOGY FOLLOW-ON PROGRAM-PHASE II NOISE SUPPRESSOR NOZZLE DEVELOPMENT- Vol. IV Performance Technology Summary		5. Report Date 11 Mar 1975	6. Performing Organization Code
7. Author(s) 10 R. S. Armstrong	8. Performing Organization Report No. 14 D6-42479		10. Work Unit No.
9. Performing Organization Name and Address Boeing Commercial Airplane Company P.O. Box 3707 Seattle, Washington 98124		11. Contract or Grant No. 15 DOT-FA-72WA-2893	13. Type of Report and Period Covered 14 Final Report Task III
12. Sponsoring Agency Name and Address Federal Aviation Administration Supersonic Transport Office 800 Independence Avenue S.W., Washington, D.C. 20590		14. Sponsoring Agency Code 16	
15. Supplementary Notes S. Blatt, DOT/SST Technical Monitor			
16. Abstract This report summarizes the performance technology developed during the DOT phase II task III program. Thrust performance design guidelines are established within mechanical constraints and acoustic criteria for low noise multitube-suppressor exhaust systems. Model-scale tests were conducted that investigated detailed performance interactions and overall performance for multitube suppressor/ejector exhaust systems. The effects of geometry, jet pressure and temperature, and external velocity on performance are analyzed. A concurrent program for the development of acoustic technology is reported upon in volume II. 6 SST Technology Follow-On Program-Phase II, Noise Suppressor/Nozzle Development. Volume IV. Performance Technology Summary.			
17. Key Words (Suggested by Author(s)) Suppressor Nozzle Multitube Suppressor/Ejector Suppressor Performance Ejector Performance Jet Noise		18. Distribution Statement Approved for U.S. Government only. This document is exempted from public availability because of restrictions imposed by the Export Control Act. Transmittal of this document outside the U.S. Government must have prior approval of the Supersonic Transport Office.	
19. Security Classif. (of this report) Unclassified	20. Security Classif. (of this page) Unclassified	21. No. of Pages 89	22. Price*

Distribution limited to U.S. Gov't. agencies only. Other requests for this document must be referred to [unclear]

*For sale by the National Technical Information Service, Springfield, Virginia 22151

390 145 ✓
not

PREFACE

This is one of a series of final reports on noise and propulsion technology submitted by the Boeing Commercial Airplane Company, Seattle, Washington, 98124, in fulfillment of Task III of Department of Transportation Contract DOT-FA-72WA-2893, dated 1 February 1972.

To benefit utilization of technical data developed by the noise suppressor and nozzle development program, the final report is divided into 10 volumes covering key technology areas and a summary of total program results. The 10 volumes are issued under the master title, "Noise Suppressor/Nozzle Development." Detailed volume breakdown is as follows:

	Report No.
Volume I – Program Summary	FAA-SS-73-11-1
Volume II – Noise Technology	FAA-SS-73-11-2
Volume III – Noise Technology—Backup Data Report	FAA-SS-73-11-3
Volume IV – Performance Technology Summary	FAA-SS-73-11-4
Volume V – Performance Technology—The Effect of Initial Jet Conditions on a 2-D Constant Area Ejector	FAA-SS-73-11-5
Volume VI – Performance Technology—Thrust and Flow Characteristics of a Reference Multitube Nozzle With Ejector	FAA-SS-73-11-6
Volume VII – Performance Technology—A Guide to Multitube Suppressor Nozzle Static Performance; Trends and Trades	FAA-SS-73-11-7
Volume VIII – Performance Technology—Multitube Suppressor/Ejector Interaction Effects on Static Performance (Ambient and 1150° F Jet Temperature)	FAA-SS-73-11-8
Volume IX – Performance Technology—Analysis of the Low-Speed Performance of Multitube Suppressor/Ejector Nozzles (0-167 kn)	FAA-SS-73-11-9
Volume X – Advanced Suppressor Concepts and Full-Scale Tests	FAA-SS-73-11-10

This report is volume IV of the series and was prepared by the Propulsion Research Staff of the Boeing Commercial Airplane Company.

PRECEDING PAGE BLANK NOT FILMED

CONTENTS

	Page
SUMMARY	1
1.0 INTRODUCTION	9
2.0 TEST FACILITIES	13
2.1 High Ratio Rig	13
2.2 Hot Nozzle Facility	13
2.3 Low-Speed Wind Tunnel	13
3.0 EJECTOR MIXING STUDY	17
3.1 Test Program Description	17
3.2 Summary of Results	21
3.2.1 Pressure Ratio Effects on Flow Field	21
3.2.2 Thrust and Flow Augmentation	21
3.2.3 Ejector Wall Pressure	24
4.0 REFERENCE NOZZLES	29
4.1 Test Program Description	29
4.2 Summary of Results	29
4.2.1 Nozzle/Ejector Performance	29
4.2.2 Secondary Flow	36
4.2.3 Ejector Flow Mixing	36
5.0 MULTITUBE NOZZLE/EJECTOR STUDY	41
5.1 Test Program Description	41
5.2 Bare Suppressor Performance	41
5.2.1 Range of Variables	41
5.2.2 Internal Performance	46
5.2.3 Nozzle Geometry Effects	46
5.2.4 Performance Trends	46
5.2.5 Performance/Noise Suppression Trends	54
5.3 Suppressor/Ejector Performance	54
5.3.1 Range of Variables	54
5.3.2 Pressure Ratio Effects	58
5.3.3 Nozzle Geometry Effects	58
5.3.4 Ejector Effects	63
5.3.5 Performance Trends	63
5.3.6 Performance/Noise Suppression Trends	67
5.4 Low-Speed Performance	67
5.4.1 Range of Variables	67
5.4.2 Pressure Ratio Effects	69
5.4.3 Nozzle Geometry Effects	72
5.4.4 Ejector Effects	77

PRECEDING PAGE BLANK-NOT FILMED

CONTENTS—CONCLUDED

	Page
5.4.5 Temperature Effects	80
5.4.6 Overall Performance Trends	83
6.0 CONCLUSIONS	85
7.0 RECOMMENDATIONS	87
8.0 REFERENCES	89

FIGURES

No.		Page
1	Wall Static Pressure Distribution	3
2	Summary of Bare Suppressor Performance	4
3	Summary of Suppression Versus Thrust Loss, Nozzle Area Ratio = 3.3	5
4	Ejector Performance Trend	6
5	Effect of Ejector Length on Performance at Forward Velocity	6
6	Suppressor/Ejector Component Forces at Forward Velocity	7
7	Effect of Tube Array on Performance With Velocity	7
8	Application of a Stowable Suppressor to an Advanced SST Exhaust System	11
9	High-Ratio Rig	14
10	Hot Nozzle Rig	15
11	Test Installation, 9- by 9-ft Wind Tunnel	16
12	Schematic of 2-D Ejector Test Apparatus	18
13	Test Installation	19
14	Ejector Flow Schematic	20
15	Change in Ejector Flow Field With Primary Pressure Ratio	22
16	Effect of Variable Changes on Weight Flow Ratio	23
17	Effect of Variable Changes on Thrust Augmentation Ratio, θ	25
18	Effect of Variable Changes on Ejector Flow Field	26
19	R/C and R/37 Nozzles	30
20	R/37 Nozzle With 8-in. Ejector (L/D = 1) and Flight Lip Inlet	31
21	Measurement of Secondary Mass Flow on Hot Nozzle Facility, R/C Nozzle With 48-in. Ejector (L/D = 6)	32
22	Bare Nozzle Performance	33
23	Effect of Ejector Length on Thrust Augmentation	34
24	Effect of Primary Jet Temperature on Ejector Performance	35
25	Ejector Nozzle Body Forces and Secondary Weight Flow Measurement	37
26	Secondary Weight Flow for a Fully Mixed Multitube Nozzle	38
27	Ejector Flow Pressure Profiles	39
28	Geometric Test Variables	42
29	Matrix of Suppressor Configurations and Test Conditions	43
30	19- and 61-Tube, NAR = 3.3 Suppressors	44
31	37-Tube, Close-Packed Suppressors NAR = 2.75 and 3.3	45
32	Comparison of 37-Tube, 3.3 Area Ratio Nozzles	47
33	Example of Close-Packed and Radial Array Nozzles	48
34	Radial Array Nozzles	49
35	Effect of Tube Length and Number on Internal Velocity Coefficient at 1150° F	50
36	Nozzle Base Drag as a Function of Tube Number, Tube Length, and Tube Array	51
37	Performance Components for Radial and Close-Packed 37-Tube Nozzles	52
38	Effect of Area Ratio, Base Array and Tube Length on Suppressor Performance	53
39	Base Ventilation Parameter for 37-Tube Nozzles	55

FIGURES—CONCLUDED

No.		Page
40	Summary of Suppression Versus Thrust Loss	56
41	Jet Noise Suppression Versus Thrust Loss	57
42	Typical Suppressor/Ejector Installation	59
43	Gross Thrust Coefficient and Body Forces for 37-Tube, NAR = 3.3, EAR = 3.1, Close-Packed, Elliptical Ramp, Elliptical Convergent Tubes	60
44	Performance as a Function of Tube Length for Various NAR = 3.3 Suppressors With EAR = 3.1 Ejectors	61
45	Effect of Nozzle Tube Number on Ejector Thrust Augmentation	62
46	Effect of Nozzle Array on Ejector Thrust Augmentation	64
47	Ejector Performance Trend	65
48	Performance Trends for 37 Elliptical Convergent Tubes, NAR = 2.75, Close-Packed Array, Elliptical Ramp	66
49	Effect of Ejector Area Ratio on Suppression and Thrust Loss for a 31-Tube, NAR = 2.75, Radial Array	68
50	General Behavior of Bare Suppressor Performance as a Function of Pressure Ratio and Velocity	70
51	Gross Thrust Coefficient for 37-Tube, NAR = 3.3, Close-Packed Array, Without Ejector	71
52	Ejector Inlet Area, A_A and A_S	73
53	Gross Thrust Coefficient for 37-Tube, NAR = 3.3, Close-Packed Array, With EAR = 3.1 Ejector, Setback = 0.25	74
54	Effect of Velocity on Base Drag as a Percentage of Ideal Thrust for NAR = 3.3 Suppressor With Various Numbers of Tubes (No Ejector)	75
55	Effect of Nozzle Geometry on Low-Speed Performance (No Ejector)	76
56	Effect of Nozzle Geometry on Low-Speed Performance With Ejector)	78
57	Effect of Setback and Velocity on Performances (Other Parameters Constant)	79
58	Effect of Ejector Length on Performance With Forward Velocity	81
59	Effect of Jet Temperature on Ejector Lip Suction	82

SYMBOLS AND ABBREVIATIONS

A_A	Minimum annular area between the ejector lip and the exit of the outer row tubes, in ²
A_B	Suppressor base area, in ² , $A_P(NAR - 1)$
A_P	Geometric flow area, in ² , of primary nozzle including temperature-induced area growth
A_S	Measured area between the outer row tubes of a suppressor, in ²
C_f	Skin friction coefficient
C_{Fg}	Gross thrust coefficient; measured (thrust-drag) divided by ideal thrust

where:

$$\text{Ideal thrust} = \frac{W_P}{g} V_{ID}$$

CPA	Close-packed array: an arrangement of tubes such that there is approximately the same distance between any two adjacent tubes
$C_{V \text{ int}}$	Nozzle internal velocity coefficient; measured $C_{Fg} + D_B/F_{ID}$
D, D_E	Ejector diameter, inches
D_B	D_{base} : nozzle base drag in pounds, calculated from static pressure measurements taken at area weighted taps on the base
D_{eq}	Exit diameter of a single round convergent nozzle having the same area as the total effective flow area of a multitube suppressor, inches
EAR	Ejector area ratio; ejector throat area divided by A_P
F_{ID}	Ideal primary nozzle thrust; $\frac{W_P}{g} V_{ID}$
F_{lip}	Ejector inlet lip (suction) force, lb; derived from static pressure measurements on lip
fps	Feet per second
L, L_E	Ejector length; distance from flight lip highlight to ejector exit
L/D	Ejector length-to-diameter ratio

L_T	Nozzle tube length measured on outside of the tube; distance from exit to baseplate
NAR	Nozzle area ratio; area inside a circle circumscribed around the outside of the outermost tubes divided by A_p
P	Pressure
P_{amb}, P_{∞}	Ambient pressure, psia
P_B	Average nozzle base pressure, psia
PR	Primary nozzle pressure ratio, P_{TP}/P_{amb}
psia	Pounds per square inch absolute
P_{TP}, P_{TO}	Primary nozzle charging station total pressure, psia
P_{TS}	Secondary nozzle charging station total pressure; also total pressure of induced secondary flow at ejector inlet, psia
P_{wall}	Ejector wall static pressure, psia
R	Universal gas constant
RA	Radial array; an arrangement of tubes in radial lines
R/C	Round convergent reference nozzle with 10° internal exit half-angle
Re	Reynolds number
R/37	37-tube reference nozzle; NAR = 3.3 close-packed array, $L_T/D_{eq} = 1.1$ (average)
SB	Setback; axial distance from nozzle exit plane to the flight lip highlight of the ejector, inches
T_T, T_{TP}	Average total temperature of primary flow at nozzle charging station, $^\circ F$
T_{TS}	Average total temperature of secondary flow, $^\circ F$
u'	Average velocity fluctuation in x direction
U	Average mean velocity
V_{ID}	Ideal velocity of primary flow at P_{TP} (isentropically expanded to ambient pressure), feet per second

V_{∞} Wind tunnel test section velocity, knots

$$W_{Scale} = \frac{W_S \sqrt{T_{TS}}}{P_{TS} A_{sec}} ; \left[\frac{2g\gamma}{R(\gamma-1)} \right]^{1/2} \left(\frac{P_{\infty}}{P_{TS}} \right)^{1/\gamma} \left[1 - \left(\frac{P_{\infty}}{P_{TS}} \right)^{\frac{\gamma-1}{\gamma}} \right]^{1/2}$$

W_P Measured primary weight flow, air (and fuel when air is heated) pounds/second

W_S Measured secondary airflow, pounds/second

θ C_{Fg} (ejector/suppressor configuration) divided by C_{Fg} (primary nozzle alone)

γ Specific heat ratio

SUMMARY

Advanced supersonic aircraft require a variable convergent-divergent nozzle geometry to provide near-ideal engine exhaust expansion for maximum thrust performance at supersonic cruise. During takeoff a suppressor can be used in conjunction with an ejector, formed by the divergent part of the exhaust system, to provide required noise suppression and good takeoff thrust.

A critical factor in the development of jet noise-suppression devices for exhaust nozzle systems is the maintenance of acceptable levels of thrust performance over the flight regime. Application to advanced supersonic aircraft demands that the suppressor cause little or no performance loss at cruise conditions. This constraint generally means that the suppressor must be retracted out of the jet stream at other than takeoff and approach flight modes and this in turn severely limits the range of suppressor hardware parameters that can be considered for practical configurations.

This volume summarizes the technology program that has been directed toward the establishment of performance design guidelines within mechanical design constraints and acoustic criteria for low-noise multitube-suppressor exhaust systems.

A matrix of multitube-suppressor configurations were tested at model scale to develop a detailed understanding of performance loss mechanisms for design trade studies. Major parameters included number, length and array of tubes, size (area ratio) of array, and the effects of the addition of ejectors and of forward speed. Additional experiments were conducted to study detailed mixing phenomena in ejectors including evaluation of initial flow conditions on mixing and performance in a two-dimensional model and secondary air handling characteristics of axisymmetric configurations. The 2-D test program used a multi-slot nozzle and ejector to determine the effects of initial flow characteristics (velocity profiles, turbulence levels, initial base thickness) on ejector thrust augmentation and secondary air handling and mixing rates.

Results of the 2-D ejector testing show that initial jet conditions have a pronounced effect on flow within the ejector as demonstrated by the large changes in wall pressure distribution in figure 1. It was concluded from these results that differences in initial flow condition could be important when comparing nozzle data from different facilities and further that these effects may be responsible for a part of the difference seen in comparison of scale-model performance with the full-scale suppressor testing reported upon in volume X.

The following significant results are presented for static and forward speed operation of multitube suppressors and suppressor/ejectors.

- **Static Performance, Bare Suppressor**
Generalized multitube suppressor performance is shown in figure 2. Tube length (L_T/D_{eq}) is seen to strongly influence overall static performance. In addition the placement of tubes in a radial array produces large improvement in performance, particularly for short ($L_T/D_{eq} = 0.25$) tubes. These geometry changes were shown to control ventilation of the nozzle base which in turn was found to be the most important parameter governing static performance of multitube suppressors with a given number of tubes.

- **Performance Versus Noise Suppression**
A summary of noise suppression versus thrust loss relative to values for a reference R/C nozzle is presented in figure 3 using suppression values from volume 11. This comparison shows that highest ratios of suppression-to-thrust loss for a given number of tubes are achieved by the performance mechanism of improved base ventilation through increased tube length and/or use of radial tube arrays.
- **Ejector Effects**
Ejector effects on performance are to increase nozzle base drag while at the same time increasing overall thrust through mixing of ambient air with primary jets to increase overall mass flow and momentum at the ejector exit. Thrust augmentation increases with ejector area ratio when sufficient mixing length is available. Increases in the number of tubes reduce the effective jet diameter and thus the required ejector length to satisfy the mixing length requirement. An adequate ejector-inlet area is shown to be a critical requirement for efficient ejector operation and performance. The general performance trend with changing inlet area is illustrated in figure 4. Too small an inlet causes flow choking that starves the ejector and severely penalizes performance.
- **Forward Speed Effects**
The low-speed flight effect on suppressor/ejectors is to reduce performance in proportion to ejector secondary air handling and the resulting ram drag penalty. This effect can be related to changes in ejector-lip suction force.

Figure 5 shows the effect of ejector length on lapse rate for a 37-tube nozzle with a 3.7 AR ejector. Although the static performance is much lower for the short $L/D = 1$ ejector, the lapse rate is also lower than that when $L/D = 3$. Integration of measured pressure distributions over the nozzle/ejector surface provides the component forces summarized in figure 6. Changes in ejector-lip suction are shown in the example to be the dominant factor accounting for the difference in lapse rate.

In the example, the ejector is sufficiently large in diameter that the jets do not impinge upon the ejector lip, and therefore the ejector-lip force at static ambient conditions can only be attributed to induced secondary flow into the ejector. The effect of forward velocity is to reduce ejector inlet recovery and thus the secondary air handling. This in turn is reflected by the decreasing lip-suction forces with forward velocity shown in figure 6.

A corollary to the above is that lapse rate is nearly independent of primary nozzle performance. This is demonstrated in figure 7 which shows lapse rates for two different nozzles, each tested with the same ejector. The similar lapse rates exhibited by the two ejector/nozzle configurations imply similar air handling even though the performance levels are much different.

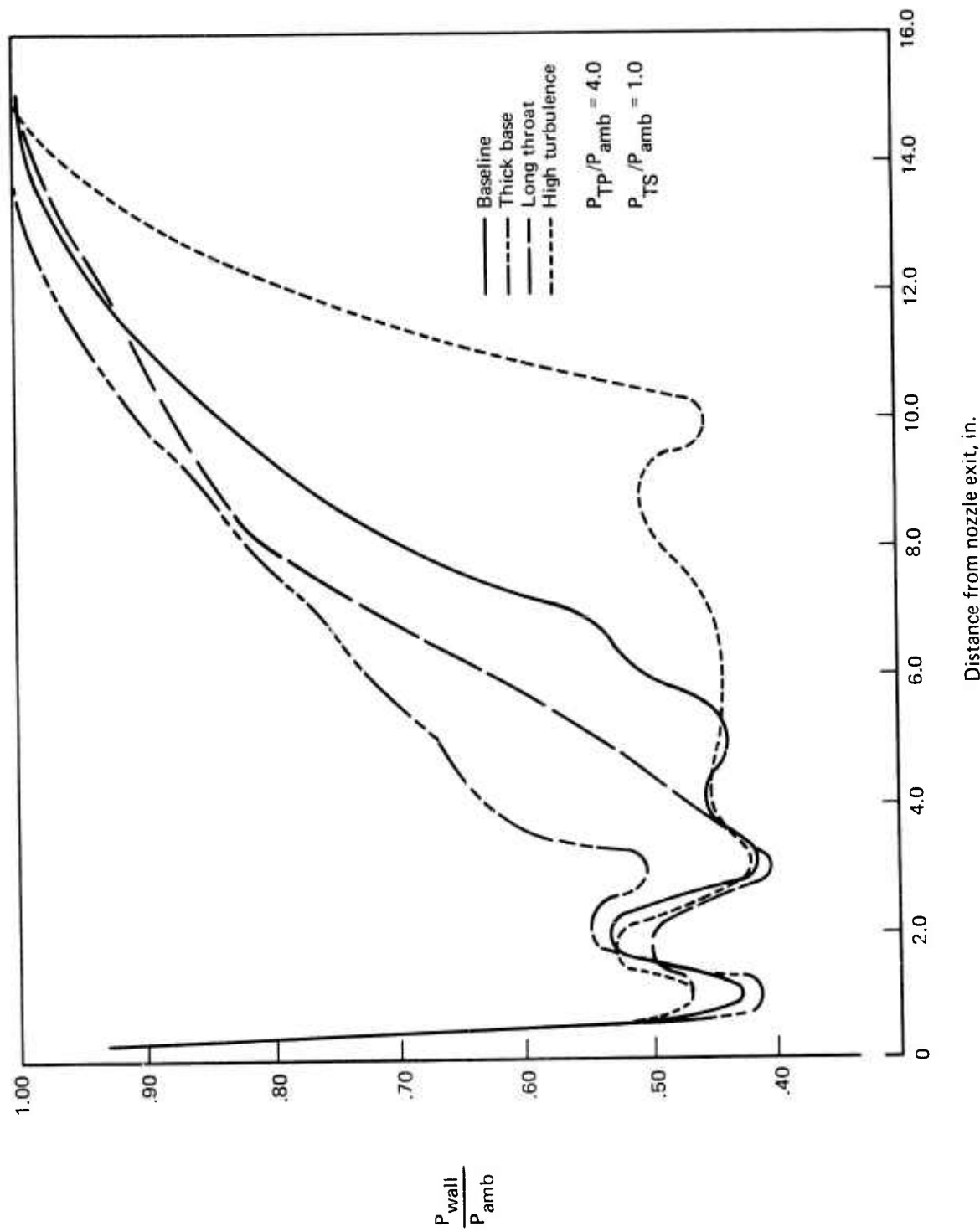
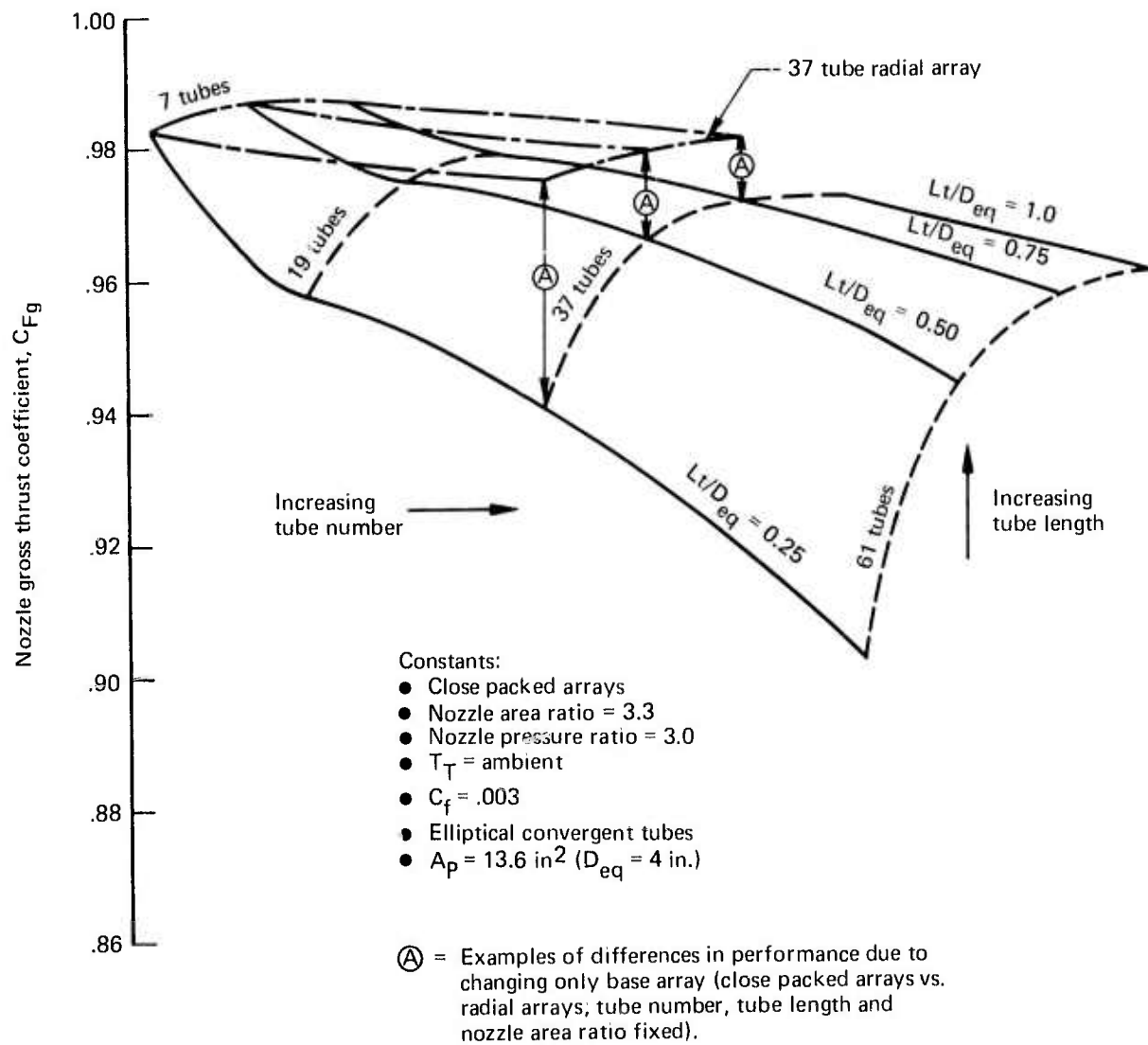


Figure 1.—Wall Static Pressure Distribution



$$\text{Area ratio} = \frac{\pi R_b^2}{A}$$

$$L_T/D_{eq} = L_T / \sqrt{\frac{4A}{\pi}}$$

Figure 2.—Summary of Bare Suppressor Performance

Typical error band
Acoustic ± 1 PNdB
Propulsion $\pm 0.25\%$

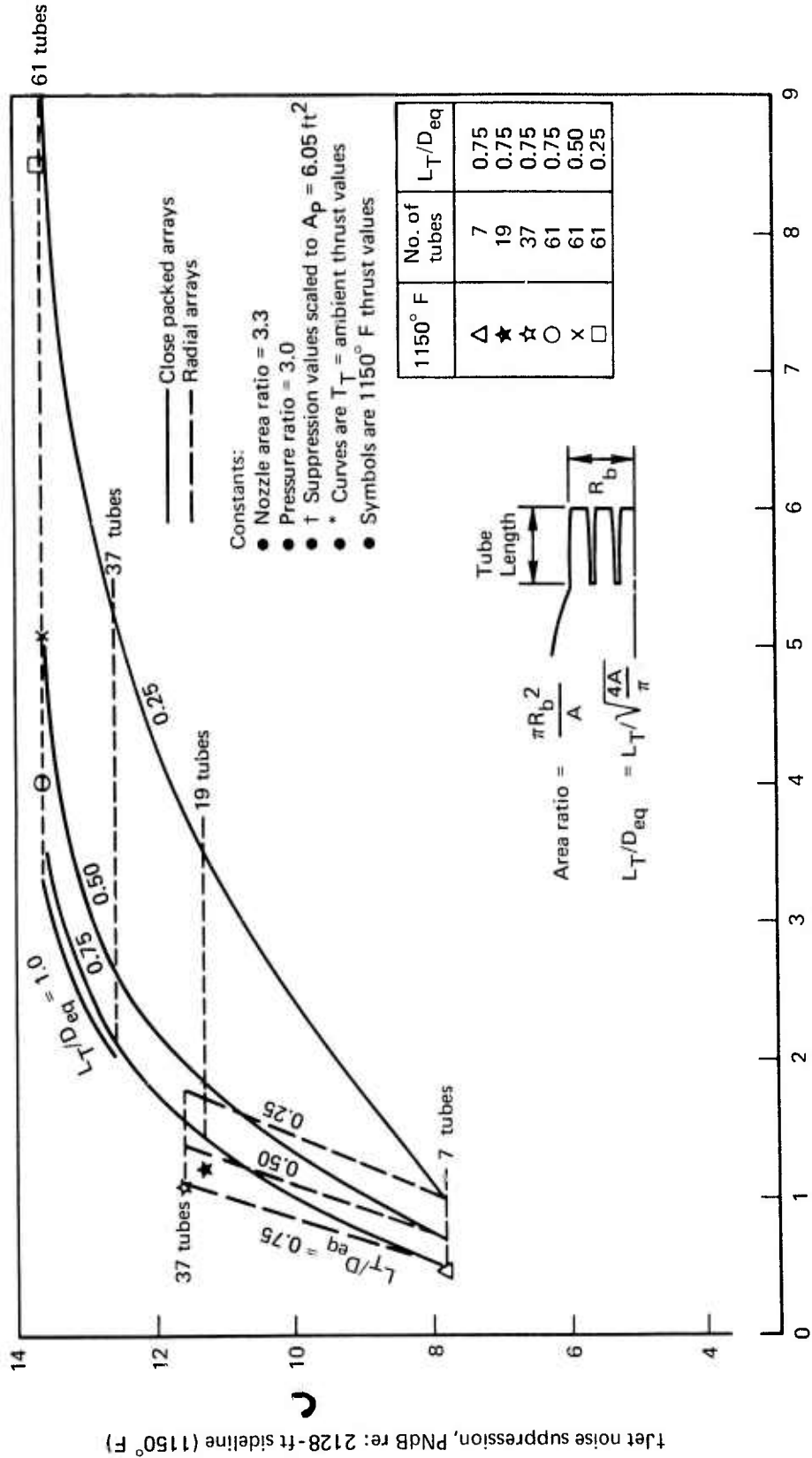


Figure 3.--Summary of Suppression Versus Thrust Loss, Nozzle Area Ratio = 3.3

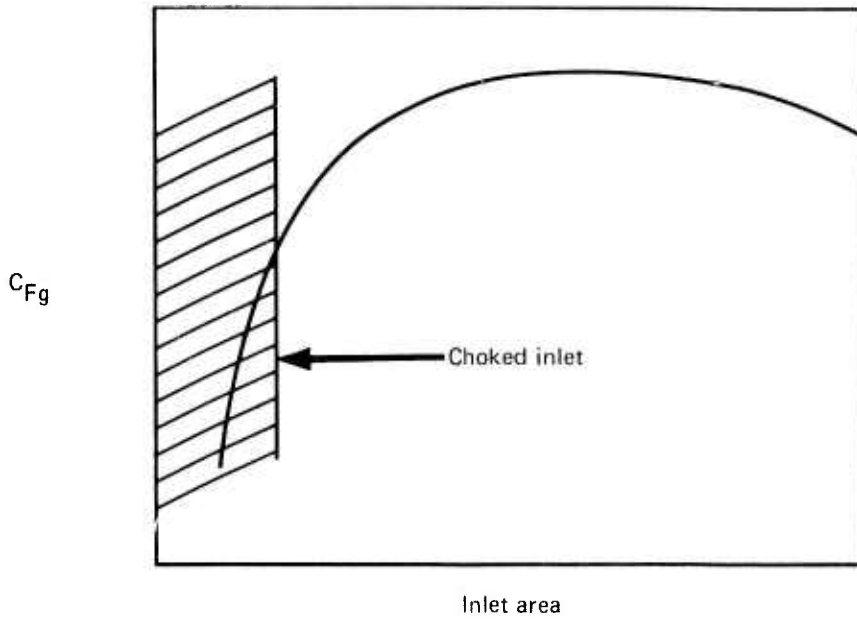


Figure 4.—Ejector Performance Trend

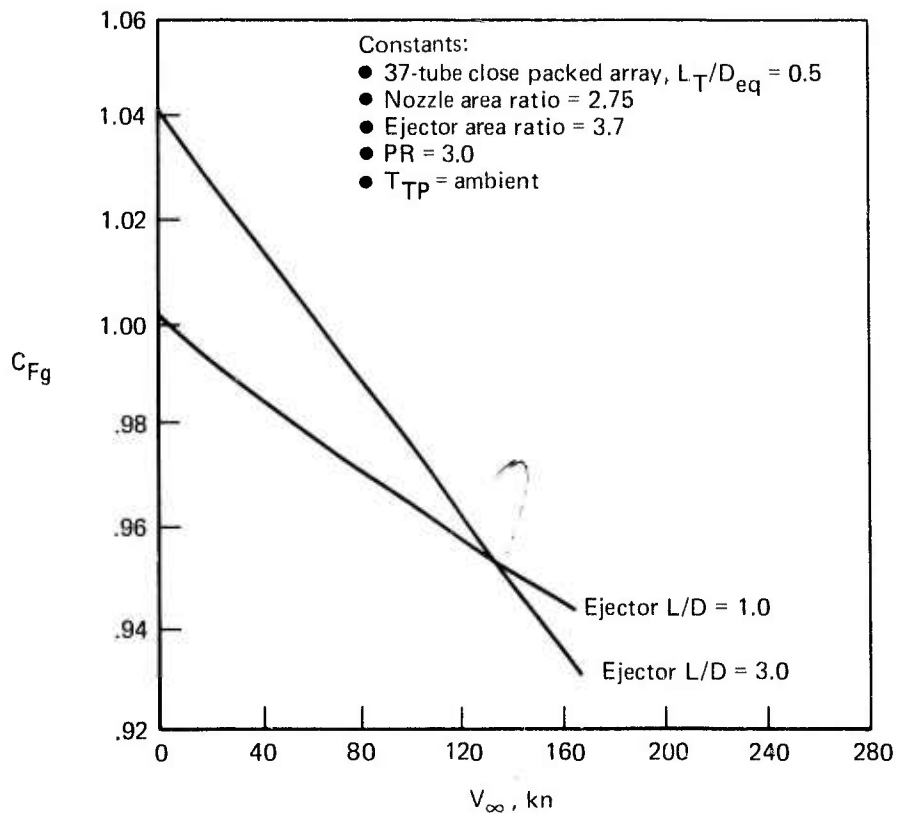


Figure 5.—Effect of Ejector Length on Performance at Forward Velocity

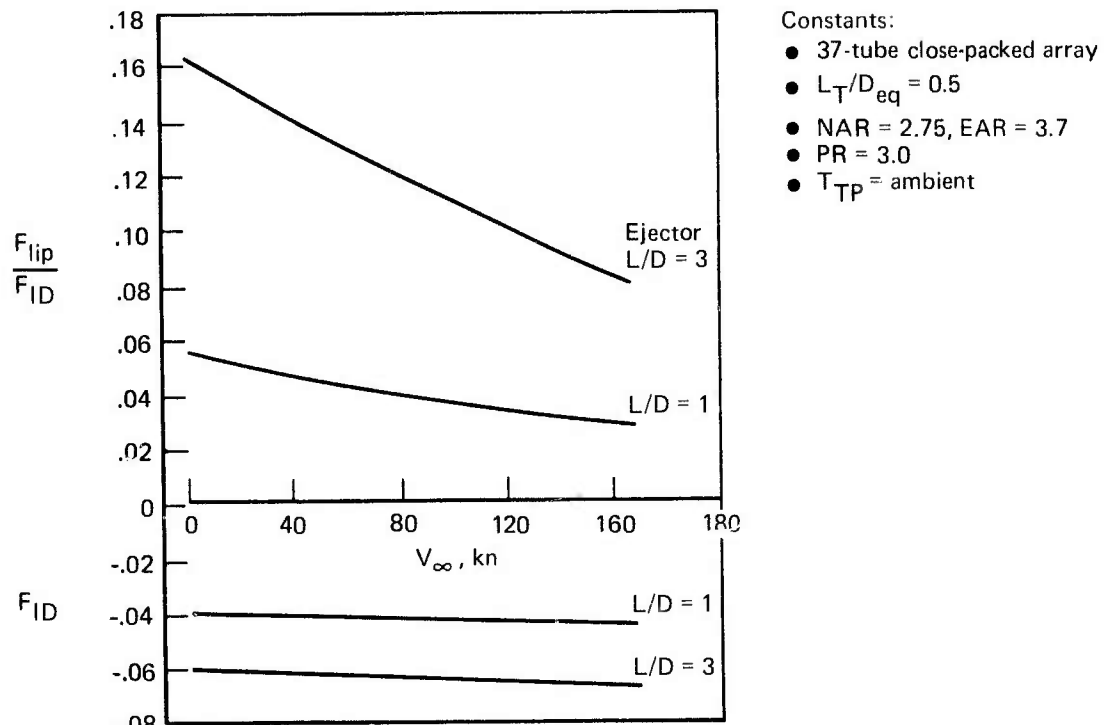


Figure 6.—Suppressor/Ejector Component Forces at Forward Velocity

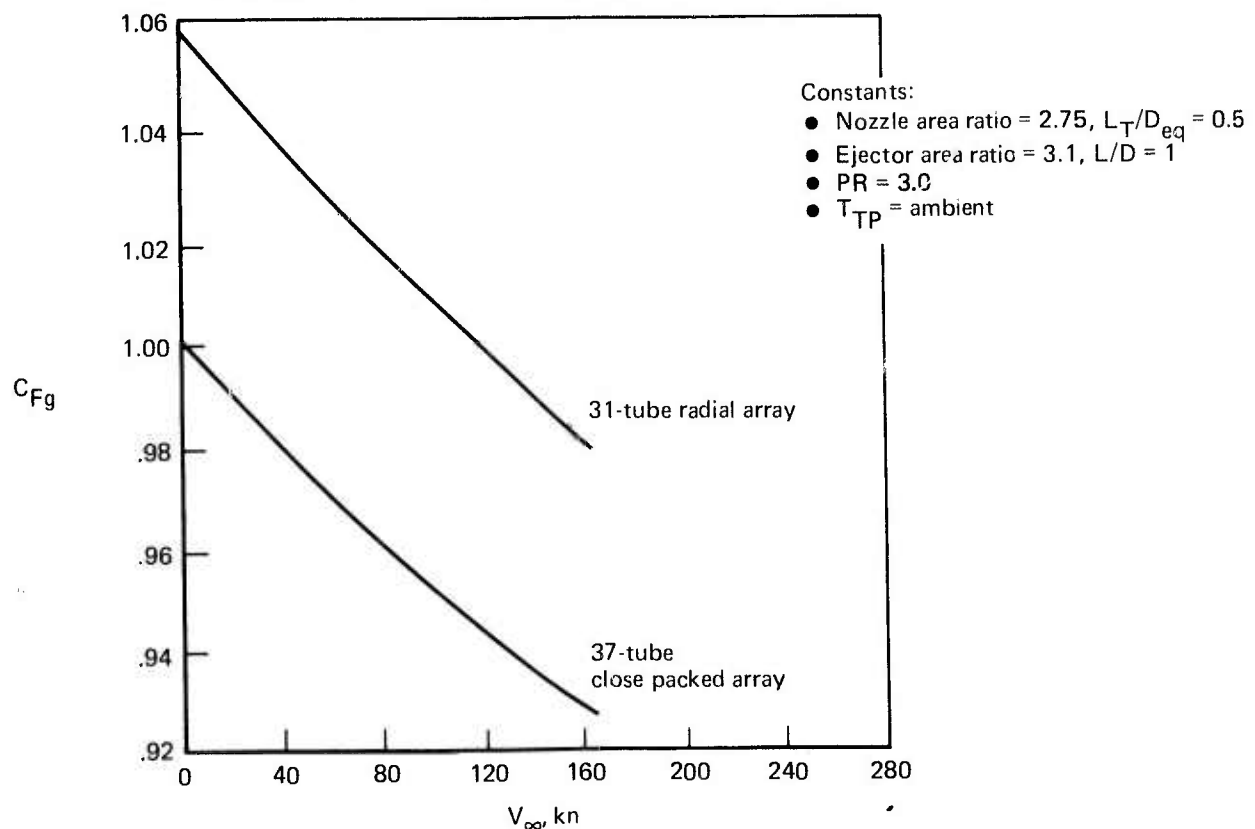


Figure 7.—Effect of Tube Array on Performance With Velocity

1.0 INTRODUCTION

Supersonic cruise necessitates the use of engines with a high thrust-to-frontal area ratio and high-exhaust jet velocities. The noise associated with the high-velocity jet can be substantially reduced by placing hardware into the primary exhaust flow to break the jet into small elements. The extreme sensitivity of the supersonic aircraft mission to nozzle performance during supersonic cruise dictates that the suppressor hardware, with its inherent thrust loss, be retracted from the jet during cruise. SST technology (ref. 1) demonstrated high suppression levels, using multitube-nozzle concepts, that could be integrated into a high cruise performance exhaust system (fig. 8).

Previous test data (ref. 2) have shown that the performance of multitube-suppressor nozzles is strongly influenced by the lower-than-ambient pressure acting on the base area between elements. The reduced pressure is the result of air entrainment by each of the discrete primary jets and is dependent upon the ability to provide sufficient ambient ventilating air to replace that entrained by the primary jets. The tube length and arrangement of the jet elements were shown to have a large effect on performance due to changes in base ventilation and thus base drag.

The addition of an ejector as is currently envisioned for an SST exhaust system also influences the suppressor base drag and presents the further requirement for properly matching suppressor and ejector hardware for best performance and noise qualities.

The effects of initial flow characteristics (velocity profiles, turbulence levels, initial base thickness) on the performance of ejectors have often been ignored in test planning. Because these quantities can affect the mixing process inside the ejector they might also have a significant effect on the overall ejector performance. Finally, the adverse effect of forward velocity on the suppressor/ejector performance has been demonstrated (ref. 2) to be large and is therefore an important consideration in establishing performance-design criteria.

This report summarizes the results of a multiphase experimental program aimed at providing a definitive guide for the design of high-performance multitube-suppressor ejector nozzles. This program was conducted with the same hardware and concurrent with the acoustic technology development program summarized in volume II.

The performance technology program was conducted in five phases and is reported upon in detail in volumes V through IX. The program will be summarized in this report in the following sections.

Section 3.0—Ejector Mixing Study (vol. V)

Experiments using a two-dimensional ejector test setup to investigate the effects of initial jet flow conditions on mixing and ejector performance.

Section 4.0—Reference Nozzles (vol. VI)

The establishment of performance levels of reference conical and suppressor ejector configurations and detailed studies of axisymmetric ejector flow and performance characteristics.

Section 5.0—Multitube Nozzle/Ejector Study

A three-part experimental program which investigates detailed performance mechanisms for a wide range of multitube suppressor/ejector geometry, jet conditions, and the effect of forward speed. This study constituted a major part of the propulsion technology effort and was conducted in three separate test programs:

5.1 Bare Suppressor (vol. VII)

5.2 Suppressor/Ejector (vol. VIII)

5.3 Low-Speed Performance (vol. IX)

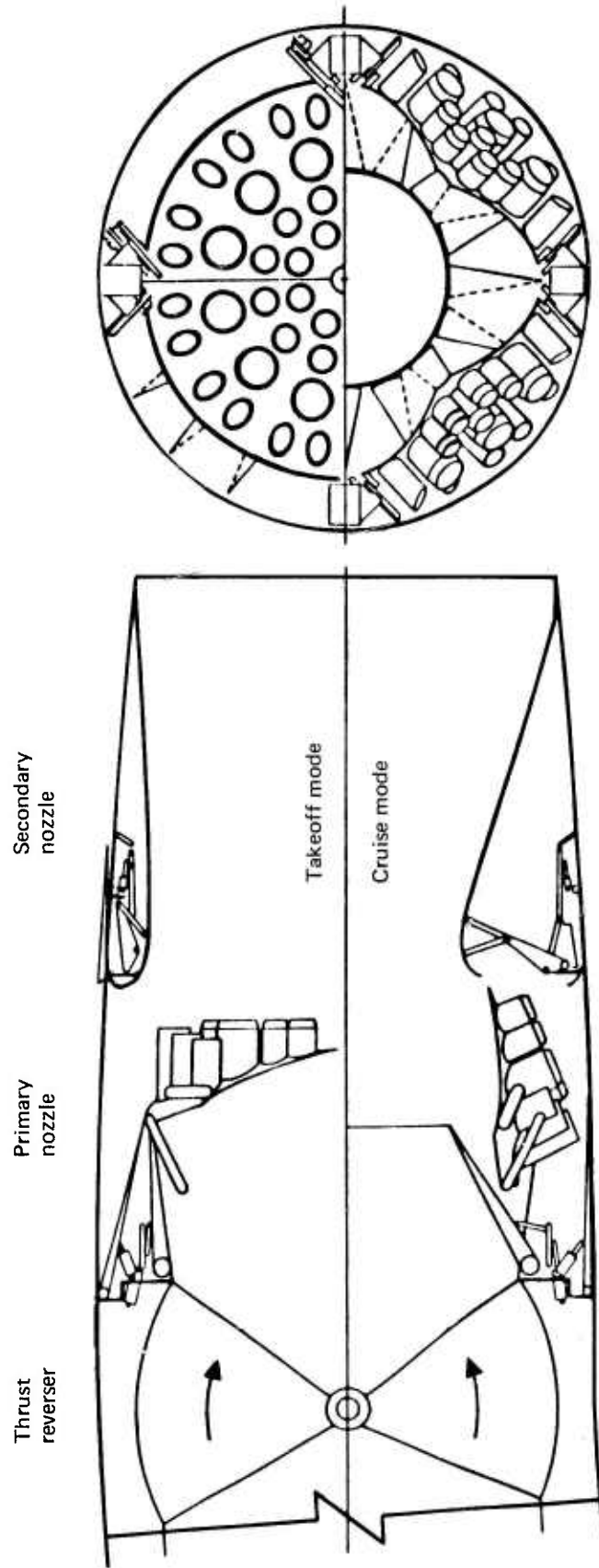


Figure 8.—Application of a Stowable Suppressor to an Advanced SST Exhaust System

2.0 TEST FACILITIES

2.1 HIGH RATIO RIG

A two-flow exhaust nozzle static performance test facility (fig. 9) was used in conducting the two-dimensional ejector mixing study described in section 3.0. This single-axis thrust rig is located at North Boeing Field, Seattle. The rig utilizes two independent air supply systems for primary and secondary flows and a strain gage load cell for reactive axial thrust measurements. Airflow rates are measured by use of critical-flow venturi meters. Static thrust testing of models up to 15 in² of primary flow area can be accommodated at nozzle pressure ratios from 1.5 to 4.0.

2.2 HOT NOZZLE FACILITY

The reference nozzles and multitube suppressor ejectors discussed in sections 4.0 and 5.0 respectively were tested for static performance on the hot nozzle test facility, North Boeing Field, Seattle. A variable-slot burner is used to obtain hot jet flow at temperatures to 1500° F. Ambient or hot flow is available at nozzle pressure ratios from 1.5 to 4.0. Flow rate is measured using a critical-flow venturi meter. Thrust is measured with a strain gage load cell providing 1/4% of full-scale accuracy over a 1000-lb range. Figure 10 shows a 6-in. reference nozzle installed on the test rig.

2.3 LOW-SPEED WIND TUNNEL

Forward velocity performance testing (sec. 5.4) was conducted in the Boeing Propulsion/Noise Laboratory low-speed wind tunnel. The facility, shown in figure 11, is an open circuit tunnel with a 9- by 9-ft test section. Driven by a gas generator and variable-pitch propeller, the tunnel velocity can be varied from 30 to 168 kn.

Suppressor configurations are installed on a strut-mounted forebody as shown in figure 11. The dual-flow forebody, enclosing a variable-slot burner, is mounted on a six-component force balance located beneath the tunnel floor. The suppressor's airflow rate is measured with an ASME long radius flow nozzle. Boundary layer suction is used forward of test models on the forebody to provide a nozzle external flow field representative of an SST nacelle installation. Test ejectors are mounted on balance using a separate strut that extends below the tunnel floor to the thrust balance.

Aerodynamic forces on the ejector strut and forebody are removed from the force data as a tare.

PRECEDING PAGE BLANK NOT FILMED

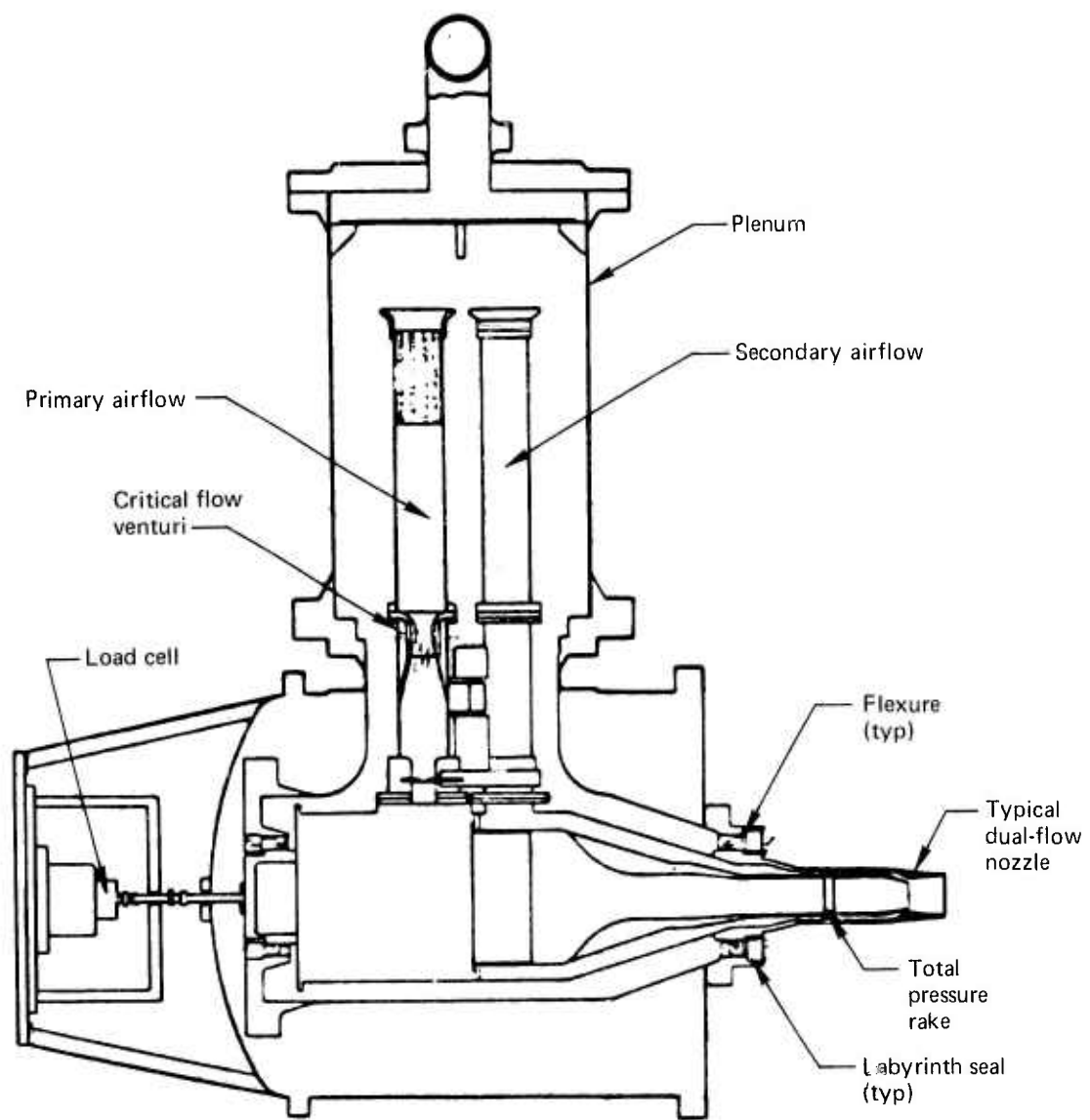


Figure 9.—High-Ratio Rig

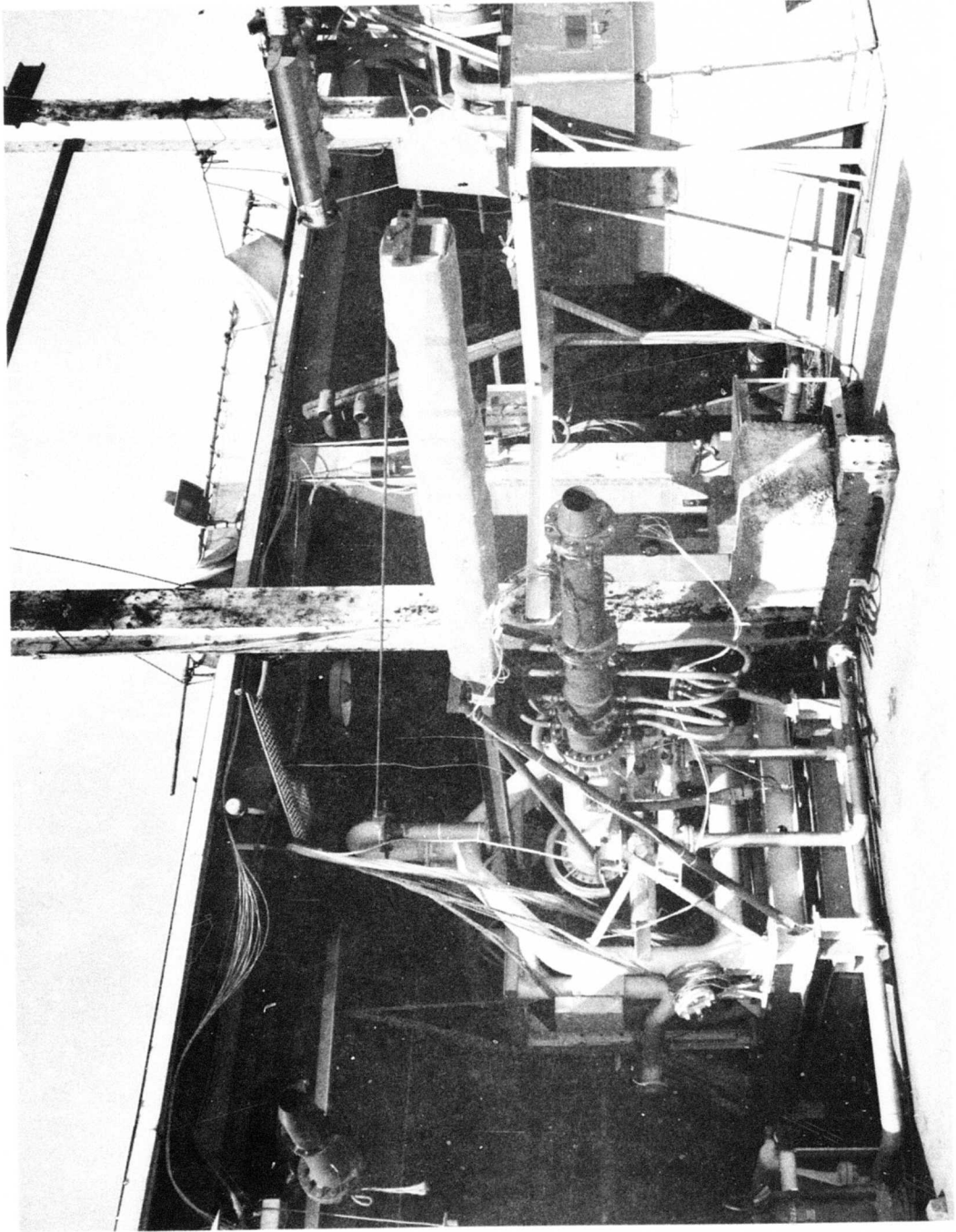


Figure 10.—Hot Nozzle Rig

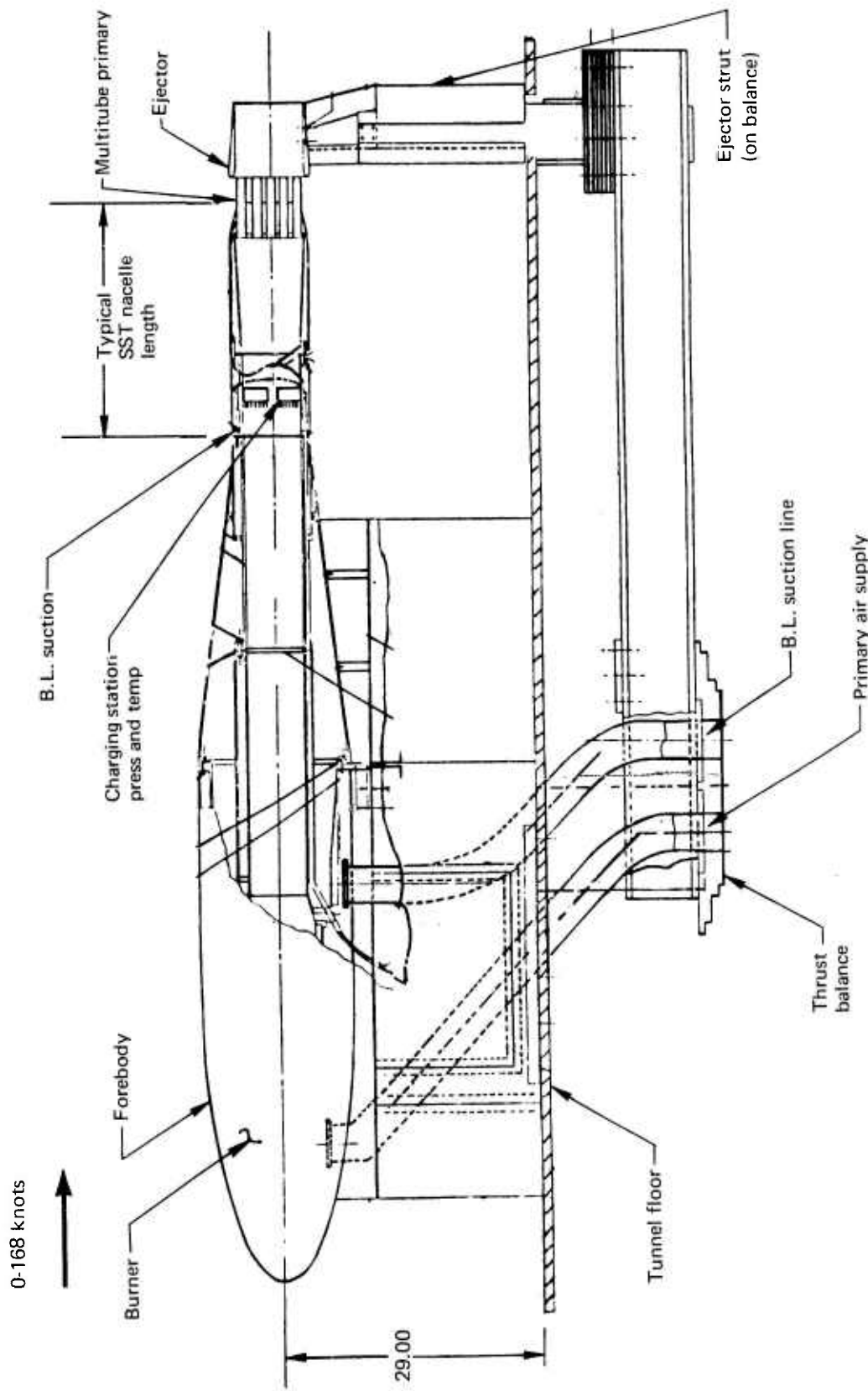


Figure 11.—Test Installation, 9-by 9-ft Wind Tunnel

3.0 EJECTOR MIXING STUDY

A two-dimensional ejector test setup was used to investigate the effects of initial jet flow conditions on mixing and ejector performance.

3.1 TEST PROGRAM DESCRIPTION

A critical concern in the design of multielement suppressor/ejector systems is maintaining acceptable performance while satisfying the acoustic criterion of rapidly mixing the jets with ambient air. Experiments were undertaken to determine the influence of the initial jet conditions on mixing in an ejector and the resulting performance. The tests were designed to study the effects of the base thickness between the jets and the induced secondary air, the jet-flow profile, and the turbulence level.

An ejector apparatus was fabricated for use on the Boeing high-ratio rig which consisted of an array of slot nozzles exhausting to a mixing section of rectangular cross section. Two opposite sides of the mixing section were of clear plastic to permit spark shadowgraph photos to be taken of the mixing flow. Both primary and secondary flows were metered and both entered the mixing section through the nozzle assembly as substantially uniform and parallel flows.

A schematic of this 2-D test ejector apparatus is shown in figure 12. The photo in figure 13 shows a typical test installation where the assembly mounted on top of the mixing section is a motor-driven pitot-static traversing probe. Static-pressure wall taps can be seen along the clear plastic sidewall of the mixing section. The entire assembly was mounted on the rig force balance system so that measured thrust performance could be obtained. Figure 14 is a schematic showing primary and secondary flow paths and illustrating the method used to measure mixing-flow profiles. The traverse probe assembly was mounted to a sliding plate which formed the upper wall of the mixing chamber. The probe could be positioned at any arbitrary station along the chamber thus allowing for detailed investigation of the flow field. A pressure seal was provided to avoid leakage along the sliding plate and at the probe blade attachment.

Base thickness was varied from 0.062 in. to 0.01 in. by chamfering the plates separating primary and secondary streams. This produced a range of base-area to primary-flow area ratios of 0.25 and 0.039, respectively. A low-angle (7° max) chamfer was employed on the low-velocity secondary side of the plates to minimize alteration of secondary flow while leaving the primary throat unchanged. The velocity-profile variation was accomplished by lengthening the nozzle throat by 12 nozzle heights using a 6-in.-long constant-area adapter section, thus producing a larger initial boundary layer thickness. Turbulence intensity was varied from a baseline u'/U value of approximately 2% to a value of 8% by insertion of upstream blockages into the primary flow. A nominal $u'/U = 0.04$ was determined for the secondary flow. Hot wire anemometer techniques were used to determine these values. Due to the hot wire strength limitations these measurements were made at a nozzle flow velocity of 300 fps. All other testing was conducted at ambient primary and secondary flow conditions over a range of primary pressure ratios from 2 to 4. The pressure of the secondary flow entering the mixing section was maintained equal to ambient.

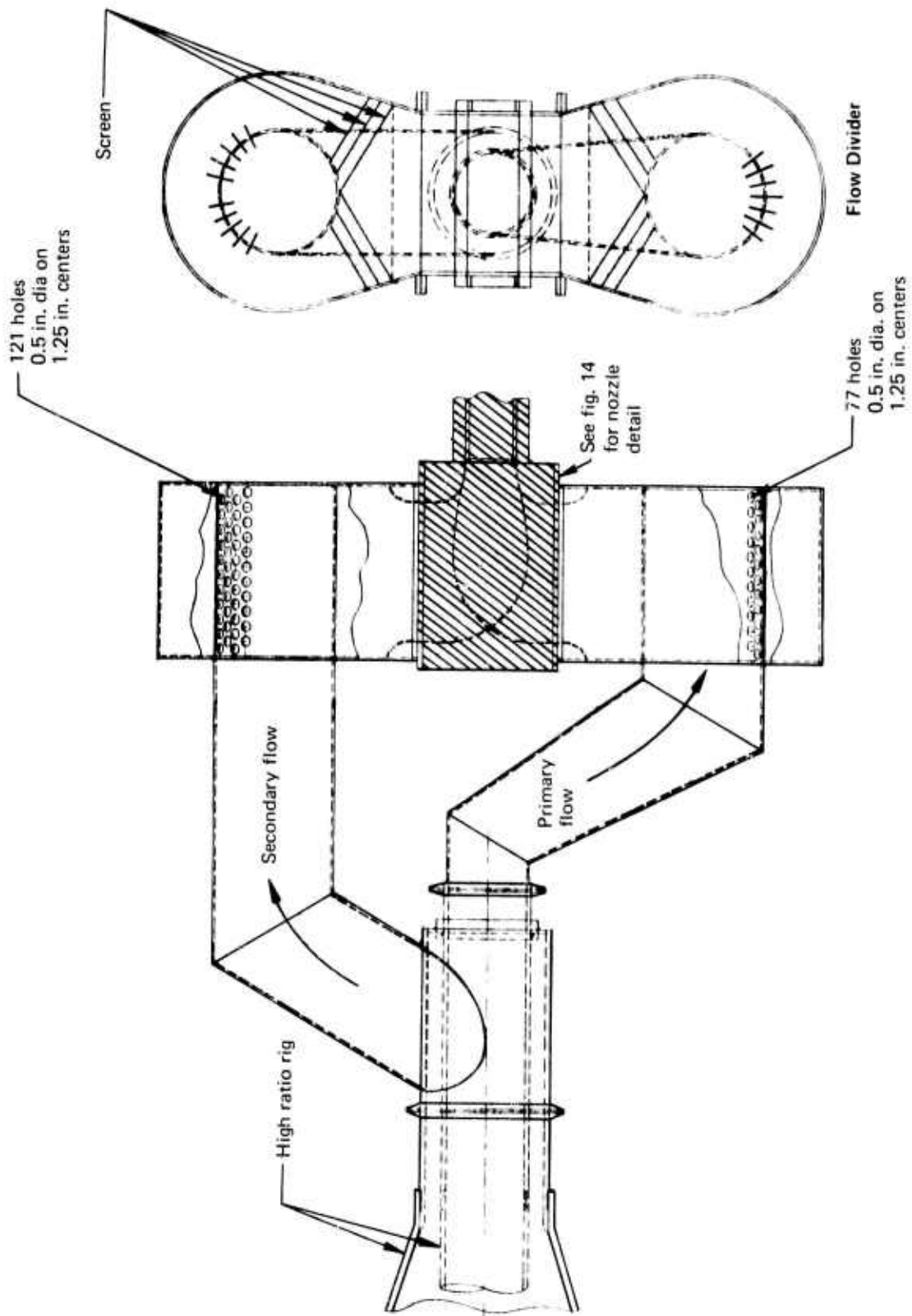


Figure 12. —Schematic of 2-D Ejector Test Apparatus

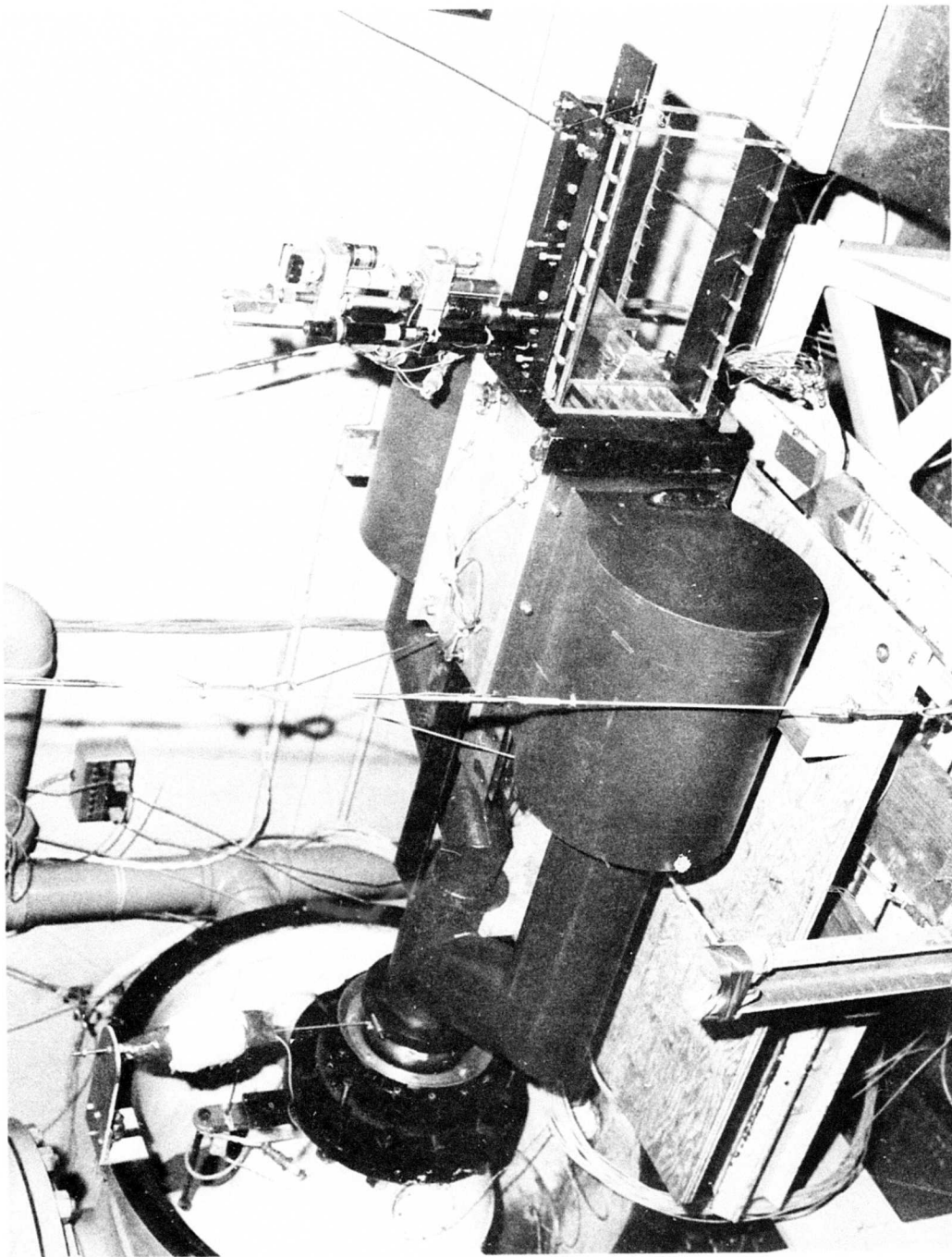


Figure 13. - Test Installation

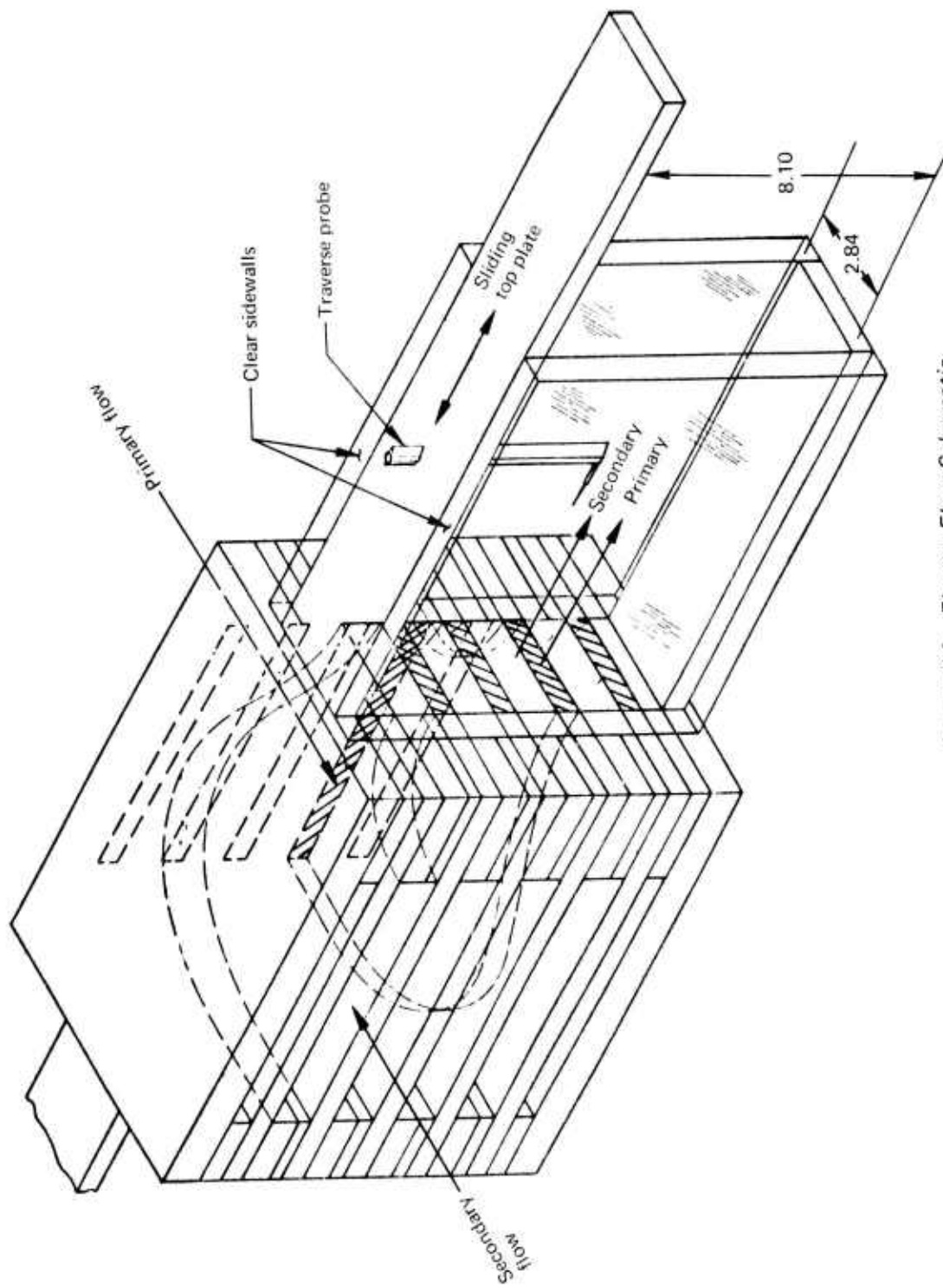


Figure 14. - Ejector Flow Schematic

3.2 SUMMARY OF RESULTS

3.2.1 PRESSURE RATIO EFFECTS ON FLOW FIELD

Spark shadowgraphs of the flow in the baseline ejector are presented in figure 15 at various primary pressure ratios. The photographs show an area including the nozzle exit illuminated by a 6-in.-diameter collimated flash. Two photographs at identical test conditions are joined to show the flow to the end of the ejector. The flow direction is from left to right and the upper three primary jets are visible. At pressure ratio 2.5 the primary flow is seen to exhibit typical characteristics of an underdeveloped free-jet exhaust from a sonic nozzle where a system of repeating but weakening normal shocks occurs. The secondary flow is shock-free and subsonic throughout. The turbulent mixing zone can be clearly seen along the jet boundaries.

At pressure ratio 3.0 the secondary flow has become sonic a short distance downstream of the nozzle exit. Farther downstream, a normal shock occurs and the resulting pressure rise is transmitted into the primary flow as an oblique shock which finally terminates in a normal shock in the primary stream. The secondary flow appears to remain subsonic beyond the first normal shock.

At still higher pressure ratios, the shocks in the secondary streams produce weak oblique shocks in the primary streams which repeat themselves farther downstream in the same manner as the more familiar repeated system of normal shocks in an underdeveloped free jet. The shock structure visibly carries through the secondary flow downstream of the first normal shock in the secondary. Apparently the mechanism for the reacceleration of the secondary flow to sonic velocities is the growth of the mixing layers. The network of weak oblique shocks in the primary stream gives way to what appears to be a normal shock farther downstream, after which the flow appears chaotic. This final normal shock is related to the beginning of the static pressure rise to ambient required of an ejector operating with subsonic flow at the exit.

3.2.2 THRUST AND FLOW AUGMENTATION

The effect of the three variable changes on weight flow augmentation can be seen in figure 16. The effect of the thick base was to reduce weight-flow ratio at the lower pressure ratios, while the long throat nozzle increased the weight-flow ratio at the higher pressure ratios. The increase in primary turbulence resulted in a slight decrease throughout the range tested.

The changes due to variations in base thickness and velocity profile (throat length) can be explained by considering the two flows before appreciable mixing has taken place. Two modes of ejector operations are possible; in the first the secondary is entirely subsonic and the minimum flow area is the geometric secondary area ($A_{\text{mixed}} - A_{\text{primary}} - A_{\text{base}}$). The second is marked by supersonic flow in the secondary with the minimum secondary area determined by the size of the expanded primary jet. The increase of the base area has the effect of decreasing the minimum geometric secondary area. In the operating mode where the minimum geometric secondary area determines the secondary weight flow (in this case

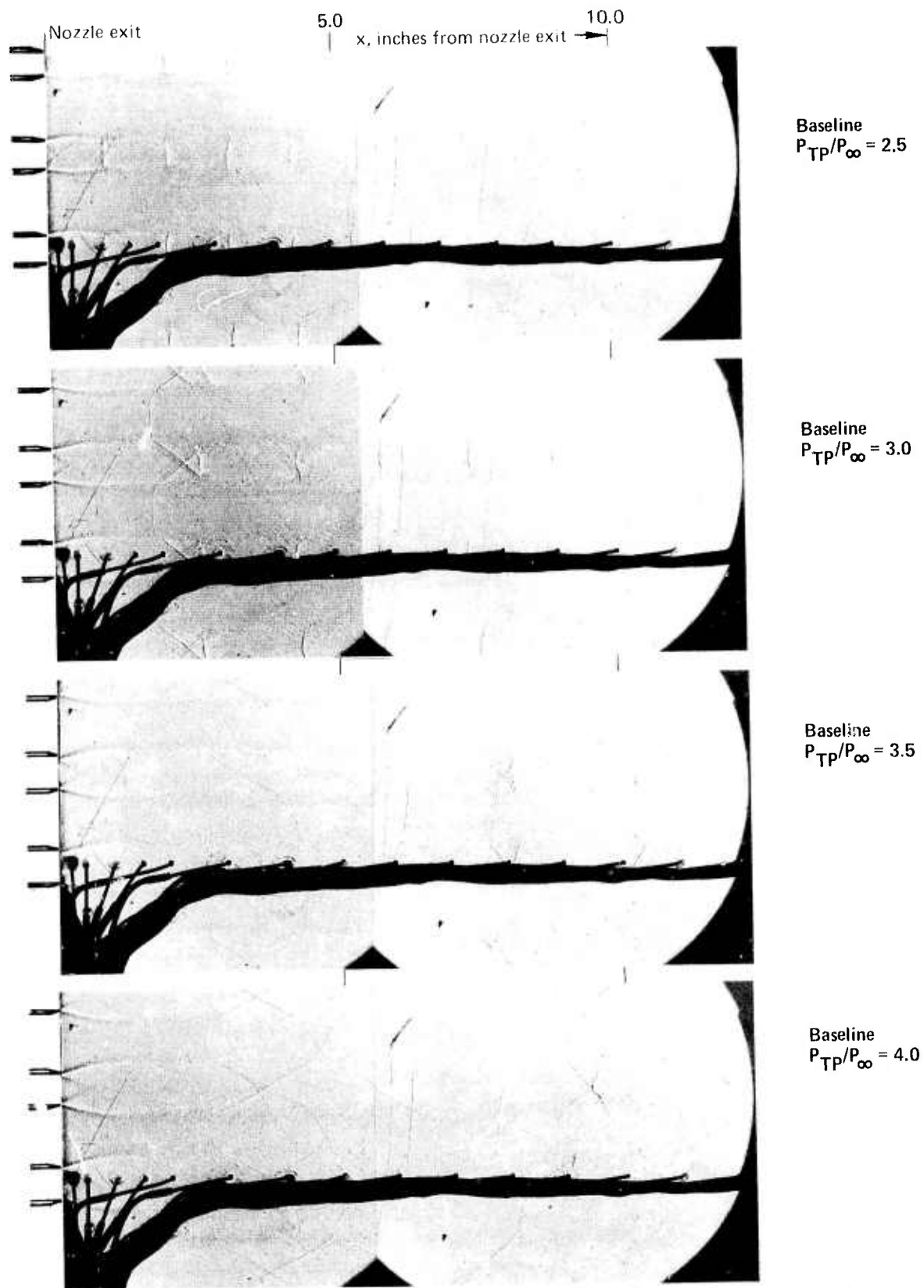


Figure 15.—Change in Ejector Flow Field With Primary Pressure Ratio

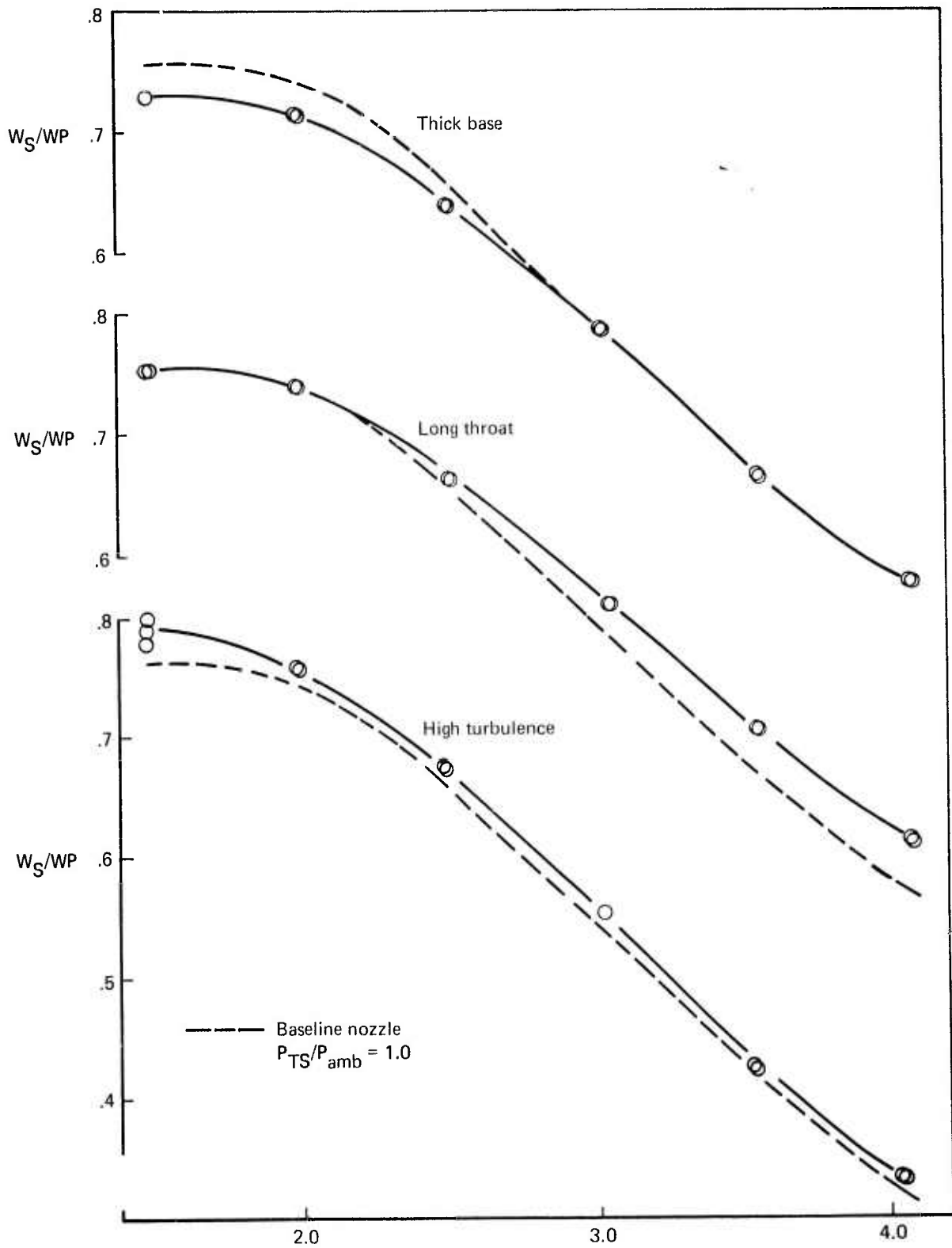


Figure 16.—Effect of Variable Changes on Weight Flow Ratio

$P_T/P_{amb} < 3.0$) the increased base area decreases the secondary weight flow. In the choked secondary operating mode, base area has little or no effect on weight flow augmentation.

The effect of the long throat (increased boundary layer thickness) is seen, on the other hand, in the secondary choked mode of operation. The total pressure loss produced by the long throat results in a lower effective nozzle pressure ratio, a smaller width of the primary nozzle jet, and a larger limiting area for the secondary flow. Thus the higher weight flow augmentation of the long throat nozzle is to be expected. The overall increase in weight flow augmentation for the case of the high primary turbulence cannot be explained in these terms since the explanation involves the mixing process itself.

The effect of the variable changes on thrust augmentation can be seen in figure 17. Both the thick base and the long throat configuration had a decrease in thrust augmentation ratio while high primary turbulence resulted in an increase. The decrease in augmentation ratio due to the thick base is the result of the increased drag of the larger nozzle-base area. The loss of augmentation ratio by the long throat nozzle can be partially explained by noting that the augmentation ratio is extremely sensitive to total pressure losses in the secondary flow. When the primary nozzle throat length was increased, the secondary was lengthened the same amount, resulting in an increased secondary total pressure loss. The gain in augmentation for the case of high primary turbulence again cannot be explained by available analysis.

3.2.3 EJECTOR WALL PRESSURE

Figure 1 is a comparison of ejector wall static pressure distribution as affected by the initial-flow condition changes for pressure ratio 4. At low pressure ratios (not shown here but discussed in volume V) trends were undistinguished with minimum pressure occurring near the nozzle exit followed by a continuous rise to ambient at the ejector exit.

At higher pressure ratios the trends were similar to those of figure 1. At this $PR = 4$ condition the static pressure remains relatively constant at a low level for some distance downstream. It then rises very steeply to ambient pressure at the exit. The axial location of this pressure rise is definitely affected by the initial condition of the primary flow. A high initial turbulence level permits the low ejector pressures to be maintained farther downstream than any other configuration. On the other hand, both the thick base and long throat version maintain this low pressure for only a short distance downstream.

The composite shadowgraphs of each configuration operating at a $PR = 4$ (fig. 18) bear out the belief that, in addition to the mixing process, a shock on the ejector sidewalls contributes to the sudden pressure rise observed. The location at which the sudden pressure rise occurs is marked on each shadowgraph. In each case this rise is about 2 in. upstream of the terminal shock in the primary jet, which follows the previously mentioned network of weak oblique shocks. It is believed that what appears to be a normal shock in the primary flow may be a Reimann-type shock wave near two intersecting oblique waves. The pressure rise at the wall, while sudden, is still smoothed out by the wall boundary layer so that it cannot be seen in the shadowgraph.

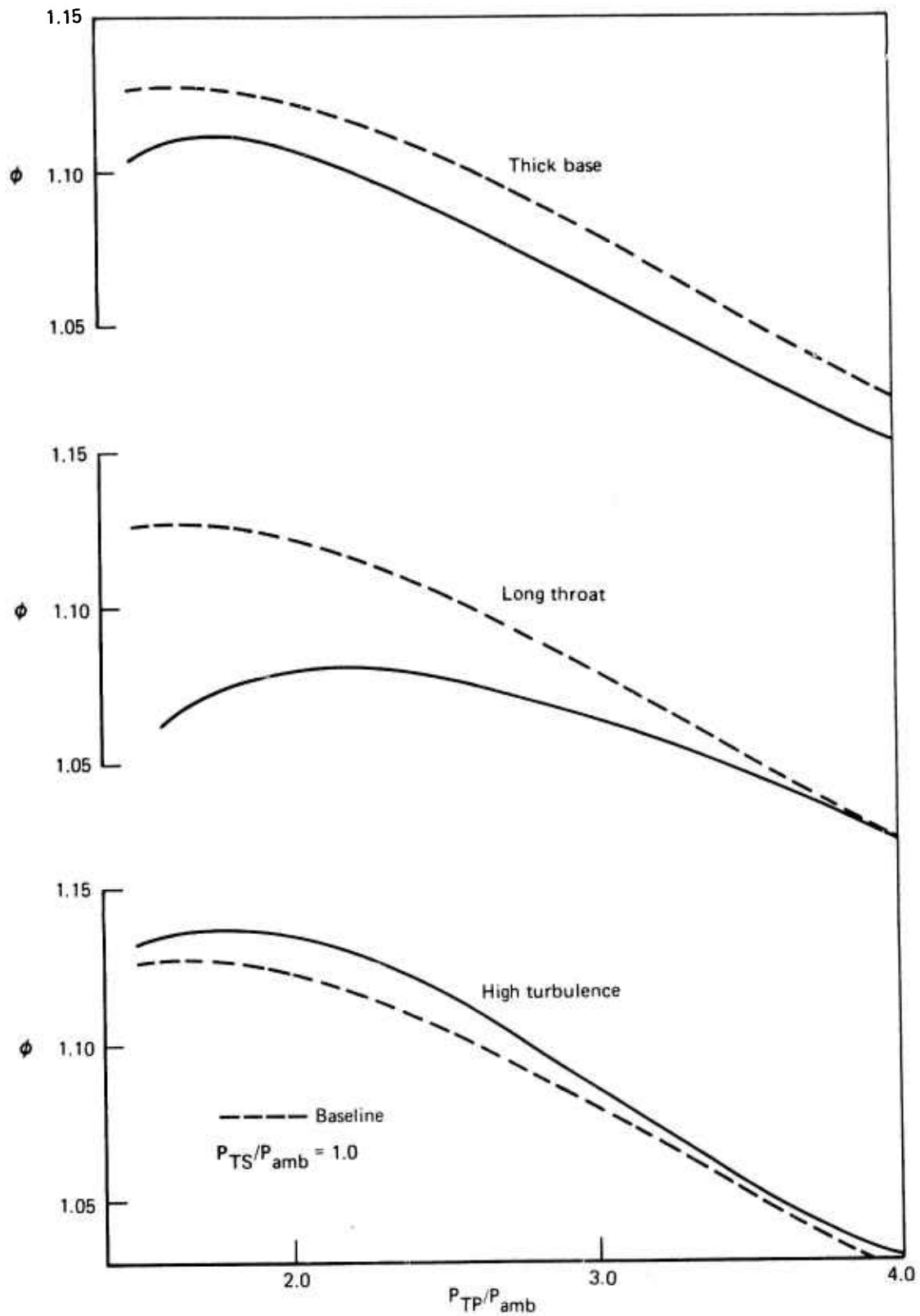


Figure 17.—Effect of Variable Changes on Thrust Augmentation Ratio, θ

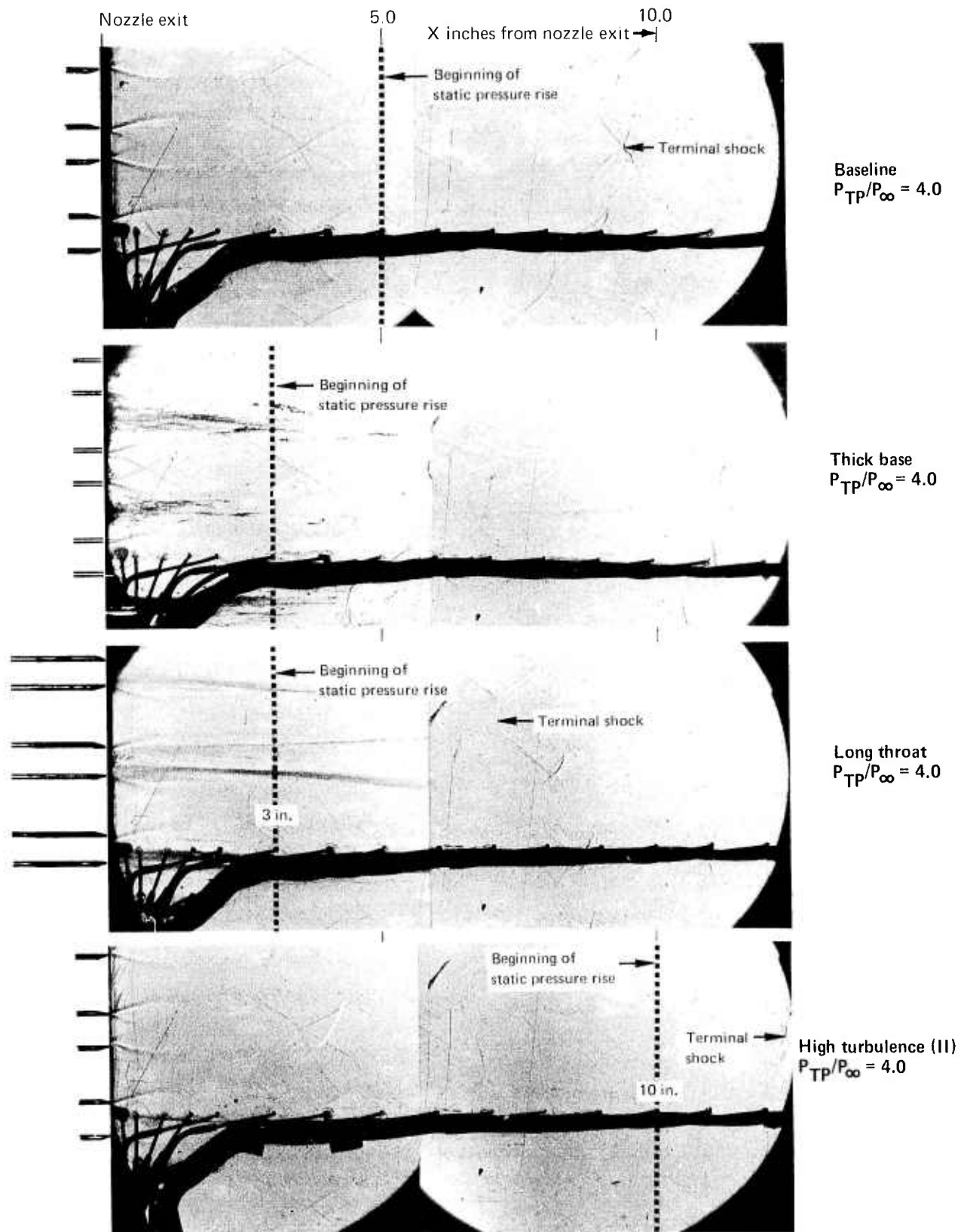


Figure 18.—Effect of Variable Changes on Ejector Flow Field

This final shock is a necessary recompression dividing the upstream supersonic ejector flow from the downstream subsonic one. If the back pressure of the ejector were lower, this recompression would occur either at the ejector exit or not at all, and the ejector would be operating completely supersonically.

It is believed that the pronounced effect of the initial conditions on the wall static pressure distribution at high pressure ratio is produced by an effect on the recompression shock location, not in the mixing process per se. Thus, the high turbulence level flow, for example, causes a more energized wall boundary layer and causes the shock to occur farther downstream. From a system performance point of view, however, the mechanism for mixing process change is not as important as the end result.

These experiments have shown that the initial jet conditions can grossly change the flow mixing process and overall performance. It is concluded that:

1. All three of the variables tested produced noticeable changes in thrust augmentation and pumping performance. Since these quantities may be different in the model-scale from full-scale nozzle system, this must be accounted for in the prediction of full-scale performance.
2. The effects of base thickness and throat length on performance are predictable with the proper one-dimensional flow analysis. Increased nozzle throat length reduced ejector performance. This effect is caused by increased secondary total pressure loss as well as the change in primary nozzle velocity profile. These effects were not clearly separated in this test.
3. Higher values of initial turbulence level in the primary produced large changes in the flow field as seen from shadowgraph and static pressure profiles. Slight increases in pumping and thrust performance also were seen. These effects are only explainable through detailed consideration of the mixing process and/or the ejector wall boundary layer.
4. The spark shadowgraph photographs of the baseline configuration in figure 15 indicate that for pressure ratios greater than 3.5 a nearly uniform primary flow exists with a shock structure composed of weak oblique shocks. This suggests that the flow region may be adequately modeled by analyses which neglect transverse pressure gradients.

4.0 REFERENCE NOZZLES

Testing is conducted to establish performance levels of reference conical and suppressor ejector configurations and details of axisymmetric ejector flow and performance characteristics.

4.1 TEST PROGRAM DESCRIPTION

A round convergent (R/C) reference nozzle was used during the DOT phase I program (ref. 2) and the NASA Lewis-sponsored testing of lined ejectors (ref. 3) to demonstrate the relative changes in performance and noise-suppression properties of different configurations. An additional reference nozzle is tested in this program in order to provide reference values of noise/performance characteristics that are more similar to those of suppressors being evaluated. A 37-tube nozzle (R/37) was designed and repeatedly tested along with the R/C nozzle for this purpose (fig. 19). These nozzles are also used in tests with various ejector configurations (fig. 20) to evaluate ejector effects on performance. Included in these studies are measurements of ejector secondary airflow and mixing profiles as functions of ejector geometry and jet pressure and temperature.

A large instrumented annular section with bellmouth entry was mounted as an extension to the normal test ejector inlet to provide for measurement of secondary flow. A typical test setup is shown in figure 21.

4.2 SUMMARY OF RESULTS

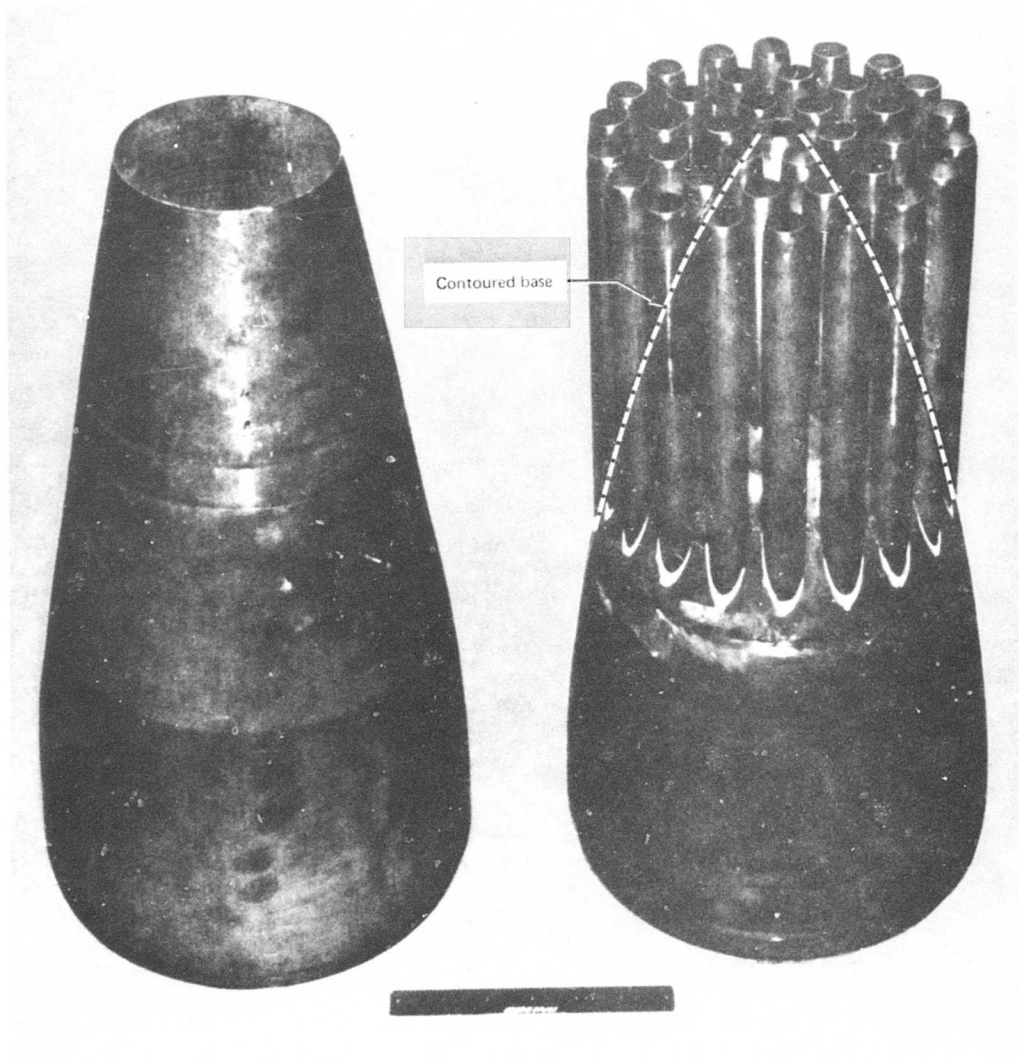
4.2.1 NOZZLE/EJECTOR PERFORMANCE

Measured baseline bare nozzle thrust performance for the two reference configurations is shown in figure 22. The predicted performance which agrees closely with measured values was derived from earlier semiempirical analysis.

Ejector studies were conducted with an $EAR = 3.7$ (ejector flow area divided by nozzle flow area). Ejector length-to-diameter ratios, $L/D = 3$ and 6 were used with the R/C and an $L/D = 1$ with the R/37. The $L/D = 6$ with R/C and $L/D = 1$ with R/37 each provided approximately 12 individual jet diameters to the ejector exit plane, thus providing equivalent mixing lengths.

Figure 23 demonstrates the similar thrust augmentation, C_{Fg} ejector/ C_{Fg} primary nozzle determined for these two configurations. Results are also shown for tests of the R/C with an $L/D = 3$ ejector. The lower performance is attributed to reduced secondary air handling because of insufficient mixing length.

The effects of jet temperature on ejector performance are demonstrated in figure 24 for the R/37 nozzle with $L/D = 1$ ejector. Shown are thrust performance and the induced body forces of nozzle base drag and ejector-entry lip suction expressed as percentages of ideal nozzle thrust. The body forces are derived from integration of measured surface pressures. The effect of increased jet temperature is shown to result in a large reduction in thrust



R/C Nozzle
Round convergent
Reference Nozzle

R/37
37-Tube Area Ratio 3.3
Close-Packed With
Round-Convergent Tubes

Figure 19.—R/C and R/37 Nozzles

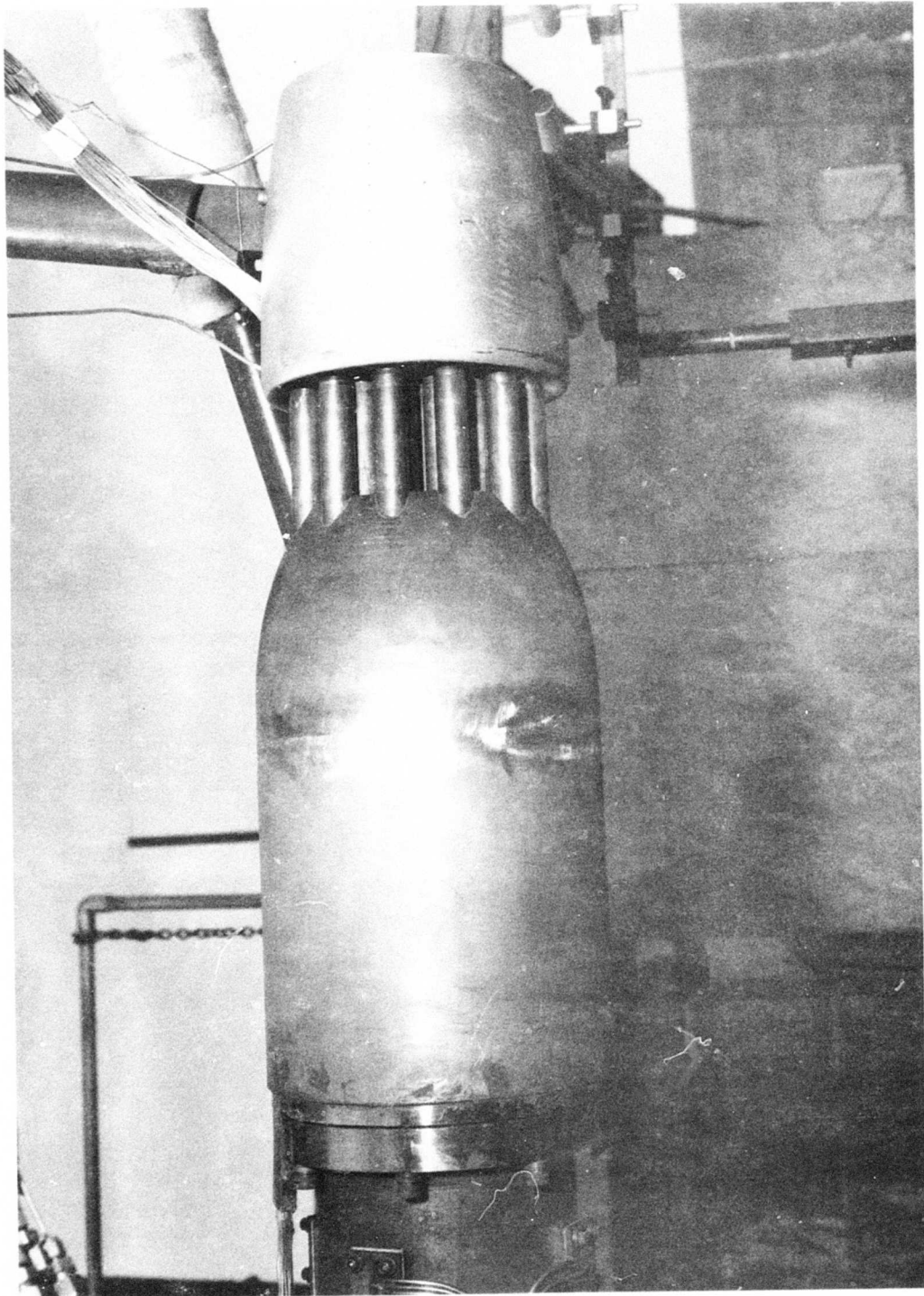


Figure 20.—R/37 Nozzle With 8-In. Ejector ($L/D = 1$) and Flight Lip Inlet

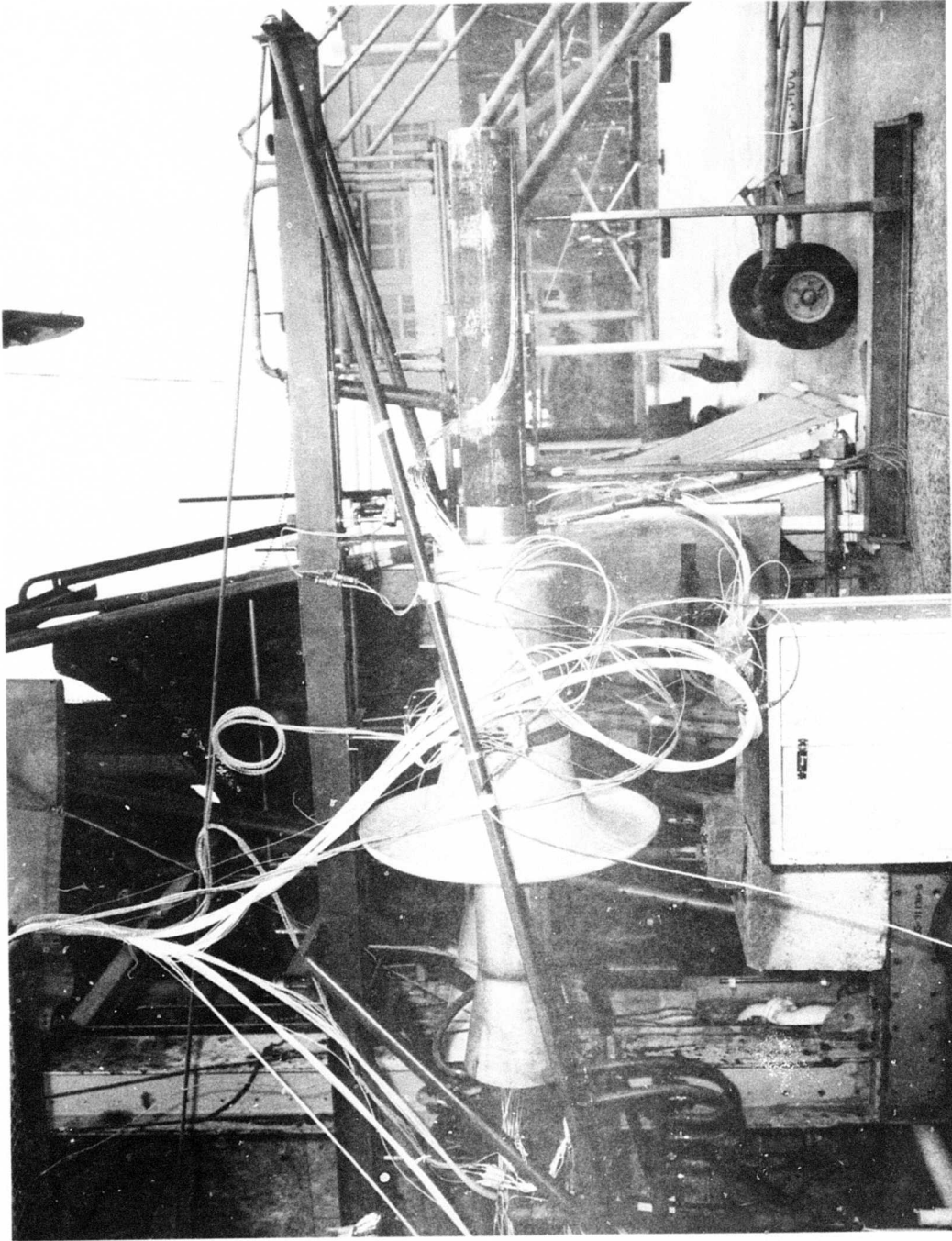


Figure 21.—Measurement of Secondary Weight Flow on Hot Nozzle Facility, R/C Nozzle With 48-In. Ejector ($L/D = 6$)

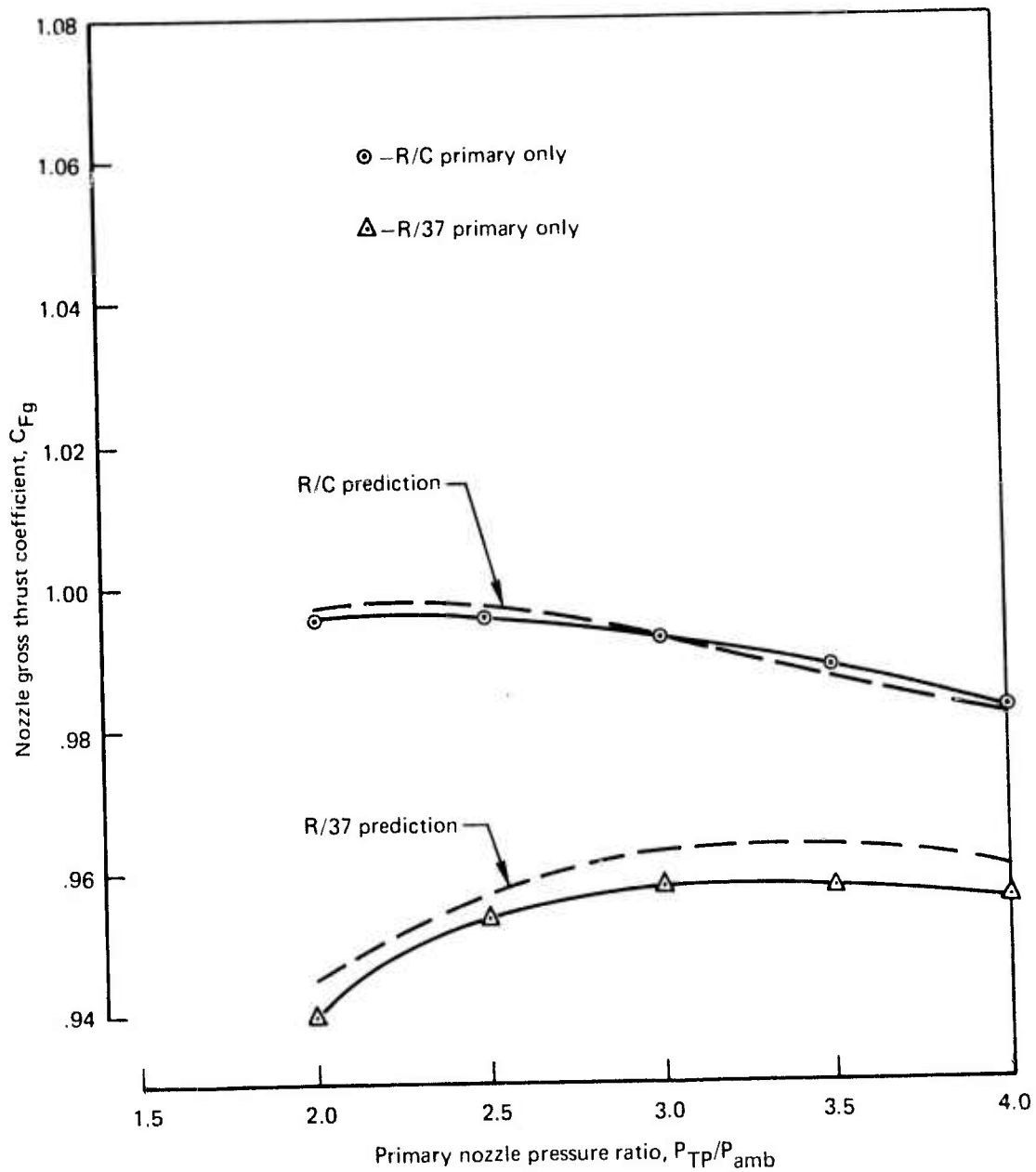


Figure 22.—Bare Nozzle Performance

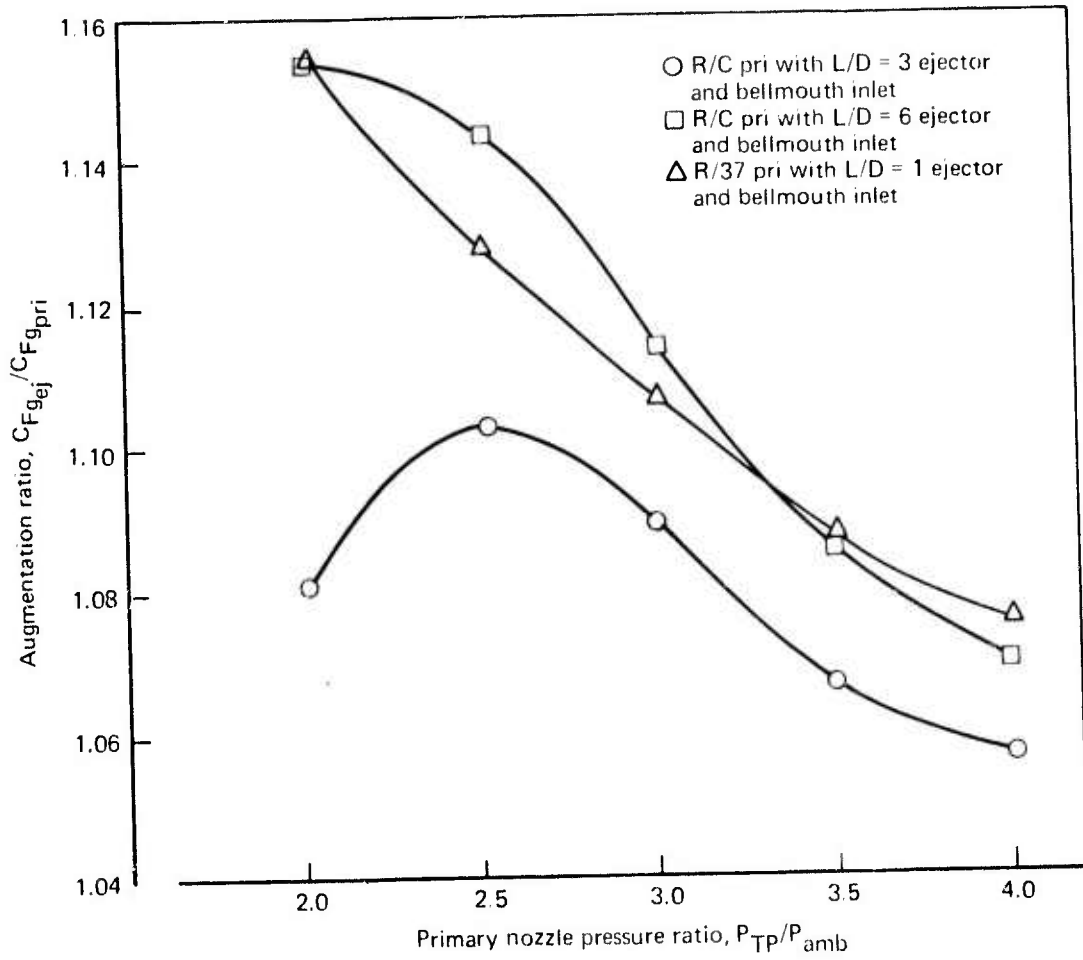
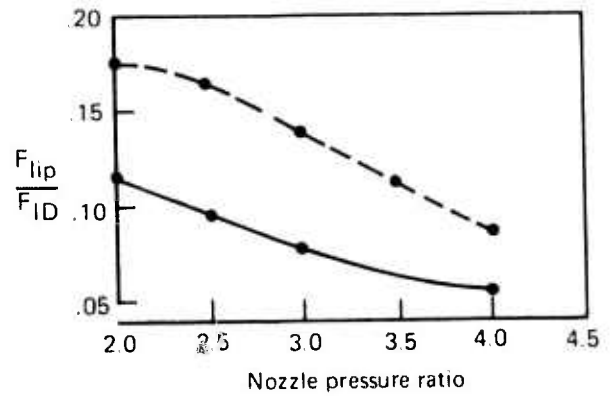
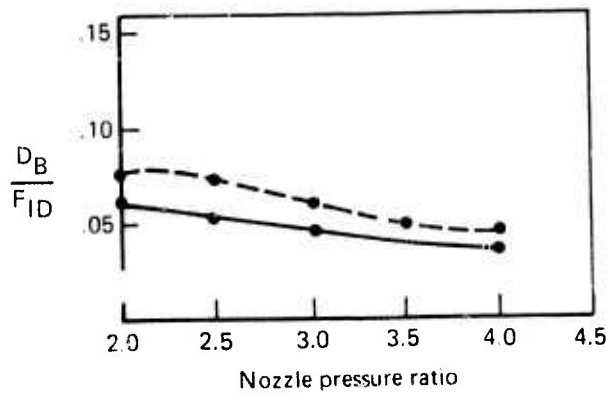
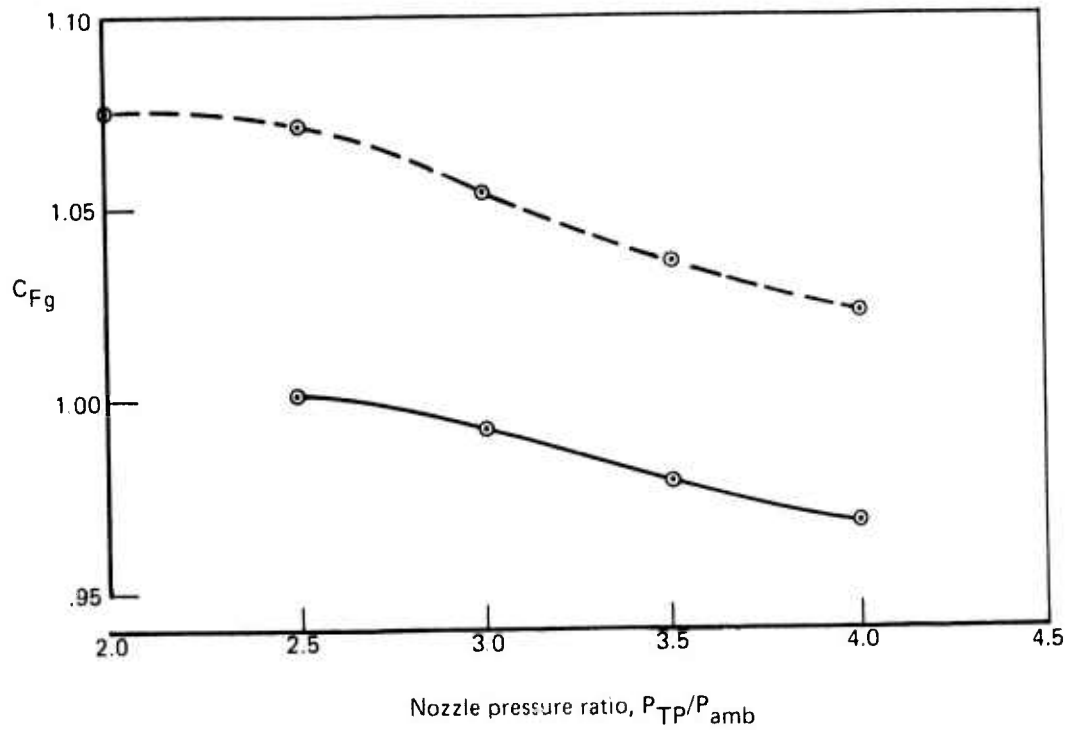


Figure 23.—Effect of Ejector Length on Thrust Augmentation



R-37 With L/D = 1 Ejector and Flight Lip Inlet

----- $T_{Tp} = \text{ambient}$
 ————— $T_{Tp} = 1150^\circ \text{ F}$

Figure 24.—Effect of Primary Jet Temperature on Ejector Performance

performance for the ejector configuration. This reduction is mostly accounted for by the change in lip suction with the remainder due to change in nozzle base drag.

4.2.2 SECONDARY FLOW

Evaluation of secondary air handling characteristics of a suppressor/ejector exhaust system presents a difficult measurement problem since the flow enters the ejector through a complex inlet path from ambient conditions and this prohibits using the inlet as a flow meter. The installation of an auxiliary flow measurement device is mechanically cumbersome and may alter the inlet flow so much as to make the measurement of little value.

The measurement technique developed and used in the present study has proven to be very effective in accurately determining ejector air handling. Figure 25 illustrates details of the test installation of figure 21 for secondary air measurement. The lower sketch in figure 25 shows the R/C and test ejector with its bellmouth inlet. The upper sketch shows the flow measurement installation which consists of a large bellmouth and annular measurement section attaching at the ejector inlet highlight. Extensive pressure instrumentation in both installations allows not only for airflow measurement but also for comparison of body forces and test ejector inlet flow conditions. Detailed analysis of this data in volume VI shows the flow to be substantially the same entering the ejector. Measured secondary air handling is shown in figure 26 for the R/37 with $L/D = 1$ ejector for jet temperatures of ambient and 1150°F . The increased jet temperature is seen to reduce air handling by 10% to 20% depending on nozzle pressure ratio and is shown in figure 24 to be reflected by the change in ejector lip suction. Volume VI shows conversely that measured ejector lip suction through pressure measurements can be used to infer ejector air handling.

4.2.3 EJECTOR FLOW MIXING

Finally, within the reference nozzle test phase, experiments were conducted to determine flow mixing profiles in the ejectors with the R/C nozzle. The example in figure 27 compares experimental pressure profiles in the $L/D = 6$ ejector for ambient and 1150°F jet temperatures. Profiles in the $L/D = 3$ ejector with 1150°F jet are compared with analytical predictions.

These reference nozzle experiments provide a foundation of basic nozzle/ejector performance characteristics upon which the studies in succeeding chapters will be based.

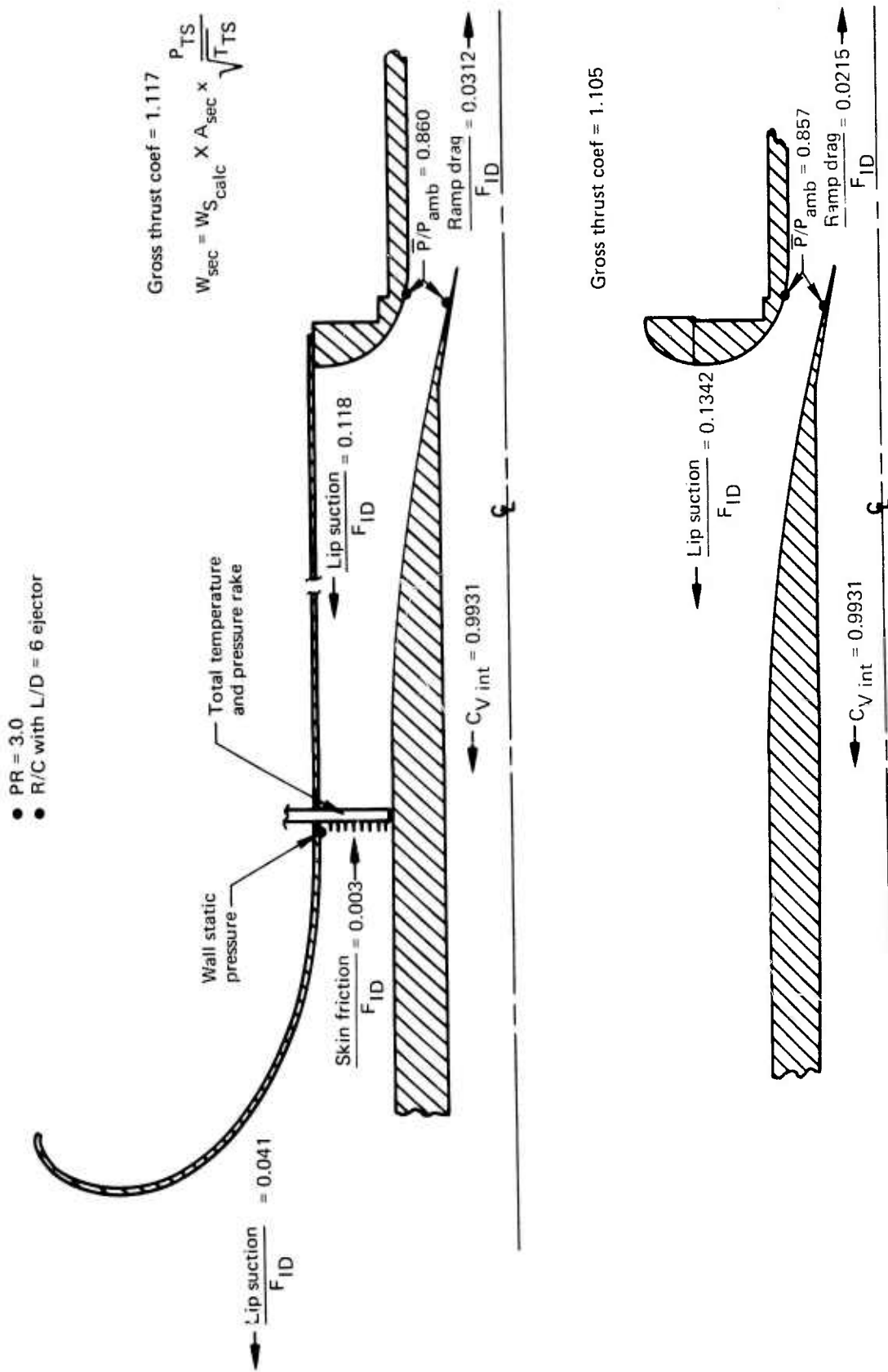


Figure 25.—Ejector Nozzle Body Forces and Secondary Weight Flow Measurement

R/37 Primary With
L/D = 1 Ejector,
Bellmouth and Annulus

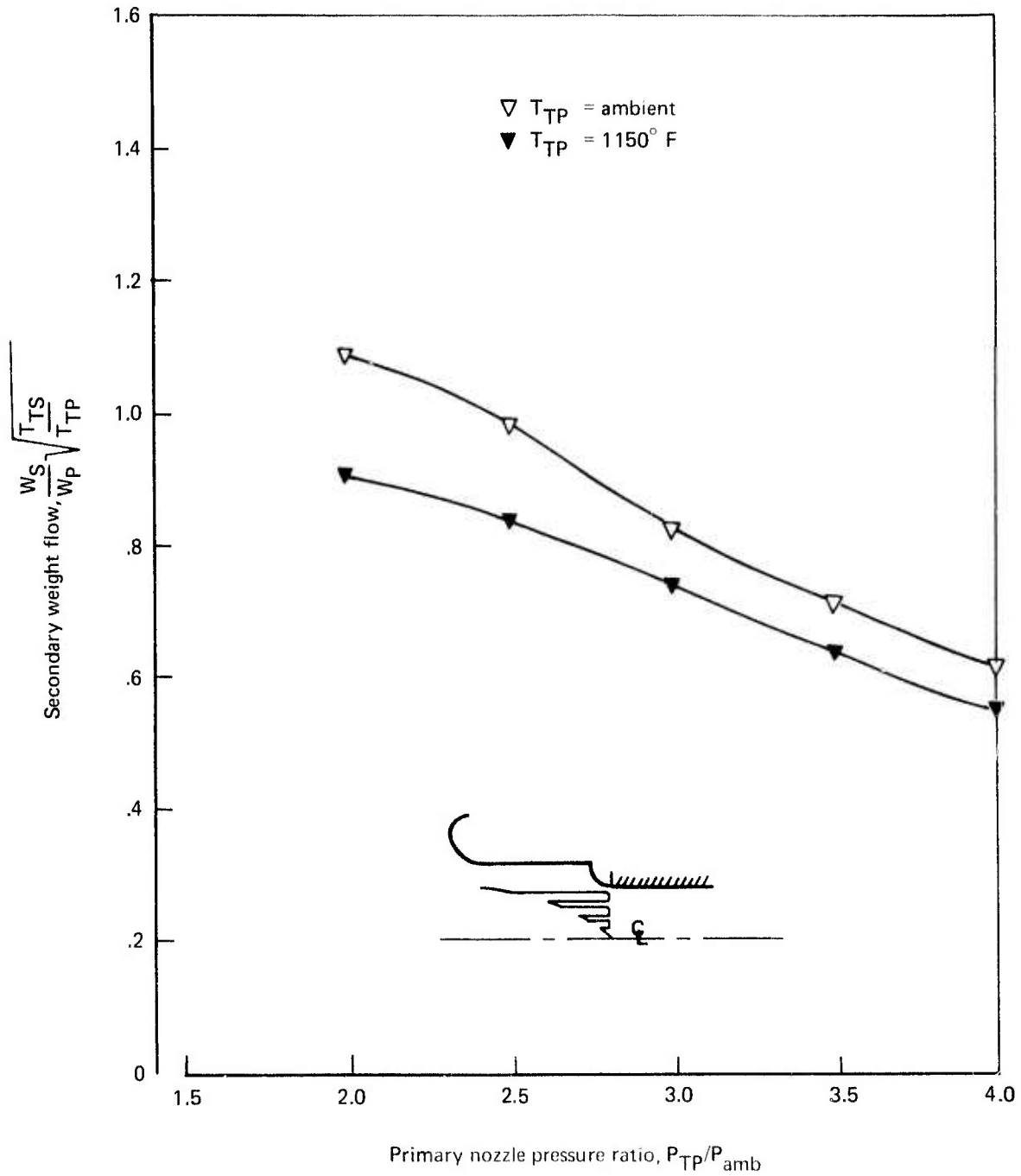


Figure 26.—Secondary Weight Flow for a Fully Mixed Multitube Nozzle

R/C Primary Nozzle and Bellmouth With Annulus Inlet $P_{TP}/P_{amb} = 2.0$

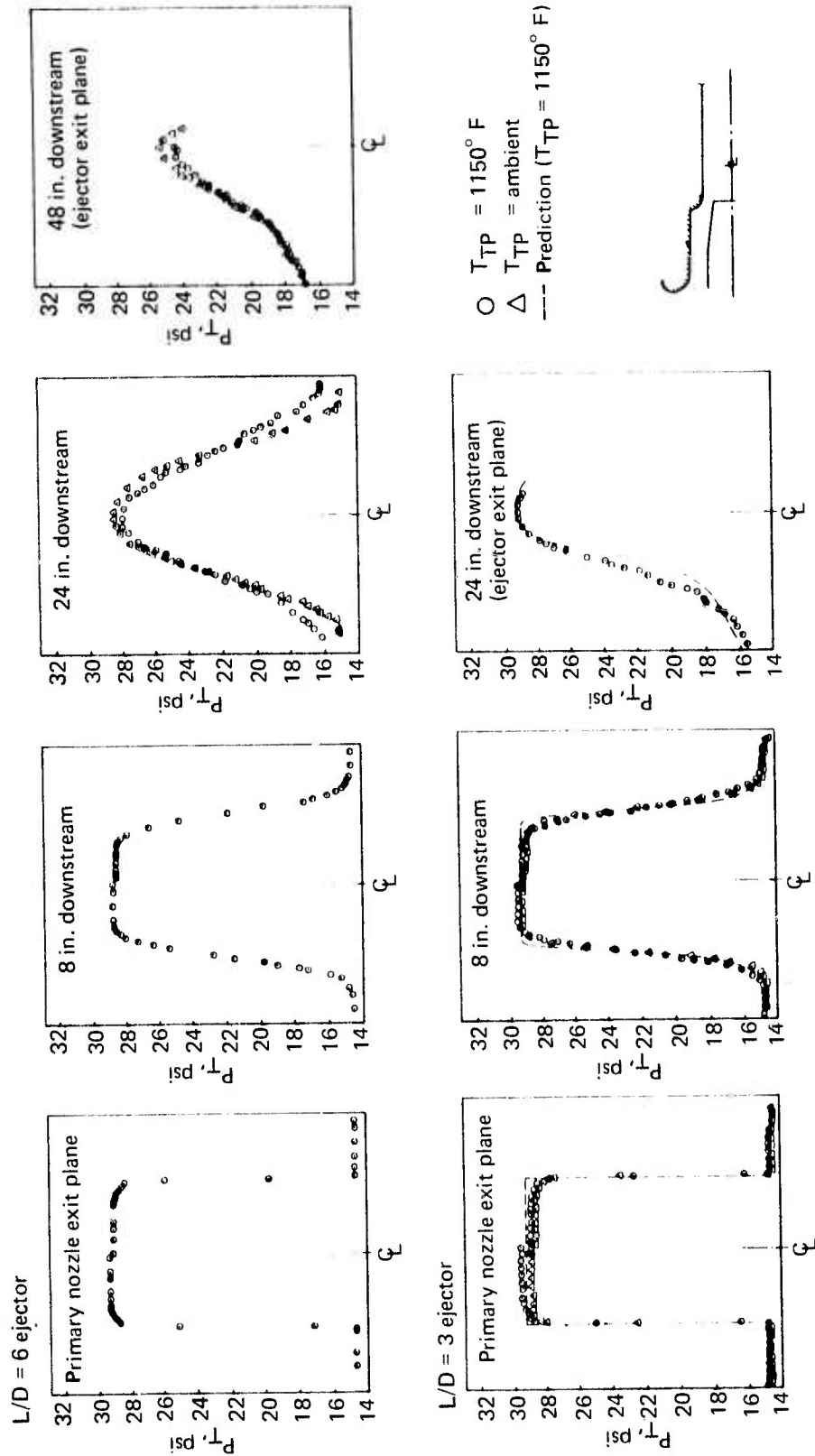


Figure 27.—Ejector Flow Pressure Profiles

5.0 MULTITUBE NOZZLE/EJECTOR STUDY

A three-part experimental program investigated detailed performance mechanisms for a wide range of multitube suppressor/ejector geometry, jet conditions and the effect of forward speed.

5.1 TEST PROGRAM DESCRIPTION

Multitube suppressor/ejector performance depends on numerous geometric parameters, as well as jet conditions and flight effects. A three-part set of experiments was conducted to investigate important parameters and establish performance design criteria for multitube suppressors. The initial testing considered the static performance interactions of suppressors without ejectors. Principal geometric variables were tube number, tube length, nozzle area ratio, and the tube placement array.

The second test series studied the effects of adding an ejector to the suppressors. Along with the nozzle parameters, ejector geometry variations included ejector area ratio, ejector length, and inlet area (controlled by ejector lip setback from the nozzle tube exit plane).

The concluding tests were conducted in the 9- by 9-ft low-speed wind tunnel to investigate flight effects. The same test hardware and geometry variations were considered as above. Wind tunnel testing covered a range of velocities from 30 to 167 knots.

All three test series investigated a range of pressure ratios from 2 to 4 at ambient and 1150°F jet temperatures. Figure 28 identifies the geometric variables and test ranges covered during the multitube suppressor/ejector performance test program.

5.2 BARE SUPPRESSOR PERFORMANCE

5.2.1 RANGE OF VARIABLES

The selection of specific test conditions throughout the multitube nozzle/ejector study was guided by a desire to obtain sufficient parametric data relative to each important parameter so that the results could serve as a definitive criterion for suppressor design. The testing of bare suppressor nozzles entailed the study of several geometric parameters, jet pressure ratio and temperature shown in figure 29. The prime variables of nozzle area ratio (NAR), tube number and tube length form the axes of the chart. Testing at ambient jet temperature encompassed all configurations while hot jet tests were confined to those configurations designated by dark symbols in figure 29. Acoustic data were also taken at these hot jet conditions. Two types of nozzle arrays were investigated; the first, called close-packed array, was designed so that all tubes in the array were approximately equally spaced, the second, called radial array, provided tubes aligned on radial lines symmetrically around the nozzle base.

Typical close-packed nozzle arrays are shown in figures 30 and 31. Figure 30 compares 19- and 61-tube, NAR 3.3 suppressor arrays. It can be seen that the tube arrangement is such that each successive row moving outward has six additional tubes. Therefore the selection of

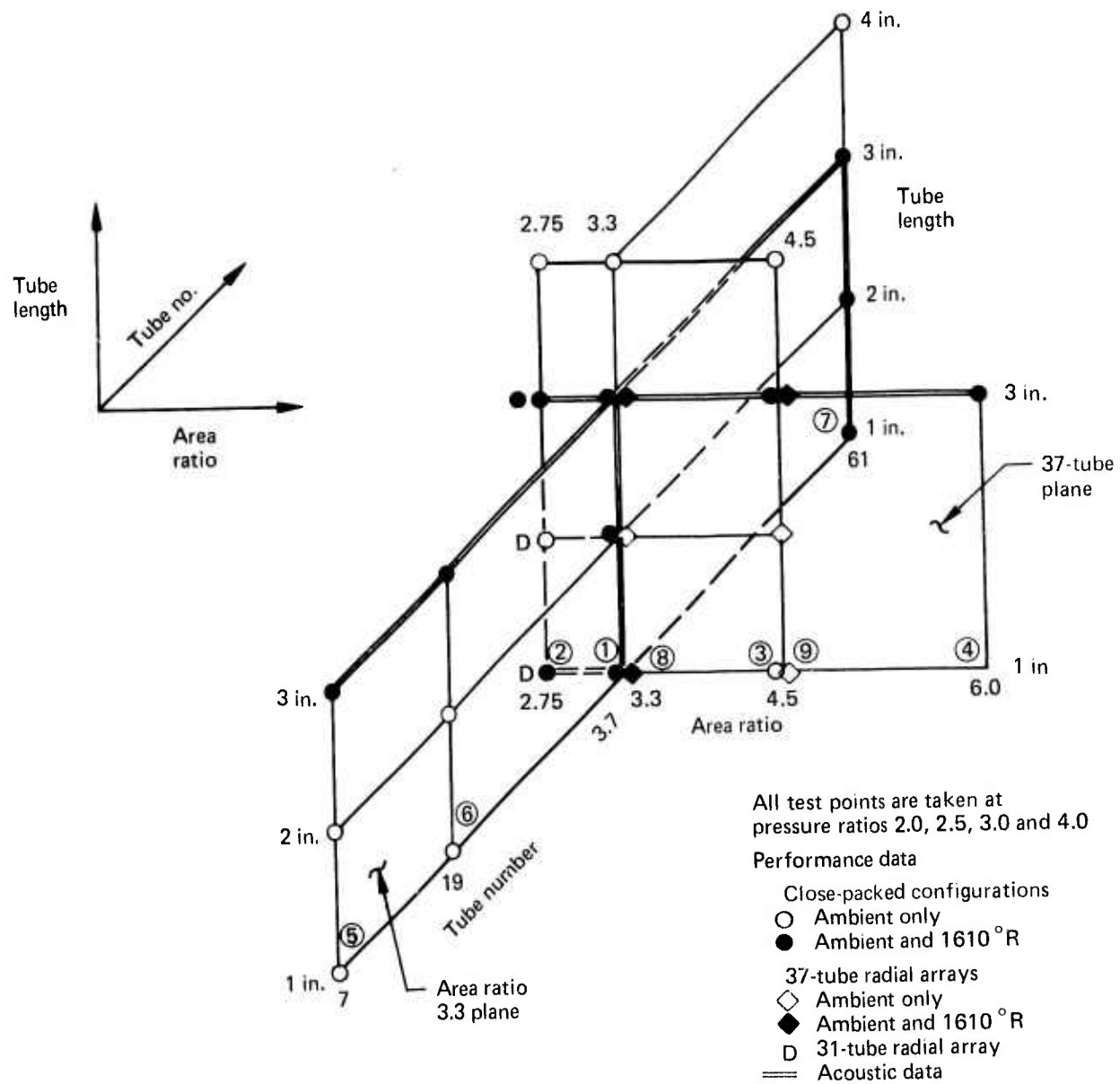


Figure 29.—Matrix of Suppressor Configurations and Test Conditions

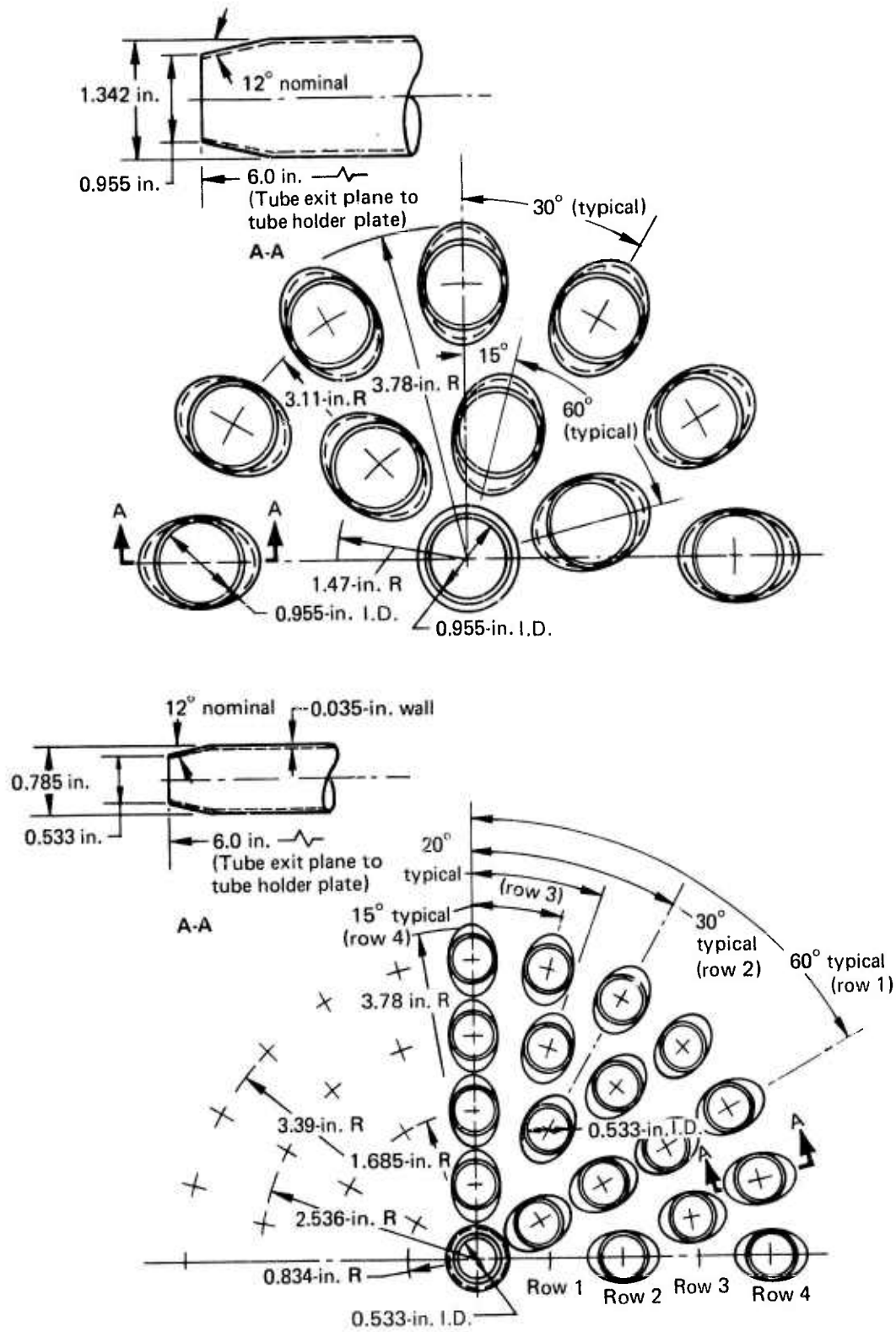


Figure 30.—19- and 61-Tube, NAR = 3.3 Suppressors

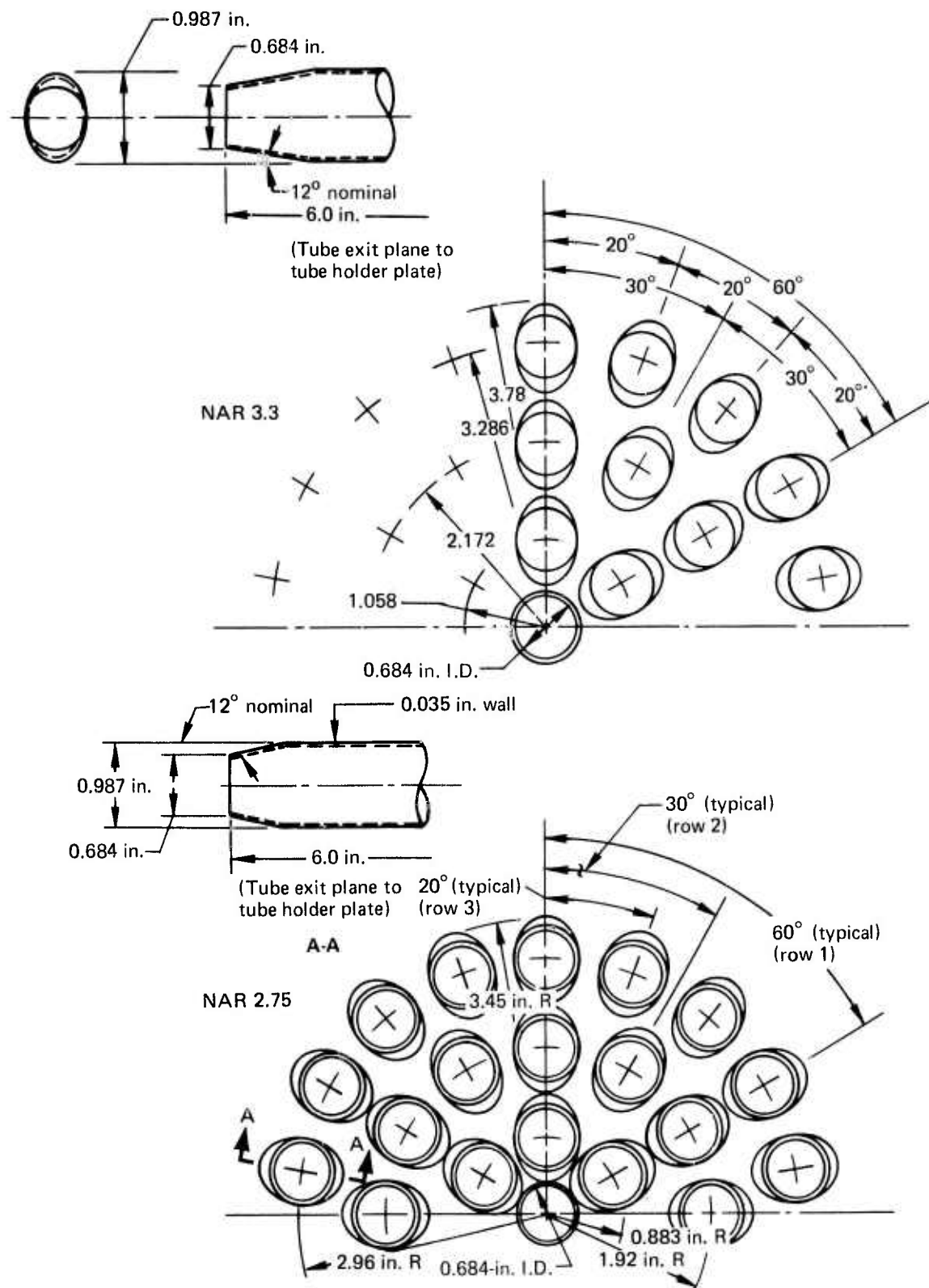


Figure 31.—37-Tube, Close-Packed Suppressors NAR = 2.75 and 3.3

7, 19, 37 and 61 tubes in the overall study was based on adding successive tube rows to form a geometrically similar family of configurations. Geometric similarity was also maintained in the design of nozzles with different area ratios (NAR) as in the example of figure 31 which shows 37-tube nozzles with $NAR = 2.75$ and 3.3 . Previous studies (ref. 2) identified base drag as the dominant performance-loss element in multielement suppressor nozzles. Attempts to minimize this loss included variations in the nacelle afterbody shape approaching the nozzle base. This was not expected to affect static performance but is included in bare nozzle tests to establish baseline data for the wind tunnel tests to be described later in section 5.4.

An example of configurations used to investigate the effects of afterbody shape on performance is shown in figure 32. The figure compares 37-tube nozzles with a circular arc boattail intersecting the base just outside the outer row of tubes and with an elliptical contoured boattail meeting the base between tubes in the outer tube row.

Close-packed and radial tube arrays are compared in figure 33 while details of 31- and 37-tube radial array configurations are shown in figure 34.

5.2.2 INTERNAL PERFORMANCE

An analysis of internal performance of multielement nozzles (vol. VII) is developed in the current study. Changes in internal performance with variations in number and length of tubes and nozzle pressure ratios are shown in figure 35 for a jet temperature of $1150^{\circ}F$. For the fixed nozzle area represented, the performance is seen to be a weak function of tube number for the shortest $L_T/D_{eq} = 0.25$ (potentially stowable) tube lengths considered.

5.2.3 NOZZLE GEOMETRY EFFECTS

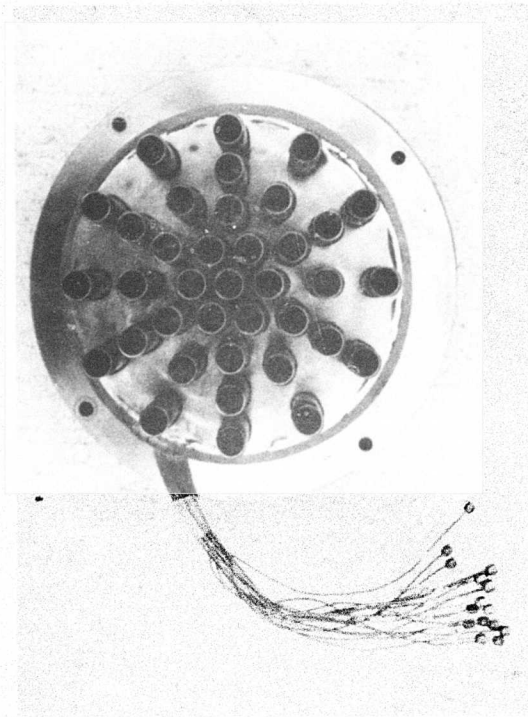
As mentioned earlier the dominant nozzle performance-loss factor is base drag. Detailed pressure instrumentation on nozzle base surfaces allowed the assessment of base drag as a function of number and length of tubes and nozzle array shown in figure 36. Extraordinary drag penalties are seen for $L_T/D_{eq} = 0.25$ tubes with increasing tube numbers for close-packed arrays. The large advantage of well-ventilated radial tube arrays is clearly demonstrated in this example (see corresponding radial array data) and by the breakdown of nozzle losses in figure 37. Internal nozzle contours including the tube entry radius, tube Mach number and exit convergence angle (10°) were designed to be identical for the nozzles in this comparison and therefore internal performance, $C_{V_{int}}$, is independent of array. The entire performance differences for given tube lengths are therefore due to base drag.

5.2.4 PERFORMANCE TRENDS

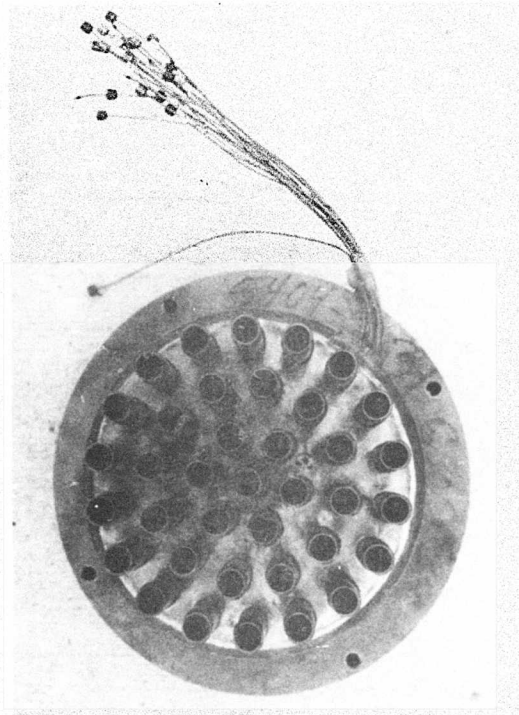
Overall performance trends for the bare tubular suppressor nozzles within this study are shown in figures 2 and 38 for a pressure ratio of three. The trends at other operating conditions are similar and can be found in volume VII. Tube number and especially length (which controls base ventilation) are seen in figure 2 to be the strongest performance variables for close-packed arrays. Where short (stowable) tubes are a configuration requirement, the use of radial tube arrays offers large performance improvements. The effects of nozzle area ratio on performance in figure 38 are relatively small at ambient conditions for the



Figure 32.—Comparison of 37-Tube, 3.3 Area Ratio Nozzles



Close-Packed Array



Radial Array

Figure 33.—Example of Close-Packed and Radial Array Nozzles

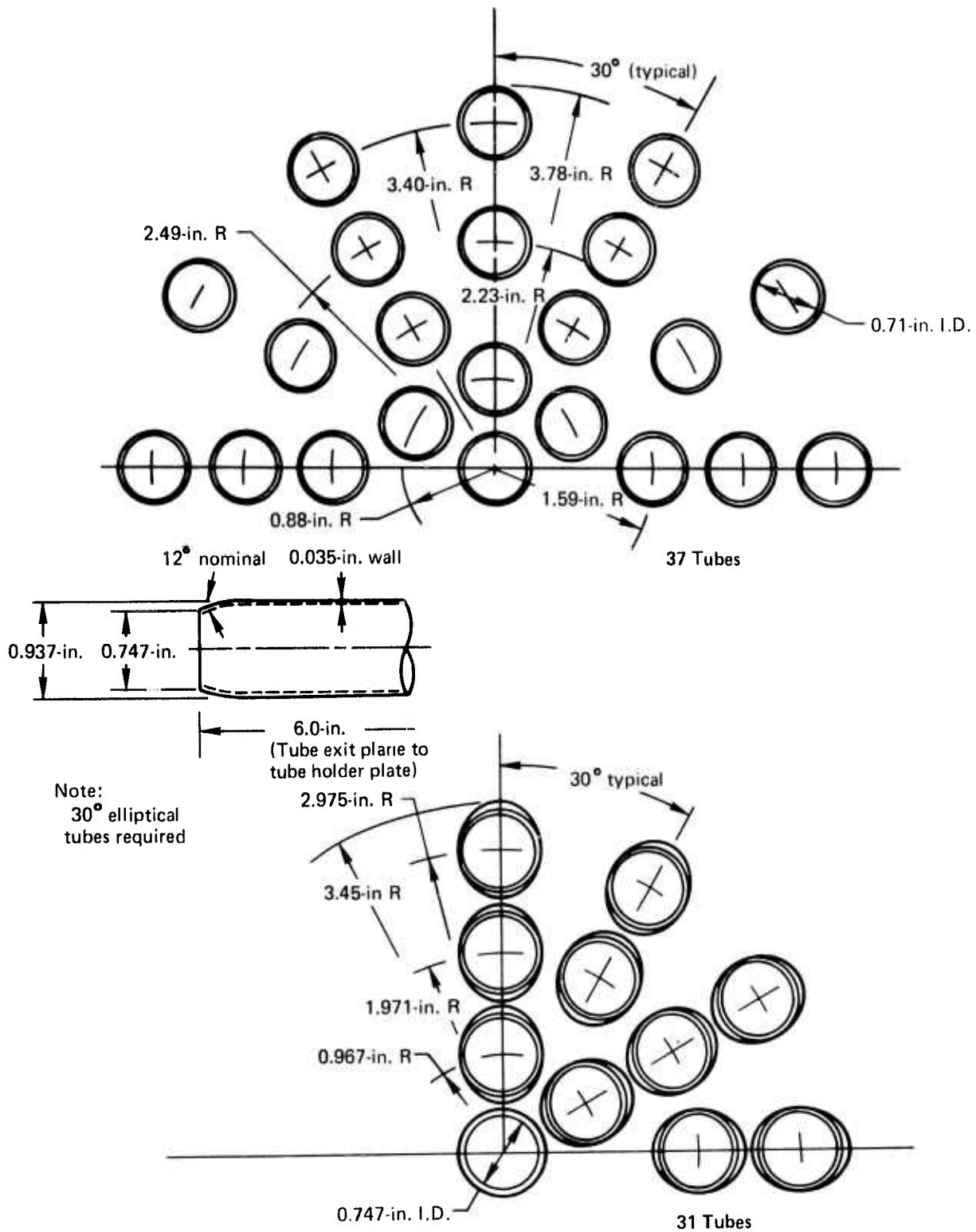


Figure 34.—Radial Array Nozzles

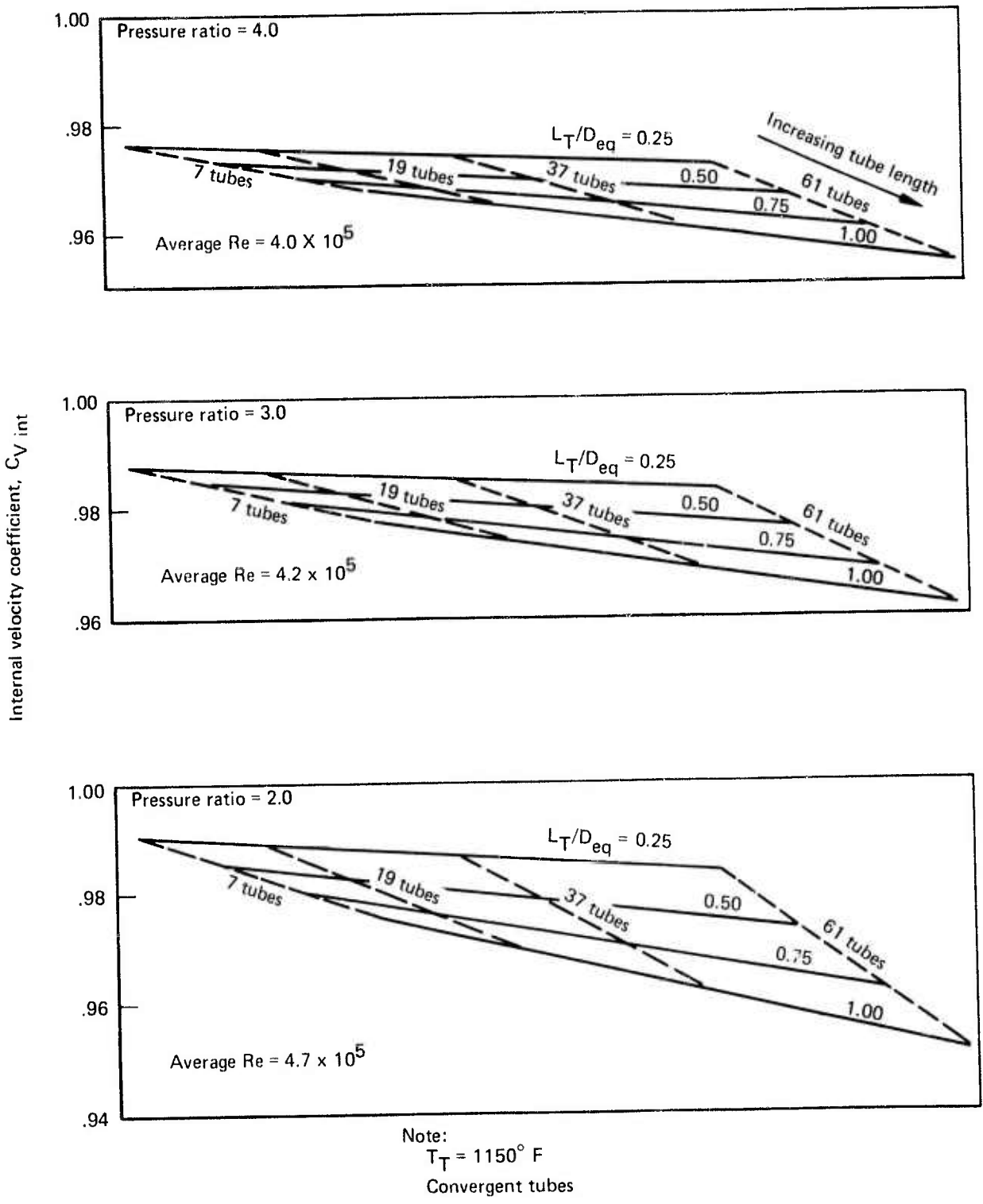


Figure 35.—Effect of Tube Length and Number on Internal Velocity Coefficient at 1150° F

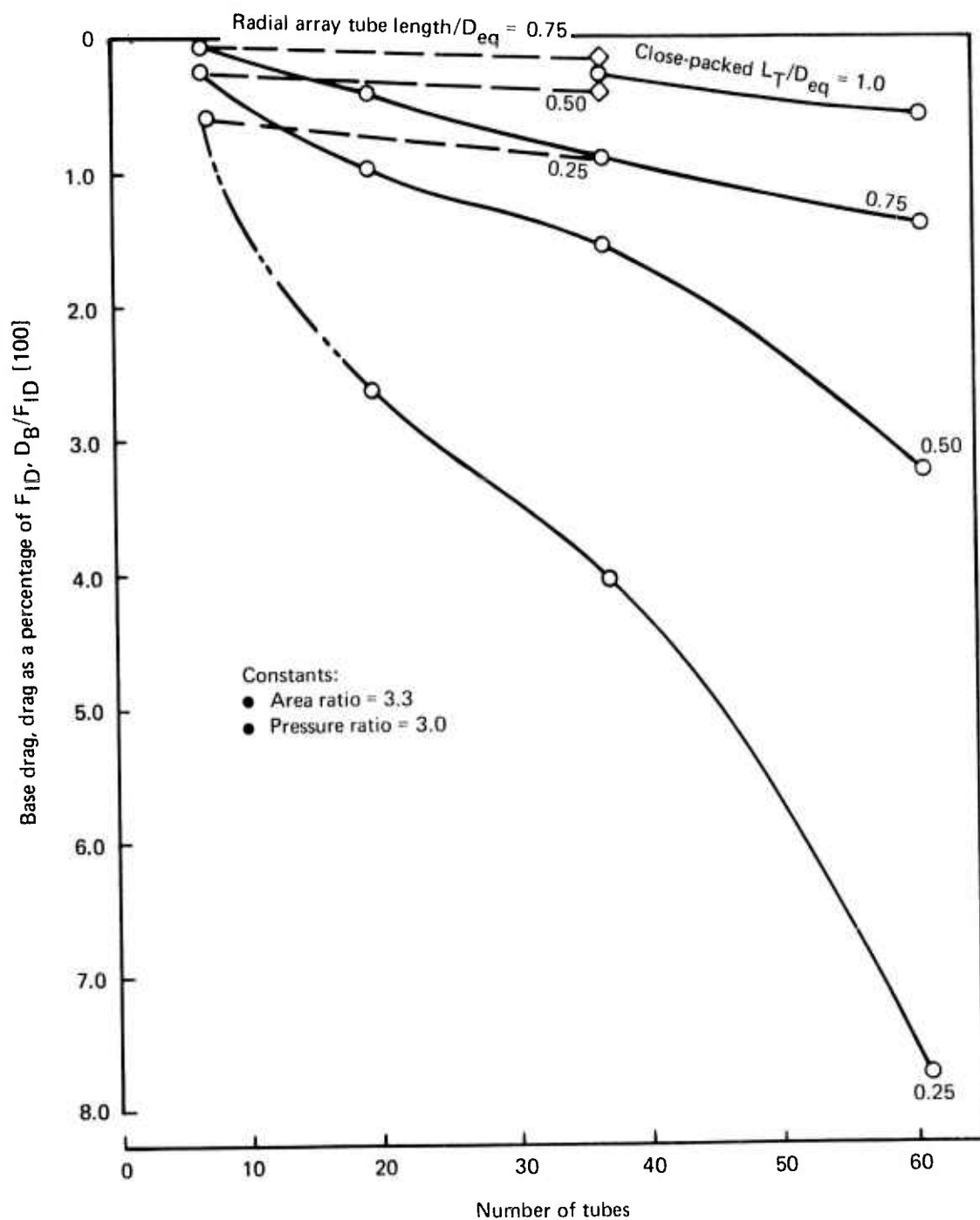


Figure 36.—Nozzle Base Drag as a Function of Tube Number, Tube Length, and Tube Array

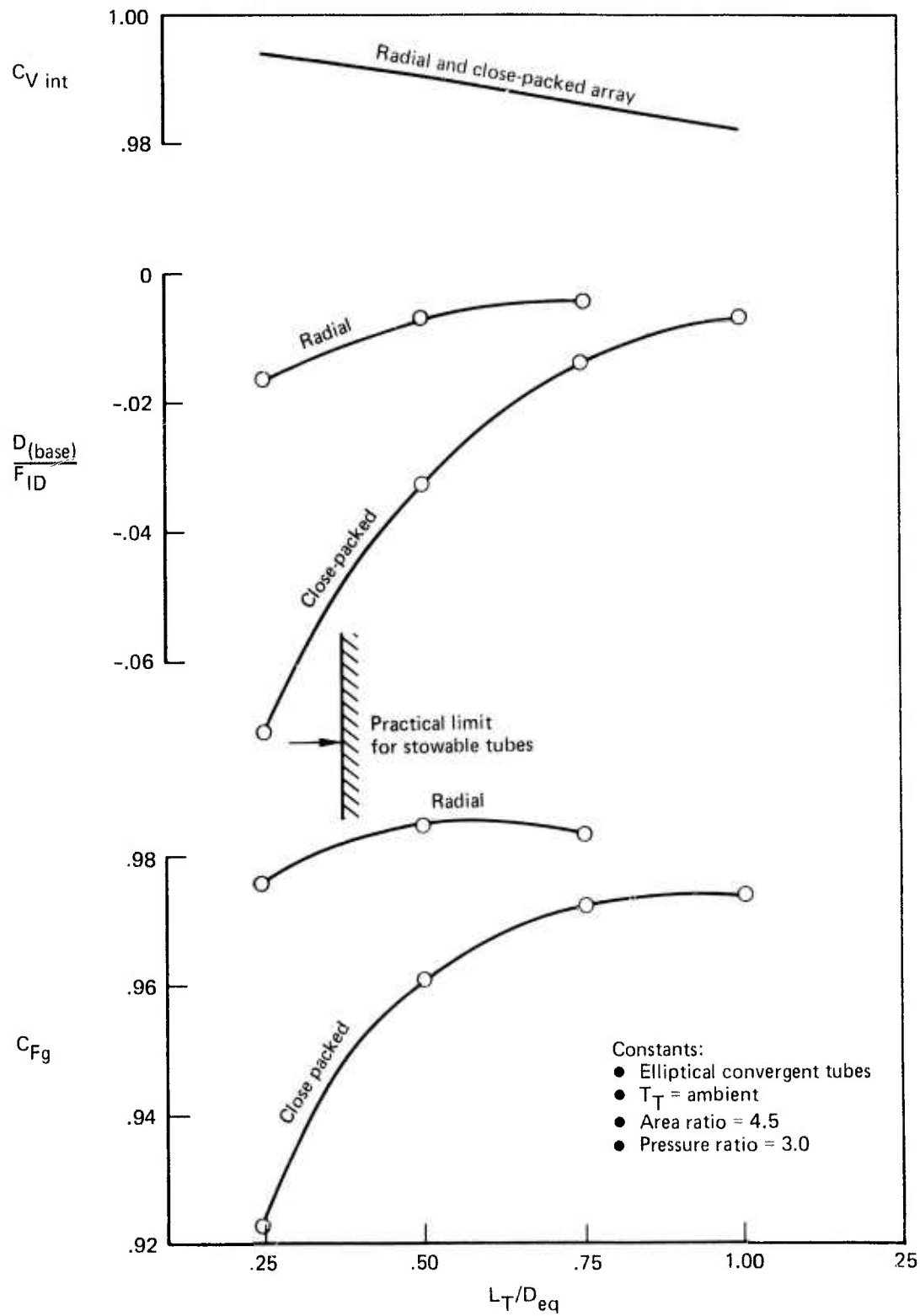
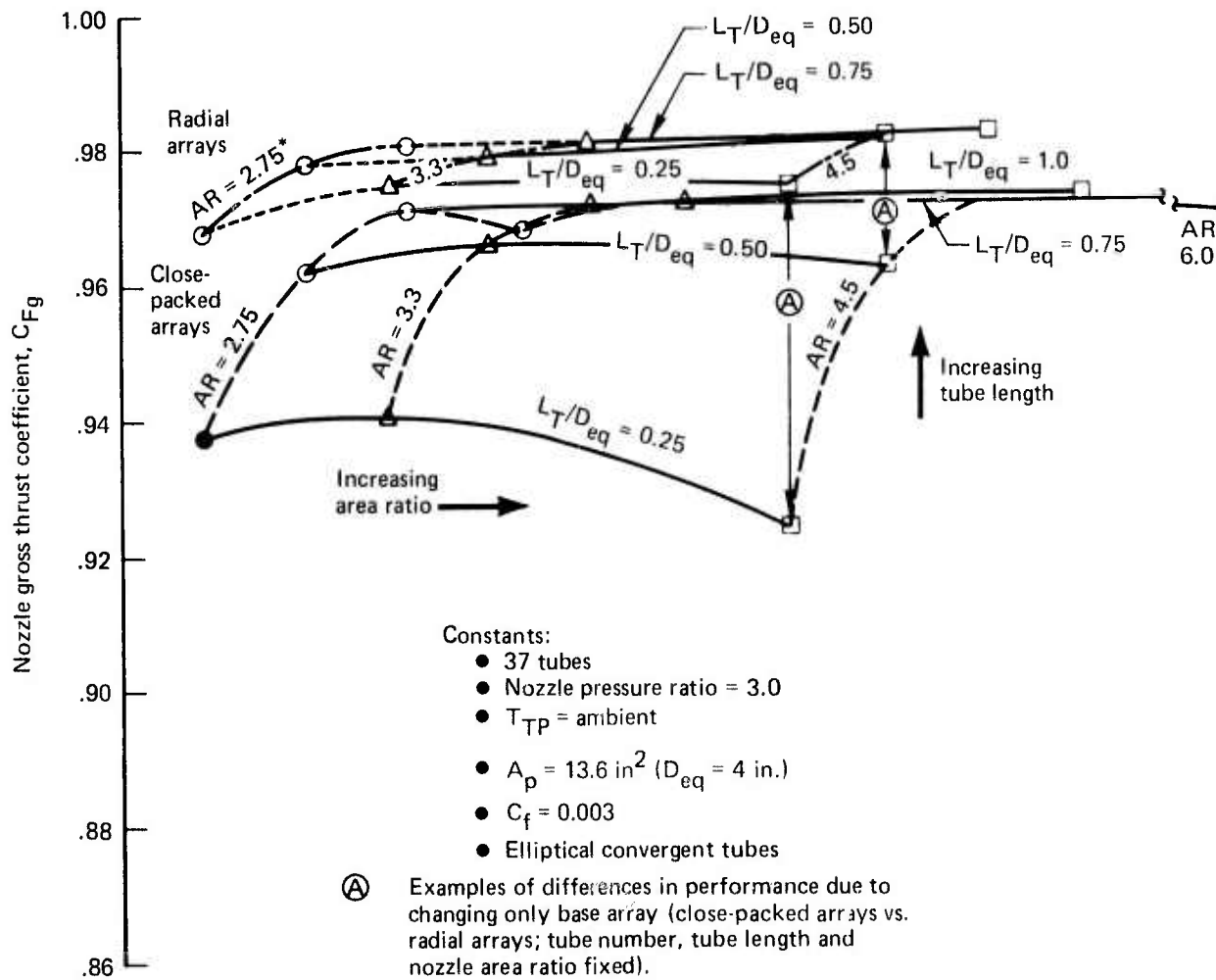


Figure 37.—Performance Components for Radial and Close-Packed 37-Tube Nozzles



Note:

*NAR = 2.75, radial array is a 31-tube configuration

Figure 38.—Effect of Area Ratio, Base Array and Tube Length on Suppressor Performance

family of 37-tube close-packed-array nozzles. The peak performance near $NAR = 3$ reflects the occurrence of a maximum in the base ventilation parameter A_S/A_B . This parameter is the ratio of the area between outer row tubes and the nozzle base area and is shown in volume VII to be nearly independent of tube number for similar arrays. Figure 39 shows that A_S/A_B for radial arrays increases with decreasing area ratio to the limiting case where it is not possible to construct a smaller array because of lack of room for installation of the tubes on the nozzle base.

5.2.5 PERFORMANCE/NOISE SUPPRESSION TRENDS

The complete results and analysis of the suppression characteristics are covered in detail in volume II. A summary of suppression-versus-thrust loss for the multitube nozzles is presented using suppression values quoted from volume II. The noise suppression and thrust loss characteristics at pressure ratio = 3.0 are shown (relative to a single round jet) in figure 40. The suppression values are for 1150° F jet temperature. The curves show thrust loss values for ambient-jet temperatures because hot-jet thrust measurements were not available for most configurations. The available values of thrust loss at 1150° F are plotted on the figure to produce a skeleton version of suppression-versus-thrust loss with both measured at the elevated temperature. As shown in volume VII, the temperature effect on the gross thrust coefficient is small and thus the curves are expected to be representative of hot jet thrust-versus-noise characteristics for all configurations.

Radial arrays provide the best suppression-to-thrust-loss ratio. Within the range of interest, increasing tube length results in large performance gains without measurable changes in suppression. The effect of area ratio on suppression and thrust loss is summarized in figure 41. It is observed that neither performance nor suppression characteristics are strongly influenced by nozzle area ratio for bare suppressors at static ambient conditions.

5.3 SUPPRESSOR/EJECTOR PERFORMANCE

5.3.1 RANGE OF VARIABLES

The suppressor nozzles discussed in section 5.2 were tested with a series of ejector configurations that encompassed practical hardware limits for SST engine application. Figure 28 lists the important nozzle and ejector parameters that were considered in the evaluation of performance interactions at static test conditions.

Ejector lip shape variation was limited to comparison between a small elliptic-shaped lip constrained by cowl envelopes and a comparatively large bellmouth shape that served as an idealized reference.

Ejector setback, as shown by figure 28, is defined as the axial distance from suppressor tube exits to highlight of the ejector lip. A variation from 0 to 1 in. ($SB/D_{eq} = 0$ to 0.25) in ejector setback was tested for most configurations to ensure determination of performance with an adequate ejector inlet area. The ejector area ratio variation ranged from 2.6 to 3.7. The majority of ejector studies were conducted with an ejector area ratio of 3.1 which is approximately the size anticipated for a practical SST installation. The smallest ejector was

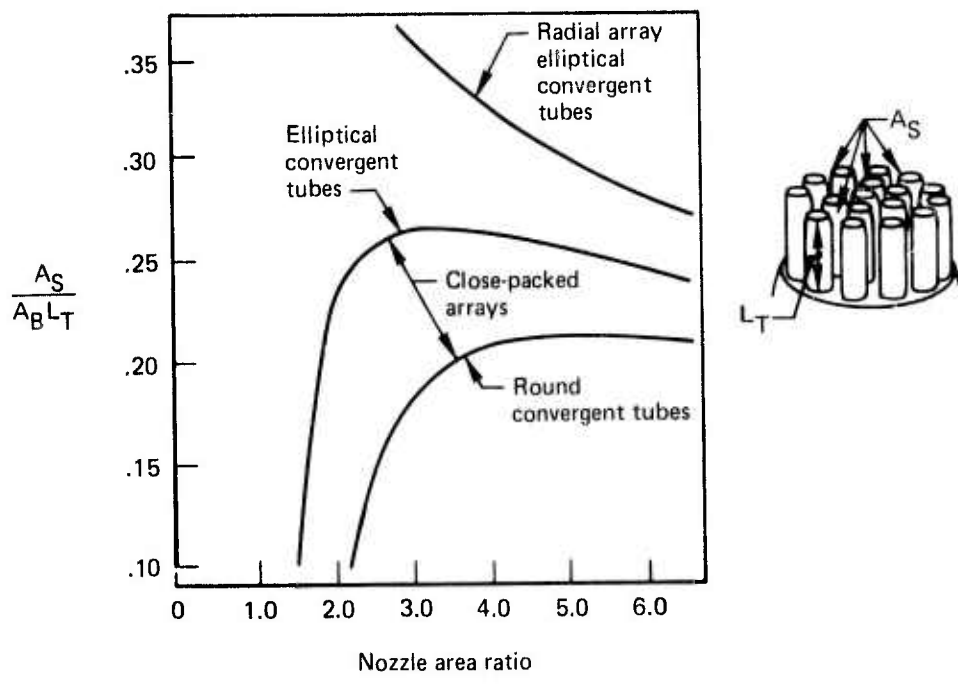
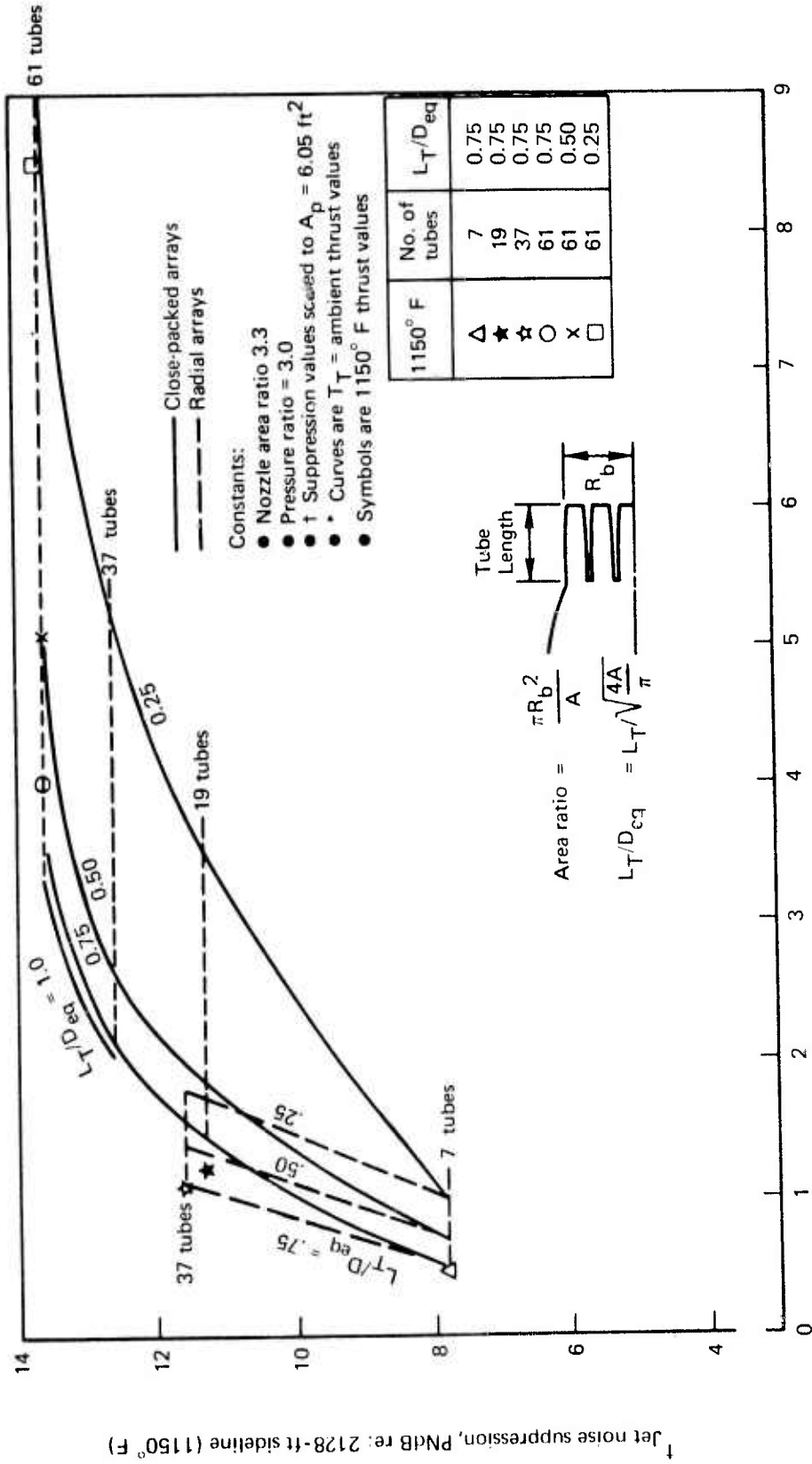


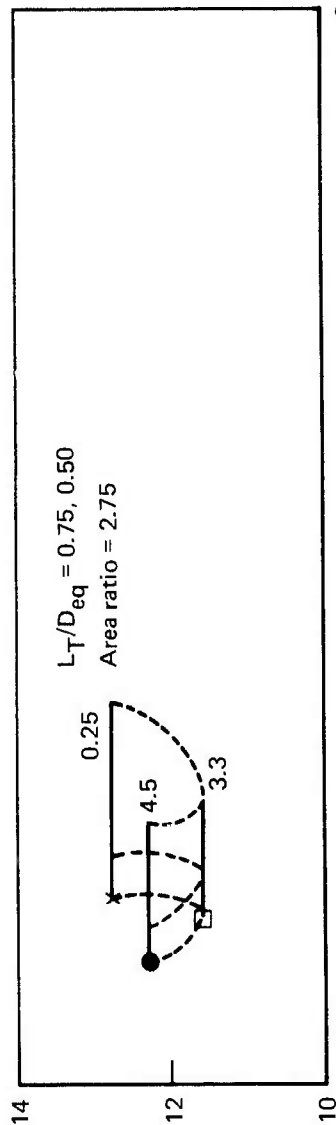
Figure 39.—Base Ventilation Parameter for 37-Tube Nozzles

Typical error band
Acoustic ± 1 PNdB
Propulsion $\pm 0.25\%$



*Thrust loss, percent re: R/C nozzle
 Figure 40.—Summary of Suppression Versus Thrust Loss

Radial Arrays



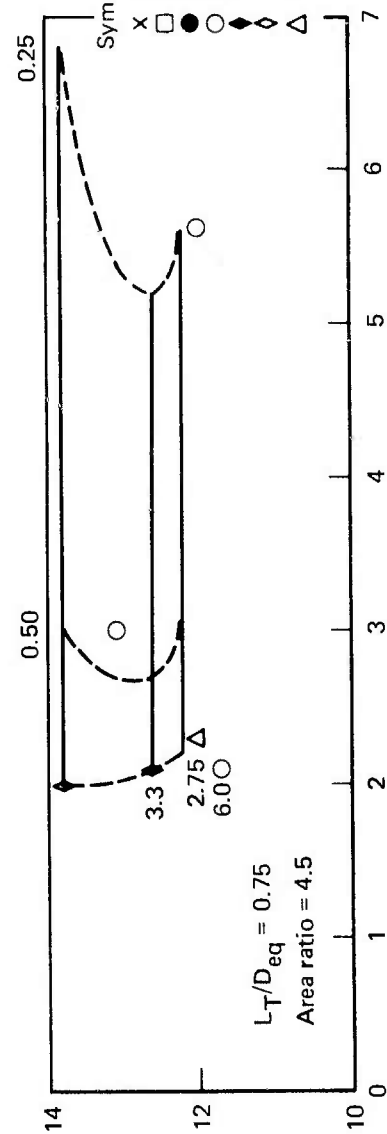
Typical error band
Acoustic \pm PNdB
Propulsion $\pm 0.25\%$



Constants:

- Pressure ratio = 3.0
- *Static noise for $A_p = 6.05 \text{ ft}^2$

Close-Packed Arrays



* Jet noise suppression, Δ PNdB re: 2128-ft sideline

Thrust loss in % relative to R/C nozzle, ΔC_{Fg}

Figure 41.—Jet Noise Suppression Versus Thrust Loss

of course tested only with the 2.75 AR nozzles whose tube-exit arrays fit within the ejector diameter.

The largest ejector area ratio tested was 3.7. Ejector length was varied from a scaled practical installation length of 8 in. to 24 in. ($L_E/D_{eq} = 2$ to 6) to establish performance trends with mixing length.

The configuration-oriented inlet losses due to ejector mounting struts were avoided by mounting the ejectors independently (but on the same force balance) from an overhead support as shown in figure 42.

5.3.2 PRESSURE RATIO EFFECTS

Figure 43 shows a typical presentation of suppressor/ejector performance as a function of nozzle pressure ratio for different jet temperatures and geometry of the configuration. Included is a breakdown of nozzle drag and ejector lip suction derived from surface pressure measurements. The example is a 37-tube, NAR 3.3 suppressor with an ejector with area ratio = 3.1.

Nozzle/ejector geometry changes are shown to dramatically affect performance levels in some instances and will be discussed later. The trends of performance with pressure ratio for given configurations are that overall performance is mildly decreased with increasing pressure ratio. This observation must be tempered by the fact that for some of the configurations a pressure ratio was reached where severe flow instability occurred and testing was halted for fear that the hardware might be destroyed by vibration. The effect of increasing jet temperature was to delay the onset of flow instability to a higher pressure ratio. The effects of pressure ratio on nozzle base drag are small in most cases as was observed during bare suppressor testing. The performance decay with increasing pressure ratio is reflected primarily by reduction in ejector lip suction force (F_{lip}/F_{ID}). This can be explained by a reduction in ejector secondary air demand (lower lip velocity and higher lip pressure) due to filling of the ejector by the increasing primary airflow with increasing pressure ratio.

5.3.3 NOZZLE GEOMETRY EFFECTS

The trends of ejector performance with nozzle tube length and tube number are demonstrated in figure 44. As expected, performance falls off rapidly with decreasing tube length due to reduced base ventilation and the changes with tube number for a given length are similar to those observed for the bare suppressors. In order to evaluate the effects of nozzle configuration on ejector operation it is convenient to express the ejector performance as a ratio to that of the particular bare suppressor.

This ratio, commonly termed augmentation ratio, is shown in figure 45 and indicates similar trends for the 37 and 61-tube nozzle/ejectors. Where reasonably good base ventilation is provided ($L/D_{eq} > 0.5$) the effect of the tube length on ejector performance is small.

It is probable, based on the detailed analysis of volume VIII, that the ejector inlet is being restricted in the $L/D_{eq} = 0.25$ tube cases and that performance could be improved by increasing ejector setback. The lower augmentation observed for the sample 19-tube nozzle

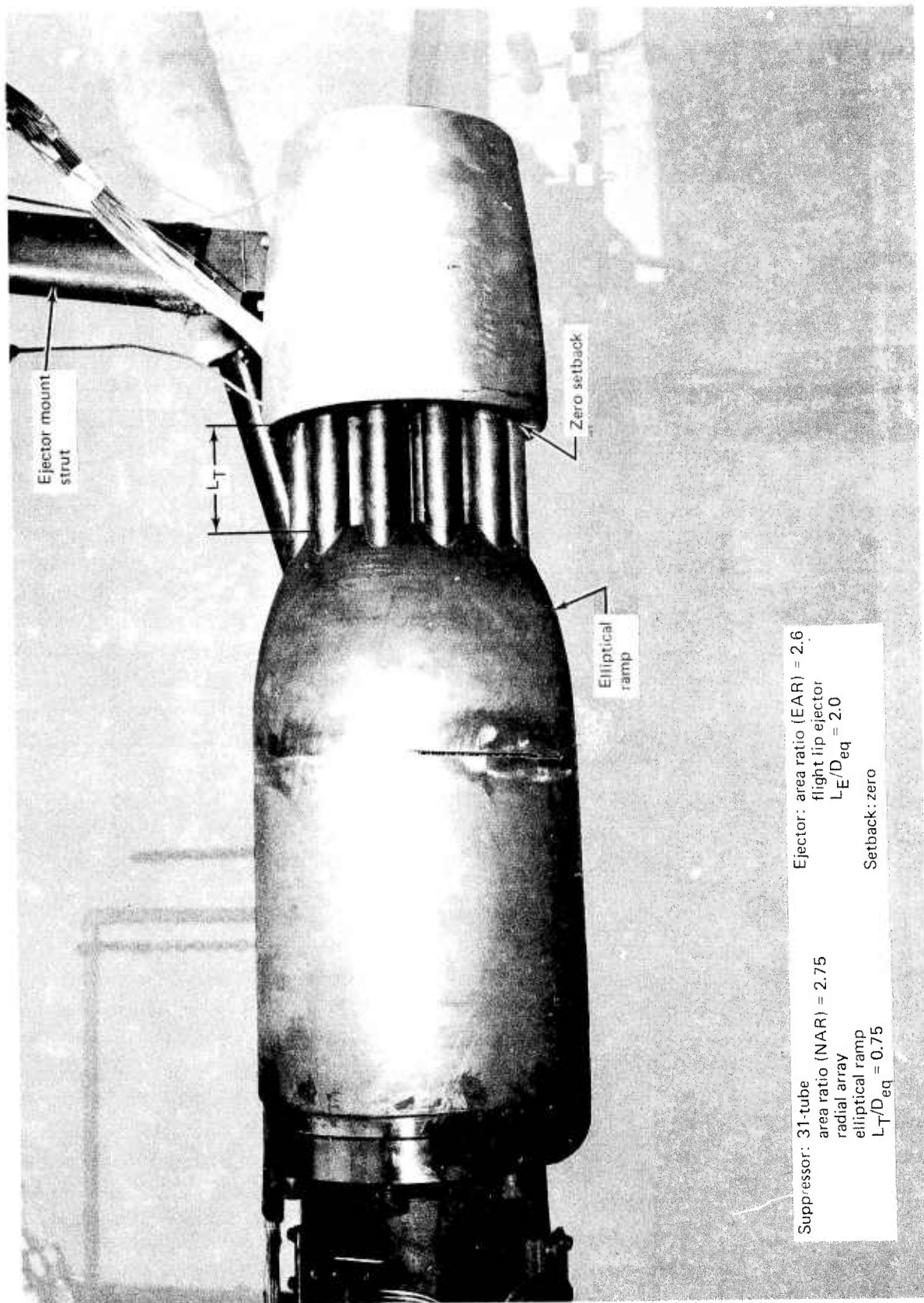
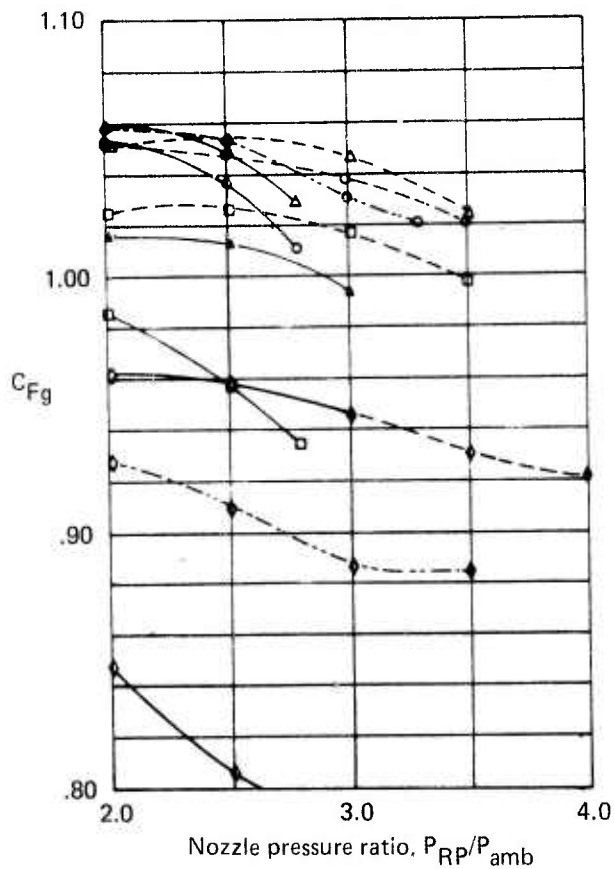


Figure 42. — Typical Suppressor/Ejector Installation



Constants:

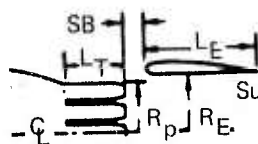
- Open symbols = ambient temperature
- Solid symbols = 1150° F

L_T/D_{eq}

- △ 1.0
- 0.75
- 0.50
- ◇ 0.25

Setback (SB/D_{eq})

- 0
- - - 0.125
- · - 0.250
- $L_E/D_{eq} = 2$



$$D_{eq} = \sqrt{\frac{\pi R_p^2}{A_E}}$$

$$\text{Suppressor area ratio (NAR)} = \frac{\pi R_p^2}{A_p}$$

$$\text{Ejector area ratio (EAR)} = \frac{\pi R_E^2}{A_p}$$

A_p = primary flow geometric exit area

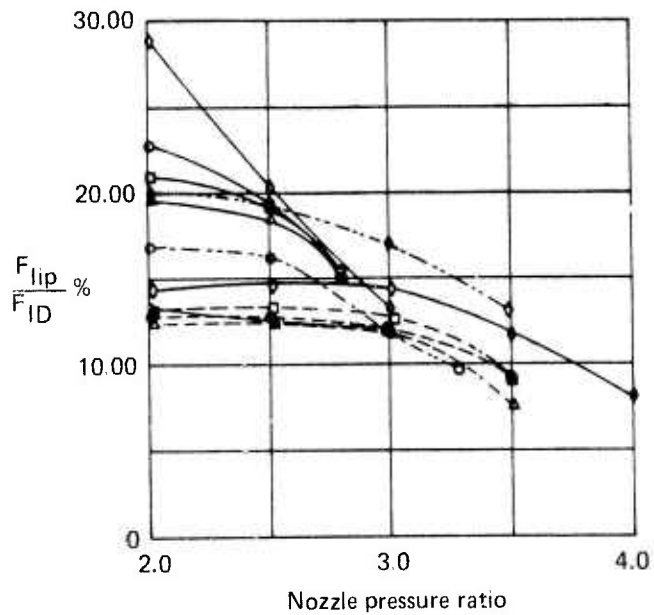
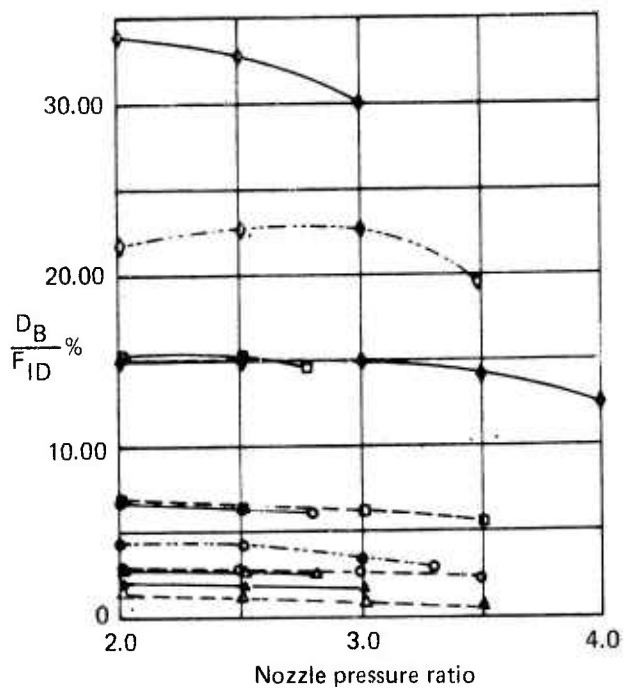


Figure 43.—Gross Thrust Coefficient and Body Forces for 37-Tube, NAR = 3.3, EAR = 3.1, Close-Packed, Elliptical Ramp, Elliptical Convergent Tubes

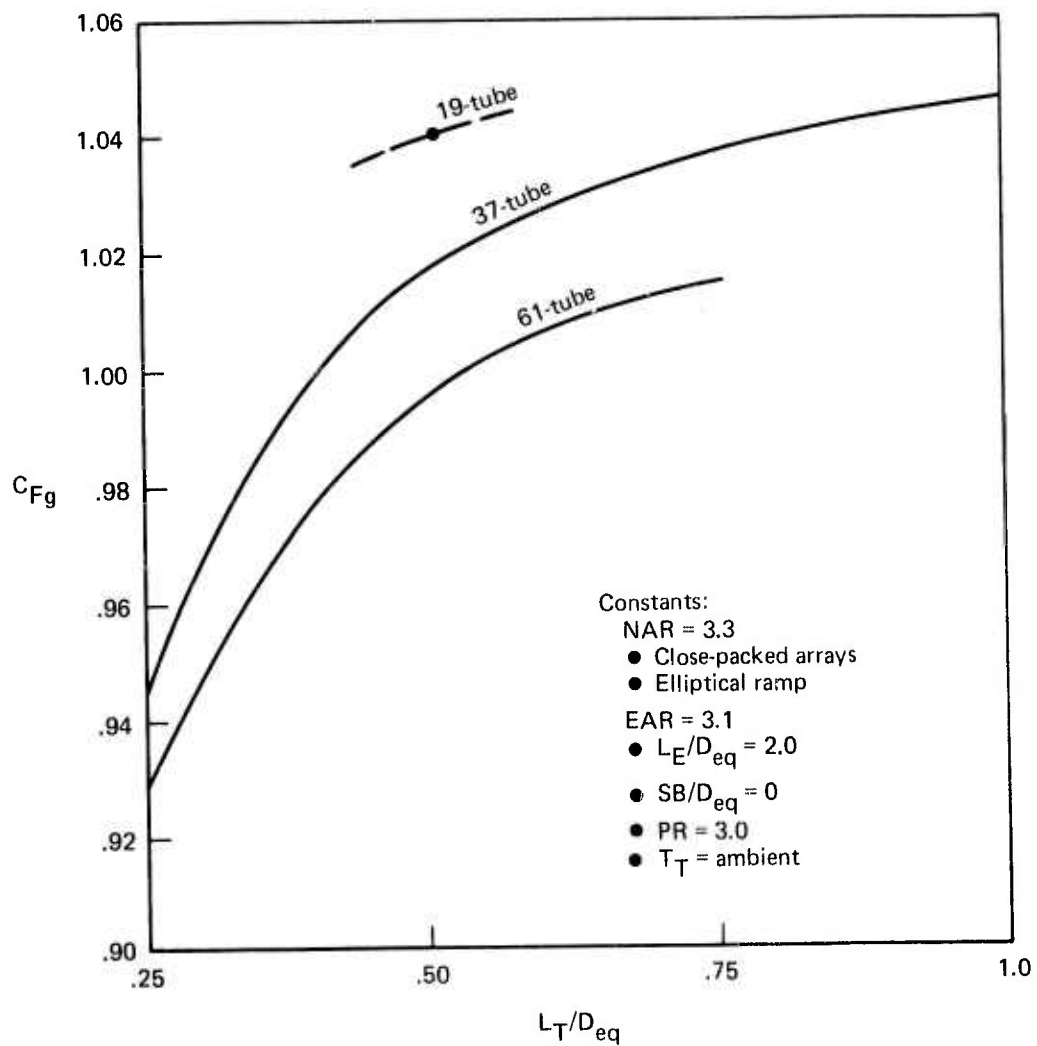


Figure 44.—Performance as a Function of Tube Length for Various $NAR = 3.3$ Suppressors With $EAR = 3.1$ Ejectors

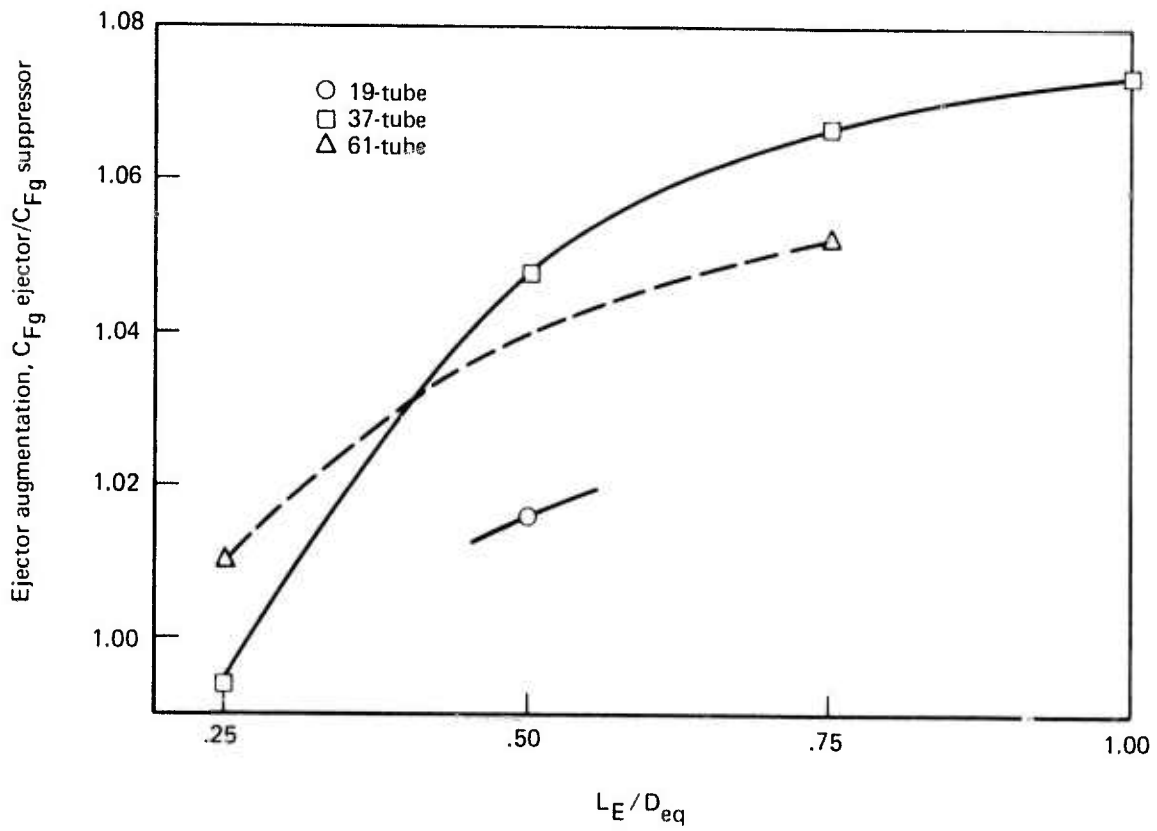


Figure 45.—Effect of Nozzle Tube Number on Ejector Thrust Augmentation

case shown is attributed to reduced ejector air handling because of the larger tube size. Increased mixing and thus performance would be achieved by increasing ejector length; this will be discussed later.

The effect of nozzle array on ejector augmentation is shown in figure 46. The significant improvement in nozzle base ventilation by the radial array over close packed is seen to also improve ejector performance through providing a less crowded ejector inlet that allows for improved flow mixing with the primary jets. It is believed that this provided an increase in ejector air handling and thus an increased thrust augmentation. This hypothesis was not directly proved by the data, however, since secondary flow was not measured.

5.3.4 EJECTOR EFFECTS

It is shown in figure 43 that very large performance changes are obtained with changes in ejector setback ratio (SB/D_{eq}). In particular, a change in setback from zero to 0.25 with $LT/D_{eq} = 0.25$ tubes affords an improvement in performance of 16% at pressure ratio 2.5. This large change is mainly due to an increase in inlet area from a condition where the inlet is too small to pass the amount of air required to satisfy the natural ejector air handling capacity. The effect of a small inlet is that the inlet velocity is increased which in turn reduces static pressure within the inlet. This is reflected as an increase in nozzle base drag and in ejector-lip suction (F_{lip}/F_{ID}) as shown in figure 43. The effects of nozzle tube length on performance are similar to those observed for bare suppressor configurations although amplified in some cases by secondary effects on ejector inlet area. By far the strongest geometric parameter affecting performance is ejector setback which directly affects inlet area. The general trend of inlet area effect on performance is shown in figure 47.

If the inlet area is too small and choking occurs, the performance is severely penalized. Since the ejector air demand is a function of the nozzle operating conditions, e.g., pressure ratio and temperature, inlet choking may not be present except for certain limiting conditions. For this reason it is extremely important in the development of ejector suppressor configurations that testing and analysis encompass the entire range of expected in-service operating conditions.

5.3.5 PERFORMANCE TRENDS

A chart format of data presentation has been developed in this program which shows general performance trends over a broad range of suppressor and ejector geometries. Each summary chart considers a particular suppressor array and identifies performance trends as a function of nozzle tube length, ejector area ratio, and setback. The summaries for all nozzle configurations provided in volume VIII are based on a nozzle pressure ratio of 3 and ambient jet temperature. Hot jet effects are shown on the charts for representative configurations. A sample summary performance chart is shown in figure 48. The example is based upon the 37-tube, NAR 2.75, close-packed-array suppressor. The numbers within the boxes at the left of the chart are measured static gross thrust coefficients for the bare suppressor (primary alone) with various tube lengths.

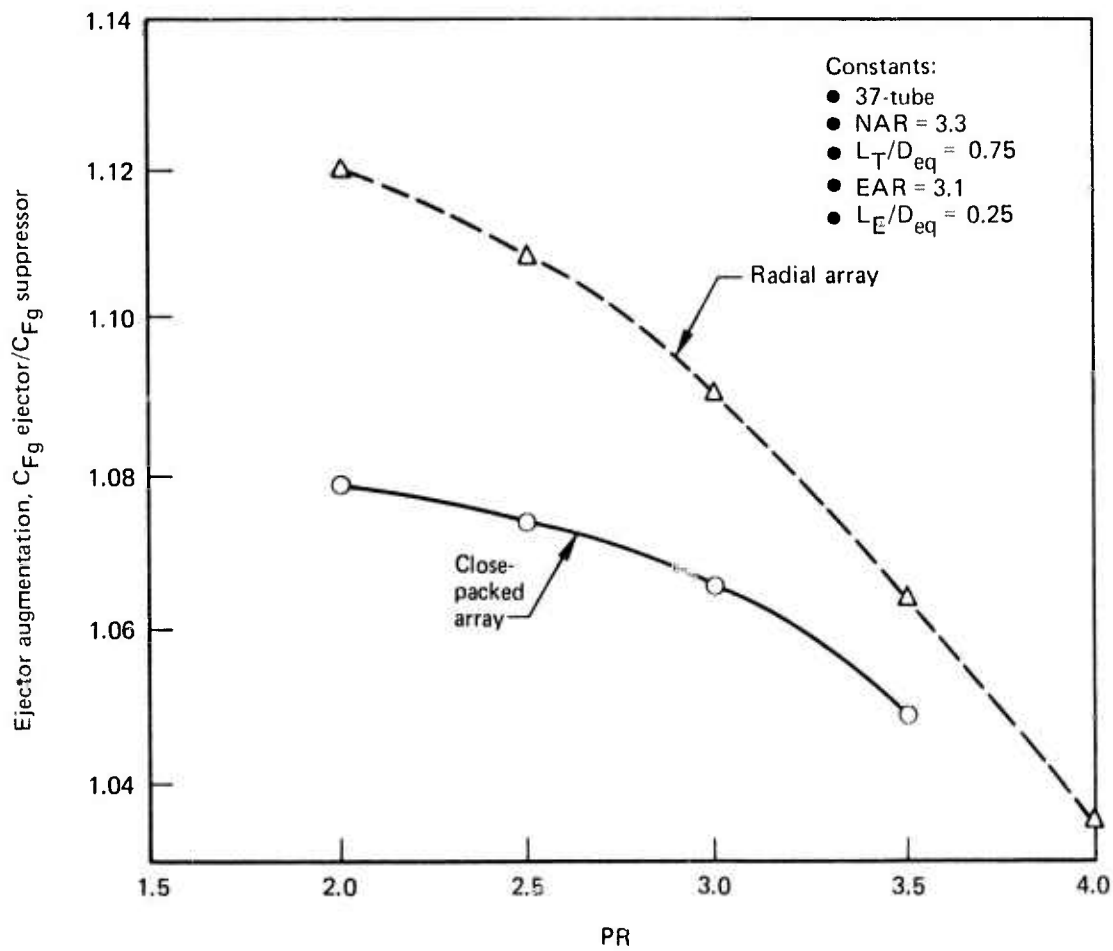


Figure 46.—Effect of Nozzle Array on Ejector Thrust Augmentation

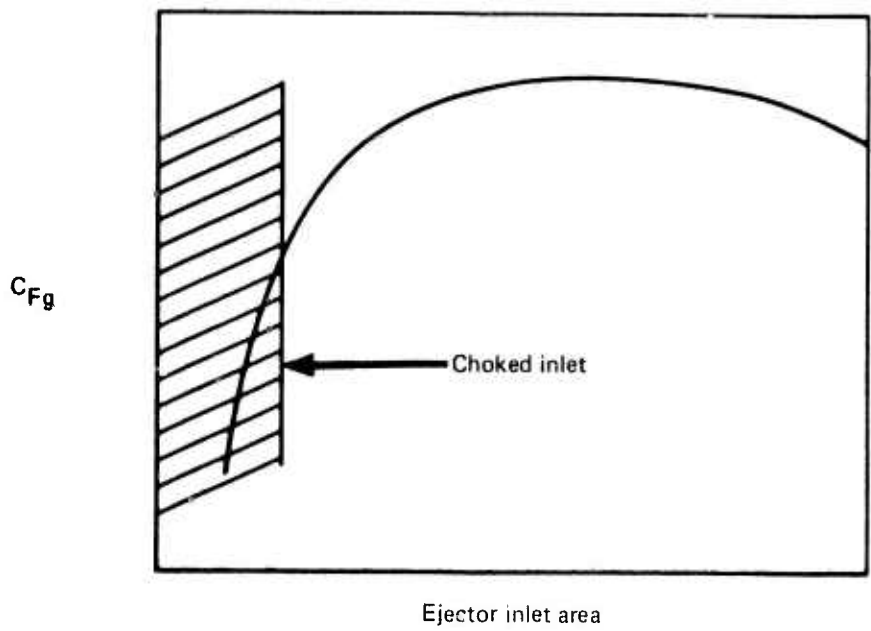


Figure 47.—Ejector Performance Trend

The effect of adding ejectors of increasing size is shown in the boxes to the right for the suppressor with given tube length. Performance with ejector setback of $SB/D_{eq} = 0.25$ is depicted in the dashed-line boxes. The arrows on lines connecting the boxes show the direction of increasing performance; the amount in percent is also shown. Following is an example of the use of these summary charts as a guide to the design of suppressor/ejectors.

Using the sample chart in figure 48 for a 37-tube suppressor, assume that installation constraints limit tube length to $L_T/D_{eq} = 0.5$ and EAR to no greater than 3.1. It is first noted that for $L_T/D_{eq} < 0.5$ or $EAR < 3.1$ performance penalties occur. Thus the installation upper limit constraints are indicated for a best performance value of 1.003 as shown. Again from the chart it is shown that a 0.5% further improvement can be realized by increasing ejector setback to $SB/D_{eq} = 0.25$.

An estimate of hot jet effects is found by comparison of performance for $EAR = 3.1$ and $L_T/D_{eq} = 1.00$ where the number in parenthesis (1.024 H) is for hot jet conditions. In this case it is observed that hot jet effects are minimal.

Finally an assessment from the chart of best geometry for the 37-tube nozzle with ejector is $L_T/D_{eq} = 0.5$, $EAR = 3.1$, and $SB/D_{eq} = 0.25$ where performance at $PR = 3$ is 1.008. Performance for this and other configurations at other pressure ratios can be determined from volume VIII.

5.3.6 PERFORMANCE/NOISE SUPPRESSION TRENDS

The suppression characteristics of the suppressor/ejectors in the present investigation are presented in volume II. An example comparison of suppression versus thrust penalty relative to measurements for the R/C reference nozzle is shown in figure 49. The suppressor is the 31-tube, NAR 2.75, radial array configuration. In this example best performance is obtained with the 3.1 AR ejector while best suppression is achieved with $EAR = 2.6$.

Performance/weight/noise characteristic trade studies would be required in an overall evaluation for selection of a "best" configuration.

5.4 LOW-SPEED PERFORMANCE

5.4.1 RANGE OF VARIABLES

Investigation of low-speed performance was conducted in the Boeing 9- by 9-ft induction wind tunnel which is described in section 5.1. Testing covered a range of pressure ratios from 2 to 4 at ambient jet temperatures. Limited testing at hot jet (1150° F) conditions showed performance/noise trends although budget constraints did not allow for sufficient data to be taken to generalize the results. Suppressor and ejector hardware were the same as in the earlier static testing and similar geometric variables were examined.

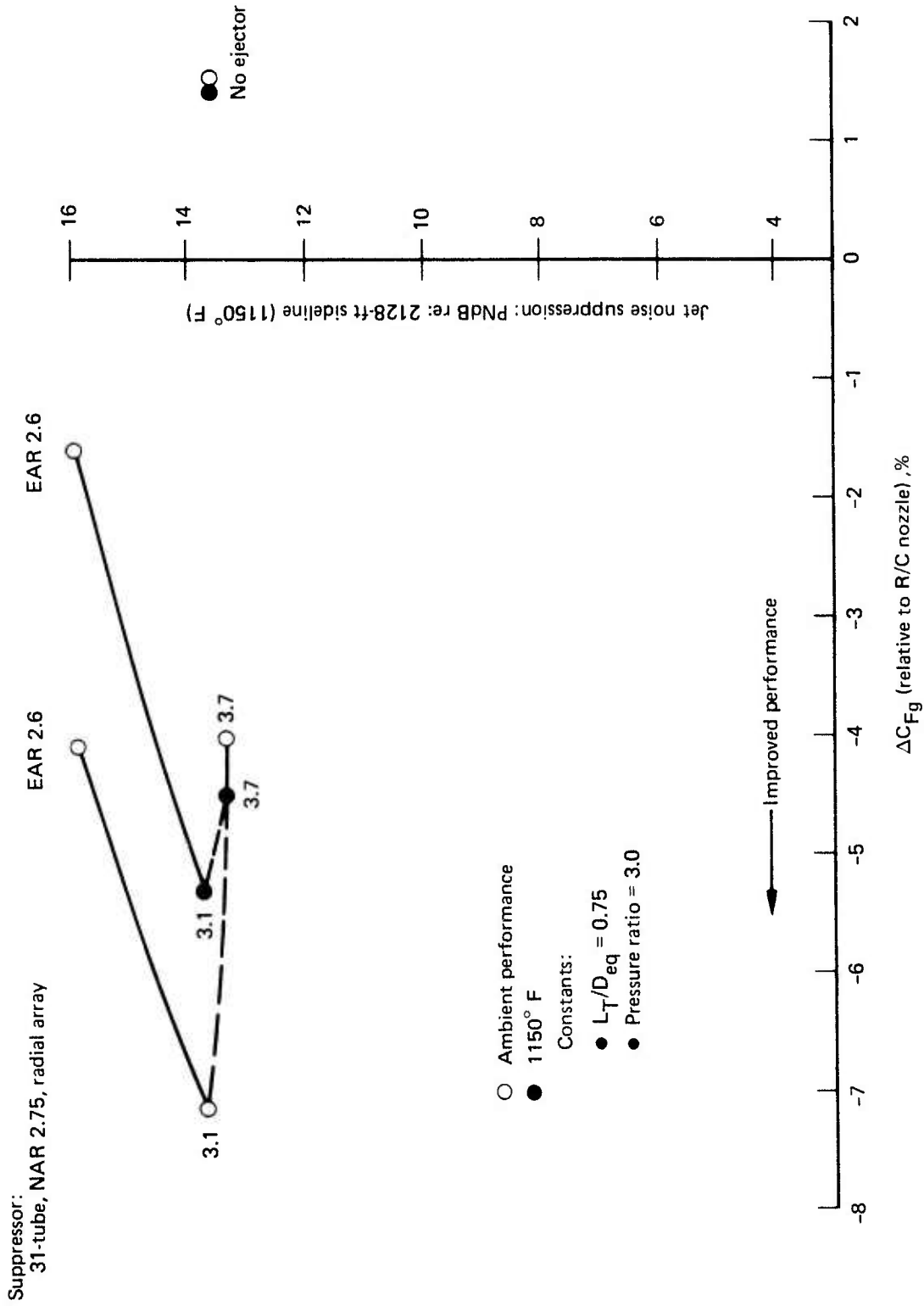


Figure 49.—Effect of Ejector Area Ratio on Suppression and Thrust Loss for a 31-Tube, NAR = 2.75, Radial Array

5.4.2 PRESSURE RATIO EFFECTS

5.4.2.1 Bare Suppressor

Volume IX provides the basis for the following observations relative to bare suppressor performance with forward velocity.

1. At any fixed wind tunnel velocity, afterbody drag becomes a decreasing percentage of ideal primary thrust as pressure ratio is increased.
2. The nozzle base drag increases linearly with increasing tunnel velocity for fixed pressure ratio conditions.
3. For a fixed pressure ratio, the ramp drag increases in proportion to velocity squared. Thus, for a fixed pressure ratio, the afterbody drag (the sum of the base and ramp drags) has a slightly nonlinear increase with velocity. The static performance of multi-tube nozzles without ejectors has been shown to be optimum at pressure ratios between 2 and 3. These combined effects result in a general behavior of bare nozzles as shown in figure 50.

A convenient way of plotting performance as a function of both pressure ratio and velocity is to use carpet plots. The carpet plot allows accurate interpolation of intermediate pressure ratio and/or velocity points. Though the value of C_{Fg} and the slope of lapse rate vary from configuration to configuration, the form shown in figure 51 always holds.

Volume IX contains the complete set of carpet plots for the suppressors tested in this program.

5.4.2.2 Suppressor/Ejector

The addition of an ejector to an exhaust system subjected to forward velocity creates these additional concerns:

- Ejector lip suction
- Increased suppressor afterbody drag
- Ejector drag
- Secondary air ram drag

The results of these effects are:

- Lapse rate ΔC_{Fg} for increased V_∞ decreases as pressure ratio increases.
- Lapse rate is nonlinear (but not a function of V_∞^2 due to the linear base drag).
- The peak C_{Fg} shifts to higher pressure ratios as velocity increases.

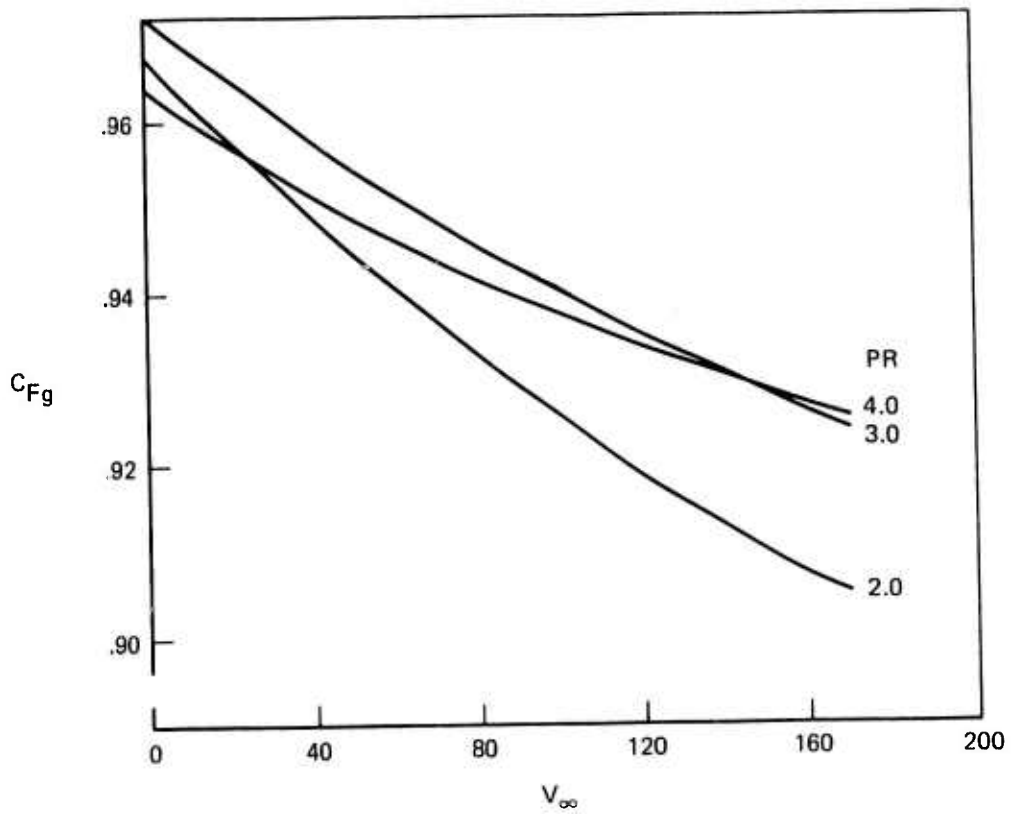


Figure 50.—General Behavior of Bare Suppressor Performance as a Function of Pressure Ratio and Velocity

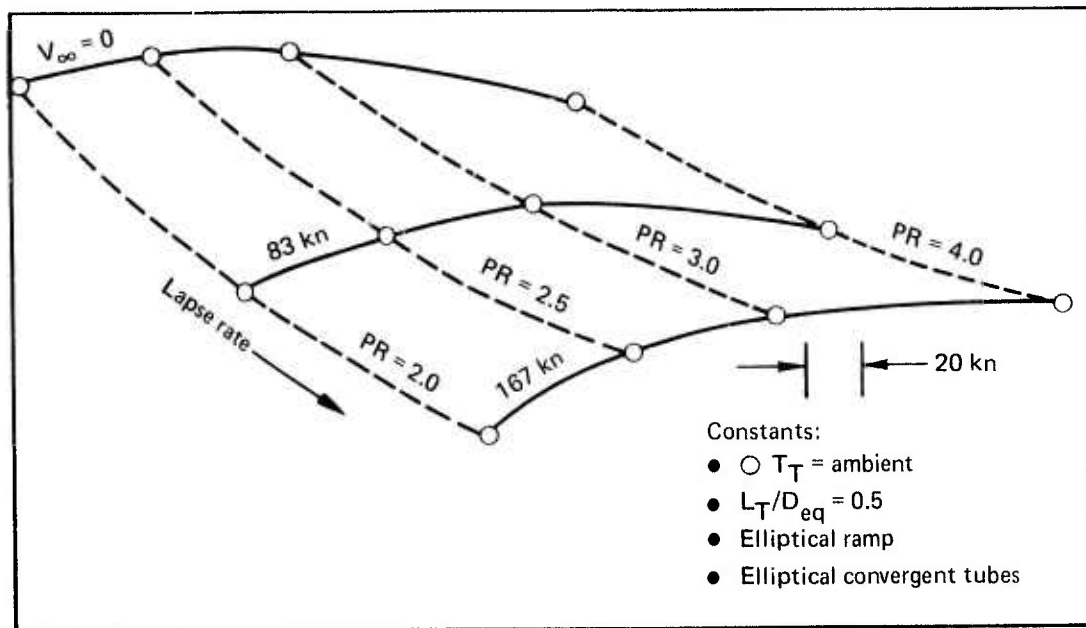


Figure 51.—Gross Thrust Coefficient for 37-Tube, $NAR = 3.3$, Close-Packed Array, Without Ejector

As the suppressor jets mix with surrounding air, flow is entrained by the jets. Ambient air moves into the regions of lower pressure created by the entrained air. When an ejector is installed this replacement air must flow into the ejector through the complex inlet provided between the suppressor tubes and through the annular opening between the outer tube row and the ejector lip as illustrated in figure 52. This inlet flow affects ejector-lip suction and suppressor afterbody drag. The lip suction, a result of the pressure reduction caused by the high velocity-flow entering the inlet, becomes a decreasing percentage of ideal primary thrust as pressure ratio increases (the lip force increases by a smaller amount than the ideal thrust).

Countering the performance benefit of the lip suction is the increased level of afterbody drag resulting from the presence of an ejector. This result is the same as for the suppressor without ejector except that the levels are higher. At any fixed pressure ratio both the afterbody drag and lip suction become a decreasing percentage of the ideal primary thrust as velocity increases.

The present investigation considers only constant area mixers; thus, the only ejector pressure drag to consider is the ejector boattail drag which is independent of pressure ratio. Skin friction drag is not considered in this investigation.

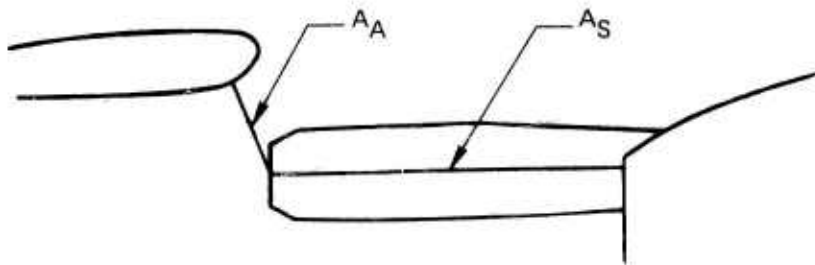
At a fixed velocity the amount of secondary air increases as pressure ratio increases. Therefore, by definition the amount of ram drag increases with increasing pressure ratio. Though it is a real component in the momentum equation, the ram drag physically manifests itself as a change in lip suction. The effect of pressure ratio on ram drag is of secondary concern when compared with its velocity effect.

The net result due to the above parameters is a pressure ratio dependence on overall performance which is similar to that of the bare suppressor case, but with steeper lapse rates. Figure 53 shows the performance of the same suppressor (shown bare in fig. 51) with an EAR 3.1 ejector installed. The skin friction, ram drag, afterbody drag, and ejector pressure drag all increase with velocity and thus increase the lapse rate for the ejector configuration.

5.4.3 NOZZLE GEOMETRY EFFECTS

The effects of nozzle geometry on performance were shown in section 5.3 to be dominated by base drag as influenced by available ventilation; and for similar internal geometries, by the number of tubes. Performance lapse rate with forward velocity is entirely due to external drag for choked nozzle conditions; in this case the change in base drag with velocity is indicative of overall lapse rate.

Figure 54 compares base drag with velocity for the 19-, 37-, and 61-tube, NAR 3.3 suppressors. Although drag levels are different, the rates of drag increase are nearly equal. Similar trends in overall performance lapse rates are found in figure 55 for these nozzles. Lapse rate for the 31-tube, radial array nozzle is significantly lower, due mainly to the smaller NAR 2.75 and in part to the improved base ventilation.



Detail A-A

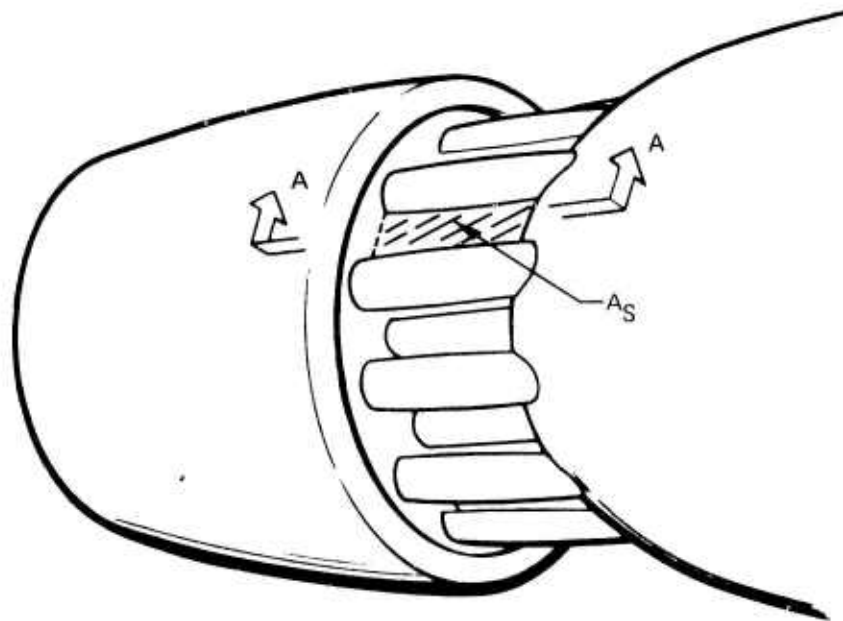


Figure 52.—Ejector Inlet Area, A_A and A_S

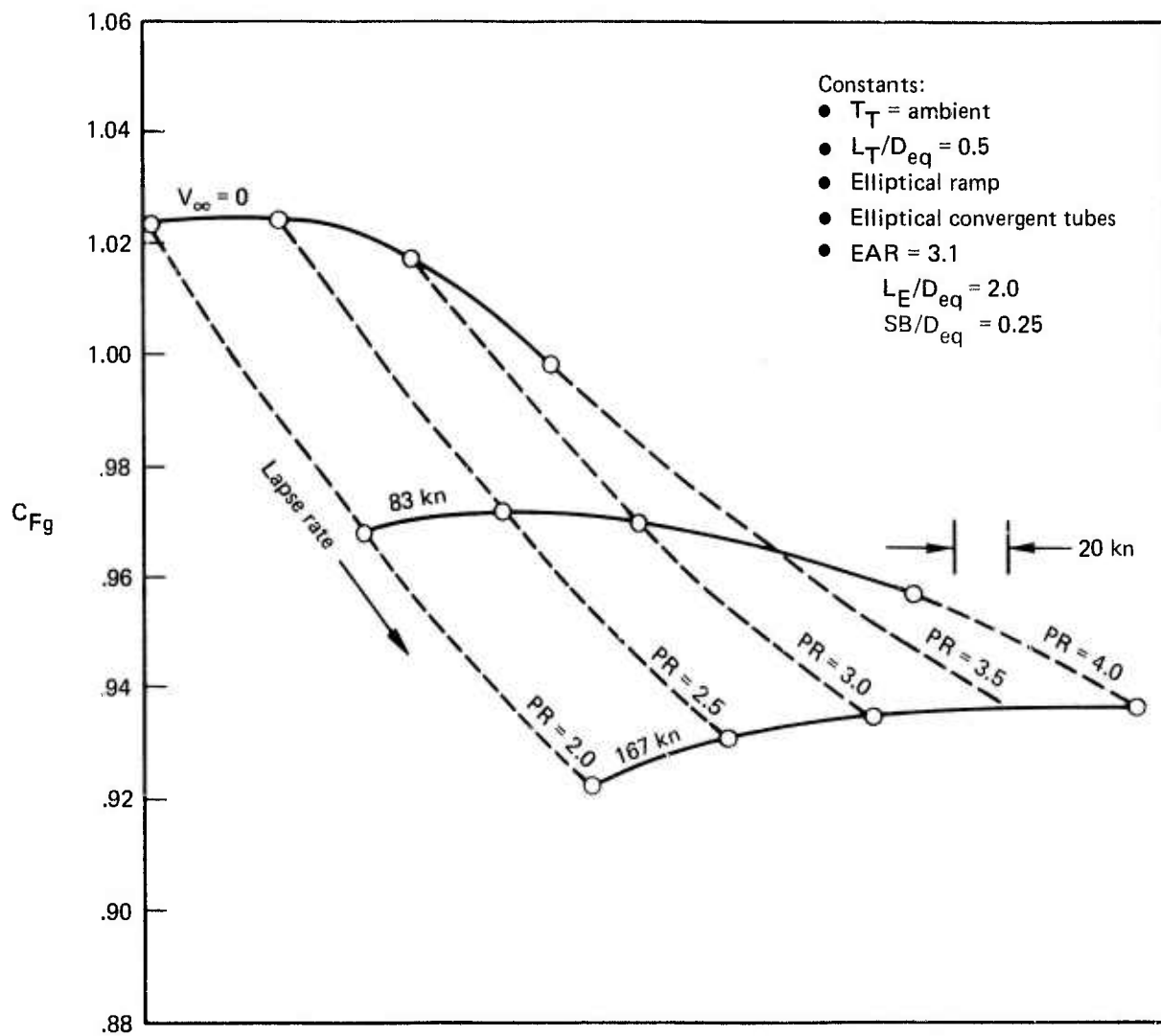


Figure 53.—Gross Thrust Coefficient for 37-Tube, $NAR = 3.3$, Close-Packed Array, With $EAR = 3.1$ Ejector, Setback = 0.25

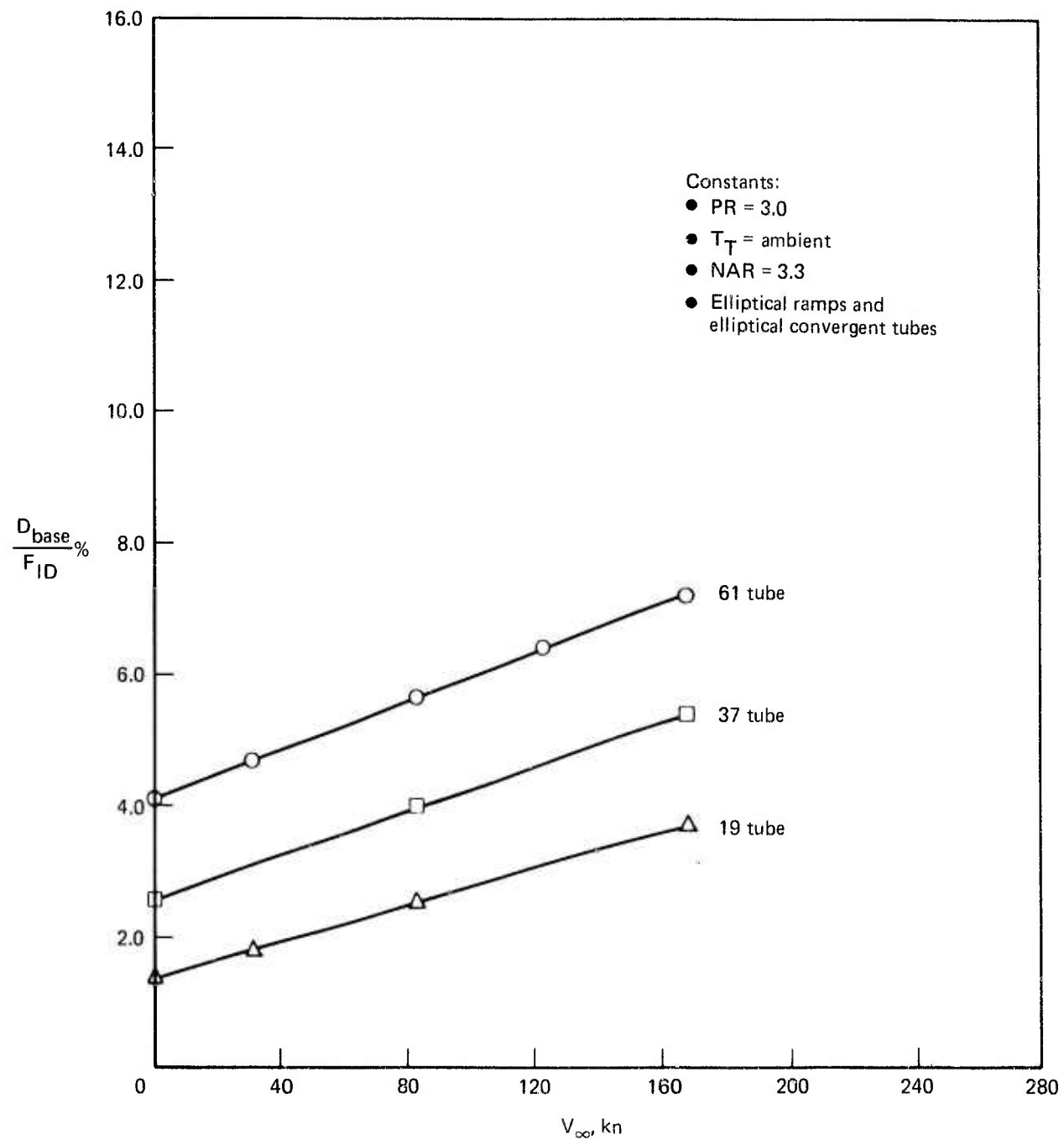


Figure 54.—Effect of Velocity on Base Drag as a Percentage of Ideal Thrust for NAR = 3.3 Suppressor With Various Numbers of Tubes (No Ejector)

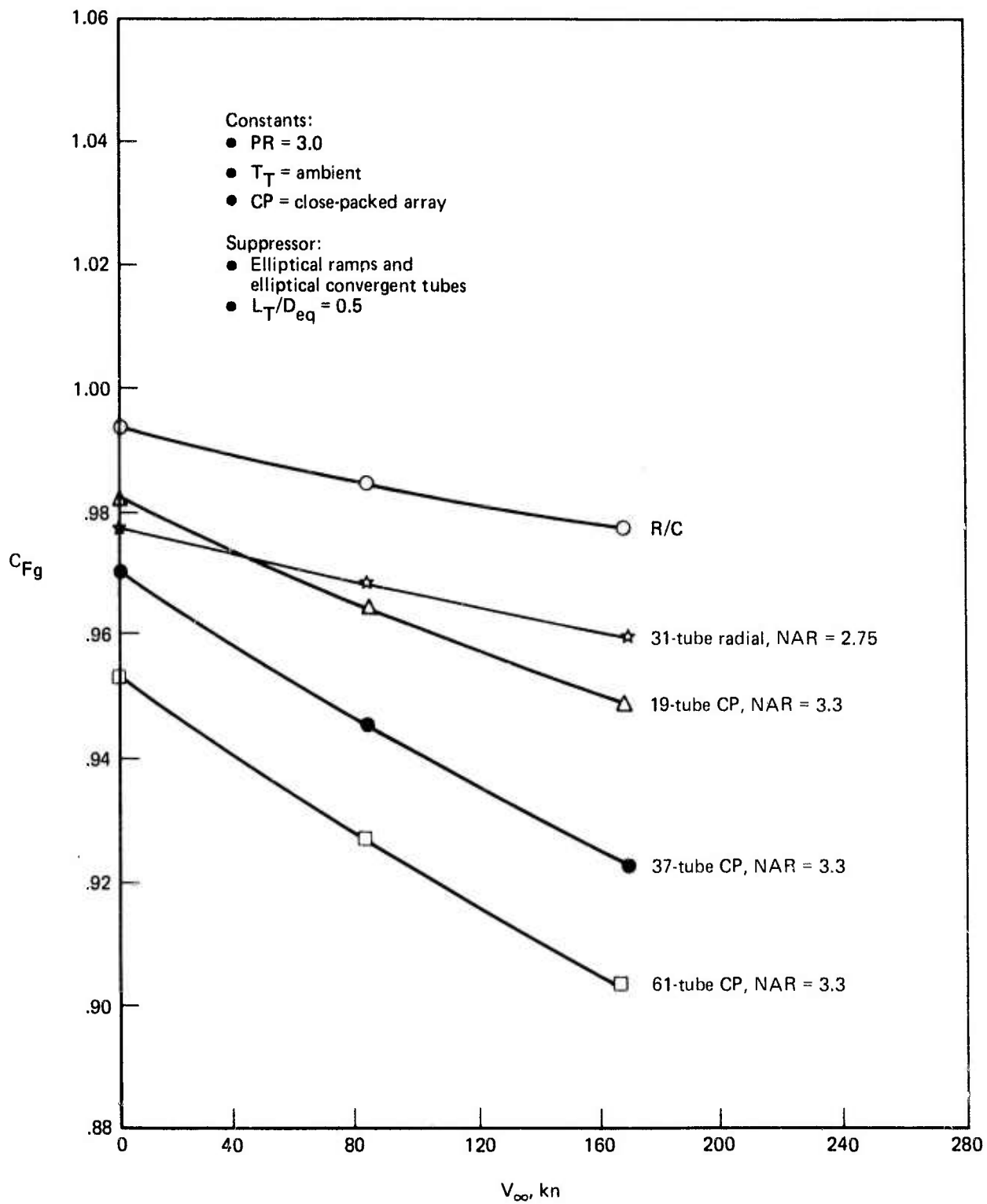


Figure 55.—Effect of Nozzle Geometry on Low-Speed Performance (No Ejector)

Lapse rate with a given ejector was found to be almost unaffected by nozzle geometry as indicated by figure 56 for various tube numbers and arrays. This finding was consistent for the range of variables in the test program, however, care should be taken when extrapolating this result. Different lapse rates would be expected when, for example, too few nozzle elements are provided for adequate mixing to achieve similar ejector augmentation and air handling.

5.4.4 EJECTOR EFFECTS

5.4.4.1 Inlet

Ejector setback was shown in section 5.3 and volume VIII to provide an important mechanism to provide optimum performance through the tradeoff between base drag and lip suction. A typical effect of setback on performance with forward velocity is shown in figure 57. Performance is seen to be a nonlinear function of setback at a given velocity. This parallels the earlier static testing where it was determined that base drag decreases asymptotically with increasing setback while lip suction has a peak value at the minimum inlet area that will pass the secondary air demand of the ejector system. These combined effects show an overall decreasing lapse rate with increasing setback for the range tested. This was true in all cases investigated and appears to provide a mechanism by which the static test optimization of inlet area through setback will also provide a minimum lapse rate.

5.4.4.2 Ejector Length and Area Ratio

The ejector length required to produce peak static thrust is a function of the suppressor element size and the ratio of the ejector to suppressor area ratios (EAR/NAR). One-dimensional ejector flow analysis (ref. 4) demonstrates that for constant primary gas conditions, the secondary weight flow rate increases as ejector area ratio increases (the analysis assumes sufficient ejector length is available for mixing and does not treat the effect of length). The peak performance of any suppressor/ejector system occurs when the ejector length is sufficient to provide optimal mixing of the primary jets with the secondary flow.

The individual element size affects the length required to mix out the primary core. As the number of primary nozzle tubes is increased, the amount of primary jet perimeter available to induce mixing increases and the ejector length required for maximum secondary air handling decreases. For the multitube suppressor the required length is conveniently non-dimensionalized by the individual tube diameter. The jet core mixes out in a length equal to 12 individual jet diameters (ref. 5). Aircraft constraints required an ejector of $L_E/D_{eq} = 2.0$. This ejector length requires 37 equal-area tubes in order to provide 12 individual jet diameters within the $L_E/D_{eq} = 2$ ejector. As the distance between the outer jets and the ejector wall increases (i.e., EAR/NAR increases) the required ejector length increases to provide enough distance for the mixing to extend across the ejector. When the ejector length is less than required for optimum entrainment the secondary air decreases, resulting in lower lip suction and hence lower static performance.

For short ejectors, entraining less than the maximum amount of secondary air, the decrease in secondary mass flow results in less ram drag penalty. Thus, the shorter the ejector (less

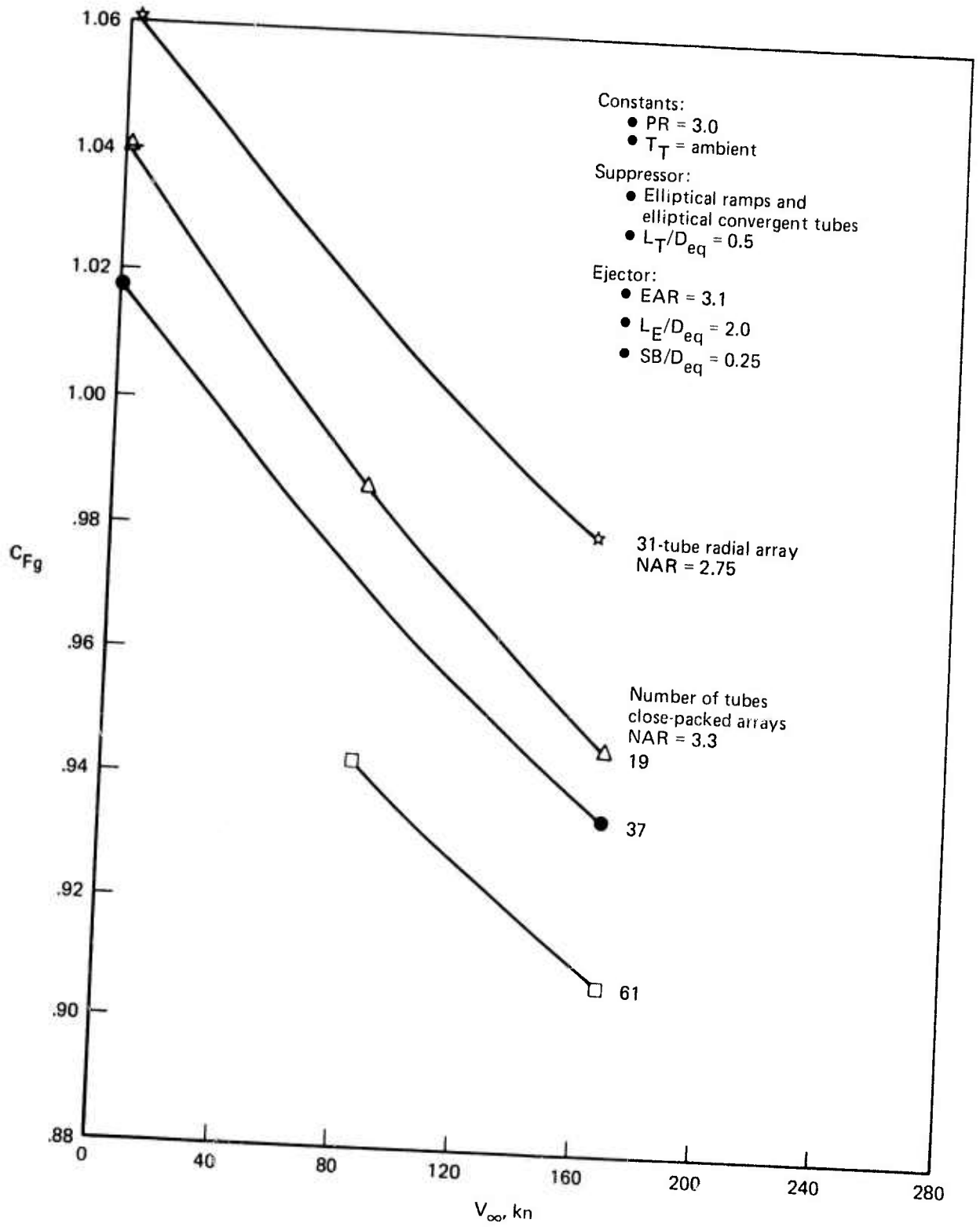


Figure 56.—Effect of Nozzle Geometry on Low-Speed Performance With Ejector

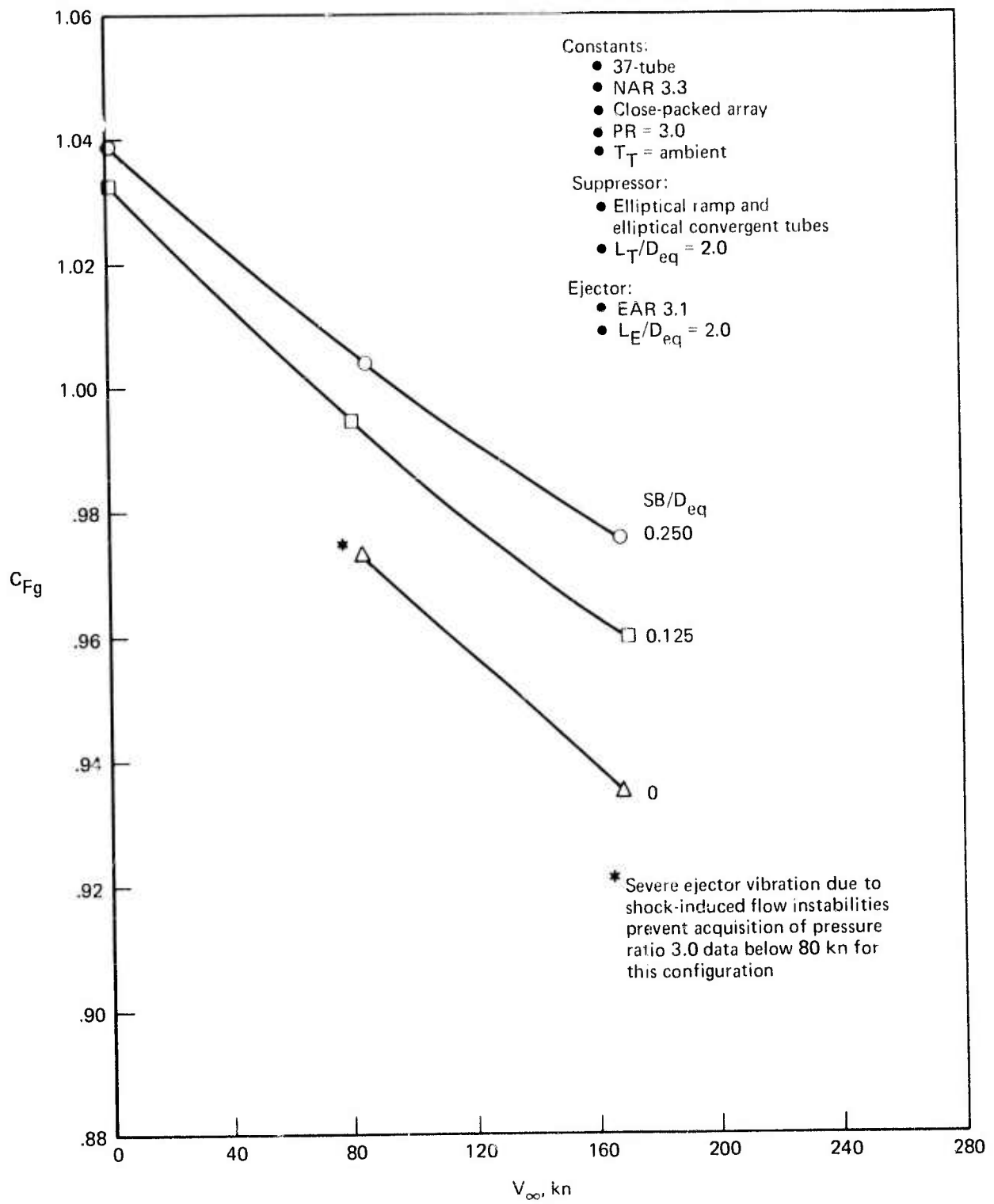


Figure 57.—Effect of Setback and Velocity on Performances (Other Parameters Constant)

than 12 individual jet diameters) the lower the static performance and the smaller the lapse rate with velocity. This results in a crossover velocity for performance of any suppressor/ejector with ejector length as the only variable. A performance envelope can be established where the highest static performance and maximum lapse rate are provided by the ejector of sufficient length to establish mixing across the ejector. The lowest lapse rate will be established by the no ejector case. The static performance and changes in ram drag due to too short an ejector are much more severe than those for too long an ejector.

Figure 58 dramatically illustrates these effects. The $L_E/D_{eq} = 2$ ejector is 12 individual jet diameters long for the 37-tube suppressor. The ejector area ratio is held constant at 3.7. The figure shows that the NAR 2.75 suppressor with the short $L_E/D_{eq} = 2.0$ ejector does not provide sufficient mixing length. The larger area ratio suppressor, NAR = 3.3, mixes out sooner and the smaller distance to the ejector wall decreases the length required for the primary flow to spread to fill the ejector. This results in greater secondary air handling and in turn a steeper lapse rate. The air handling of the EAR 3.7 ejector can be substantially increased using a long ejector. Figure 58 shows a 4% increase in static thrust due to the larger ejector on the NAR 2.75 suppressor. However, the increased air handling also increases the ram drag penalty and skin friction drag to the point where above 120 knots the shorter ejector performs better. This crossover velocity and the trade between static performance and lapse rate must be kept in mind when designing a suppressor/ejector for takeoff.

5.4.5 TEMPERATURE EFFECTS

- Base drag and lip suction both decrease with increasing jet temperature.
- The temperature effect is more pronounced on lip suction than it is on base drag.

The observed decrease in lip suction implies a decrease in secondary air handling and thus, the ram drag penalty (i.e., decrease in lip suction with increasing velocity) decreases as jet temperature increases. Figure 59 shows this to be the case. Statically, the lip suction at 1150° F is 3.39% less than the ambient value for the configuration shown. Increasing velocity produces a decrease in lip suction for both cases.

Since the ram drag is less for the hot flow, its rate of performance decrease is less. The difference in rate is small compared to the static difference in level and hence the velocity required to get the same lip suction from the hot and cold cases would be nearly 300 knots for this configuration. Volumes VI and VIII detail the decrease in base drag due to elevated temperature for static performance. The configurations tested at 1150° F to establish the effects of forward velocity on base drag showed that the base drag is slightly less at 1150° F jet temperature than at ambient for all velocities. Insufficient data were taken to quantify the amount, but it was observed that the ratio of change of drag with velocity was approximately the same for hot and cold configurations. Thus, a first order approximation would suggest that the static reduction in base drag due to hot primary flow be used as the quantity of reduction at all velocities. In this manner an approximate value can be obtained by using the hot-to-cold changes statically from volume VIII and the rate of change of drag with velocity from volume IX.

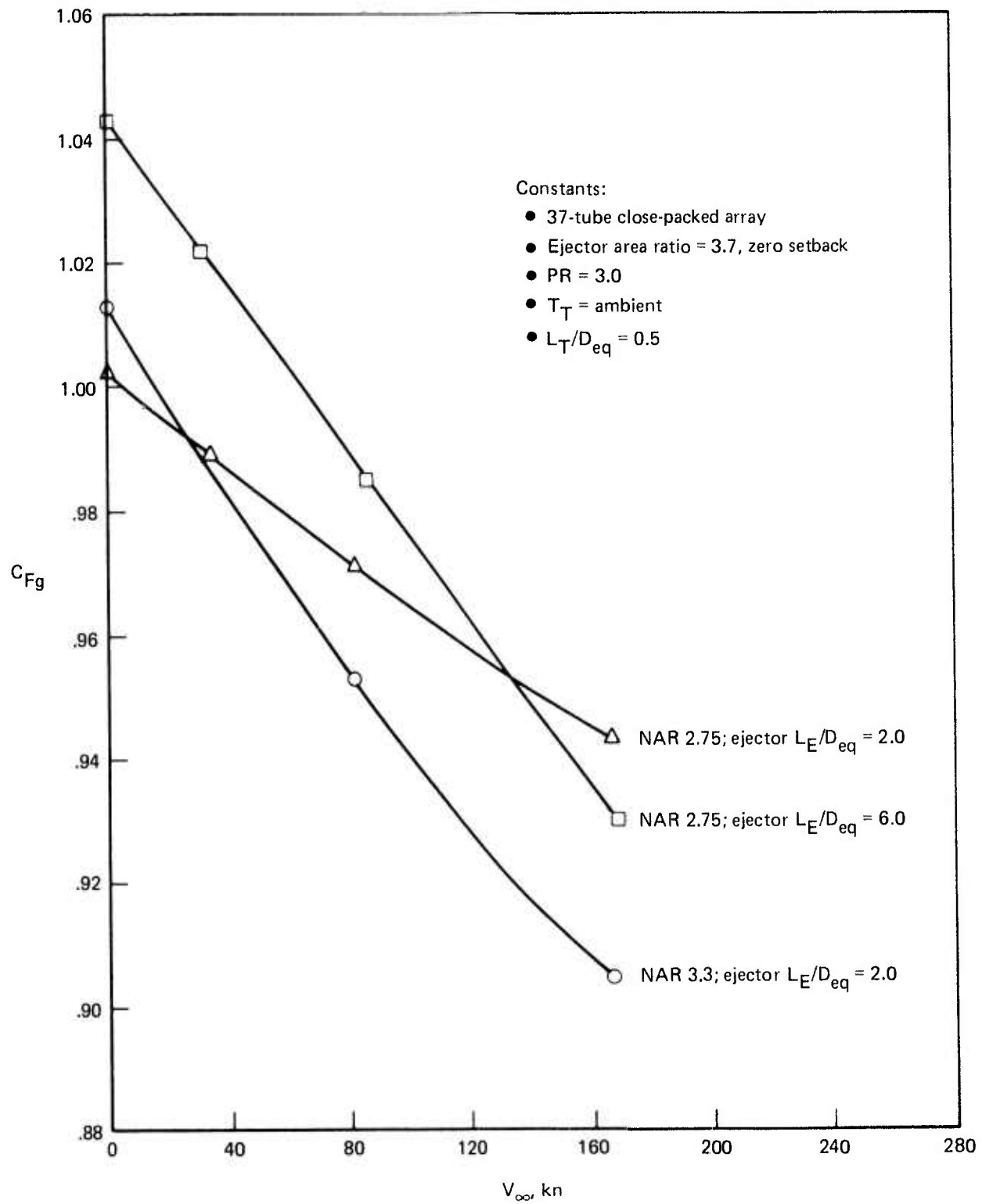


Figure 58.—Effect of Ejector Length on Performance With Forward Velocity

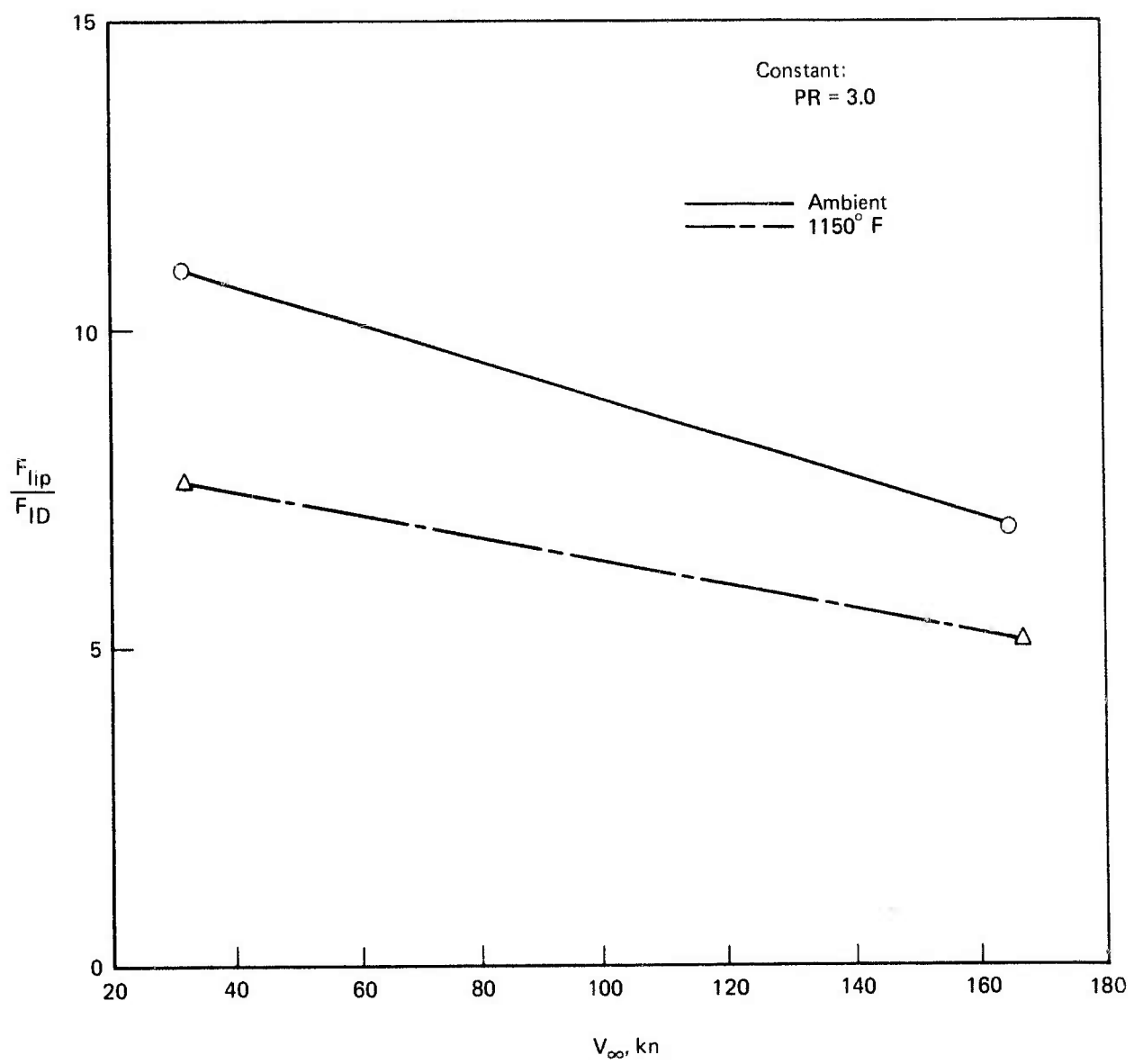


Figure 59.—Effect of Jet Temperature on Ejector Lip Suction

Unfortunately, lip suction is not as well understood as base drag. Except for the general statements about lip suction made in this section, the present investigation can only conclude that future testing must be done at the desired temperature. Performance data acquired at elevated temperatures have traditionally been much less accurate than ambient temperature data. The present program was successful in obtaining 1150° F primary-flow data statically. The limited wind-on data suggest a need for substantial development prior to future wind tunnel performance tests to ensure the correct temperature profiles and data levels and repeatability.

5.4.6 OVERALL PERFORMANCE TRENDS

The lapse rate of suppressor/ejector configurations is inherently larger (steeper) than that of the bare suppressor configuration. Though an ejector can produce a static thrust augmentation which for large ejectors can offset the inherent losses of the suppressor hardware, there is always some forward velocity beyond which the ejector becomes a performance handicap.

To the limit of ejector choking and/or flow instability, geometry changes were shown to have little effect on performance lapse rate although often grossly affecting the basic static performance level.

The selection of ejector inlet area which produces maximum static thrust for given suppressor/ejector geometry inherently produces the minimum lapse rate and thus best overall performance for that geometry.

Increasing ejector area ratio and length tend to increase air handling and thus static thrust augmentation. This benefit must be traded against the increased lapse rate which, in some cases, can result in less takeoff performance than for a smaller ejector.

Increased jet temperature reduces ejector air handling and lapse rate. Limited available data indicate that the overall result is a small performance penalty at takeoff conditions for configurations applicable to SST installations.

6.0 CONCLUSIONS

- Initial jet conditions (jet-flow profile, base thickness and turbulence level) can significantly affect the mixing process in suppressor/ejector.
- Base drag is the largest contributor to static performance losses associated with multi-tube suppressor nozzles. Base drag is least when tubes are arranged in a radial array to maximize base ventilation.
- Given sufficient mixing length and inlet area, static ejector performance increases in proportion to secondary air handling which in turn is proportional to ejector area ratio.
- Secondary air handling is the dominant factor governing ejector suppressor performance lapse rate (i.e., the rate of performance decay with forward velocity increases with increasing secondary air handling).
- The static thrust performance gains with increasing ejector size always cause increasing penalties at some forward velocity because of increasing lapse rates. This trade between static performance and lapse rate must always be considered when selecting ejector area ratio if best takeoff performance is to be realized.

PRECEDING PAGE BLANK-NOT FILMED

7.0 RECOMMENDATIONS

- Initial jet conditions were shown to significantly affect flow patterns and ejector performance. A need exists to determine if these phenomenon can be exploited to improve suppressor/ejector performance and noise suppression characteristics.
- Ejector lip suction and air handling appear to decrease significantly as jet temperature increases. The amount of decrease is not well understood except to affirm that performance lapse rate becomes less as primary temperature increases. Performance data acquired at elevated temperatures have traditionally been limited and much less accurate than ambient temperature data. Future wind tunnel testing should be based on acquisition of accurate thrust performance data at actual engine operating temperatures to ensure determination of representative takeoff performance trends.

PRECEDING PAGE BLANK-NOT FILMED

8.0 REFERENCES

1. C. P. Wright, D. B. Morden, C. D. Simcox, *SST Technology Follow-On Program—Phase I, A Summary of SST Jet Noise Suppression Test Program*, AD900-401L, FAA, Washington, D.C., February 1972.
2. M. Lu, D. Morden, et al., *SST Technology Follow-On Program—Phase I; Performance Evaluation of the NSC-119B Nozzle System; Volume I: Suppressed Mode*, AD-900-399L, FAA, Washington, D.C., February 1972.
3. J. Atvars, G. C. Paynter, et al., *Development of Acoustically Lined Ejector Technology for Multitube Jet Noise Suppressor Nozzles by Model and Engine Tests Over a Wide Range of Jet Pressure Ratios and Temperatures*, NASA CR-2382, April 1974.
4. P. Scoffield, "One-Dimensional Ejector Analysis." unpublished Boeing document.
5. J. Reid, *The Effects of Cylindrical Shroud on the Performance of a Stationary Convergent Nozzle*, Aeronautical Research Council Report and Memoranda No. 3320, Ministry of Aviation, London, England, 1963.

PRECEDING PAGE BLANK-NOT FILMED